SERI/PR-255-3057
DE88001101

September 1987

File

Polymer Reflectors Research During FY 1986

Paul Schissel
Hermann H. Neidlinger

Solar Energy Research Institute
A Division of Midwest Research Institute

1617 Cole Boulevard
Golden, Colorado 80401-3393

Operated for the
U.S. Department of Energy
under Contract No. DE-AC02-83CH10093

SERI/PR-255-3057
UC Category: 62
DE88001101

Polymer Reflectors Research During FY 1986

Paul Schissel
Hermann H. Neidlinger

September 1987

Prepared under Task No. 5120.510
FTP No. 0651

Solar Energy Research Institute
A Division of Midwest Research Institute

1617 Cole Boulevard
Golden, Colorado 80401-3393

Prepared for the
U.S. Department of Energy
Contract No. DE-AC02-83CH10093

Notice

Printed in the United States of America

Available from:
National Technical Information Service
U.S. Department of Commerce
5285 Port Royal Road
Springfield, VA 22161

Price: Microfiche A01
Printed Copy A07

Codes are used for pricing all publications. The code is determined by the number of pages in the publication. Information pertaining to the pricing codes can be found in the current issue of the following publications, which are generally available in most libraries: *Energy Research Abstracts (ERA); Government Reports Announcements and Index (GRA and I); Scientific and Technical Abstract Reports (STAR);* and publication NTIS-PR-360 available from NTIS at the above address.

PREFACE

The research and development described in this document was conducted within the U.S. Department of Energy's (DOE) Solar Thermal Technology Program. The goal of this program is to advance the engineering and scientific understanding of solar thermal technology and to establish the technology base from which private industry can develop solar thermal power production options for introduction into the competitive energy market.

Solar thermal technology concentrates the solar flux by focusing tracking mirrors or lenses onto a receiver where the solar energy is absorbed as heat and converted into electricity or incorporated into products as process heat. The two primary solar thermal technologies, central receivers and distributed receivers, employ various point- and line-focus optics to concentrate sunlight. Current central receiver systems use fields of heliostats (two-axis tracking mirrors) to focus the sun's radiant energy onto a single, tower-mounted receiver. Point-focus concentrators up to 17 m in diameter track the sun in two axes and use parabolic dish mirrors or Fresnel lenses to focus radiant energy onto a receiver. Troughs and bowls are line-focus tracking reflectors that concentrate sunlight onto receiver tubes along their focal lines. Concentrating collector modules can be used alone or in a multimodule system. The concentrated radiant energy absorbed by the solar thermal receiver is transported to the conversion process by a circulating working fluid. Receiver temperatures range from 100°C in low-temperature troughs to over 1500°C in dish and central receiver systems.

The Solar Thermal Technology Program is directing efforts to advance and improve each system concept through solar thermal materials, components, and subsystems research and development and by testing and evaluation. These efforts are carried out with the technical direction of DOE and its network of field laboratories that works with private industry. Together they have established a comprehensive, goal-directed program to improve performance and provide technically proven options for eventual incorporation into the nation's energy supply.

To contribute successfully to an adequate energy supply at reasonable cost, solar thermal energy must be economically competitive with a variety of other energy sources. The Solar Thermal Program has developed components and system-level performance targets as quantitative program goals. These targets are used in planning research and development activities, measuring progress, assessing alternative technology options, and developing optimal components. These targets will be pursued vigorously to ensure a successful program.

One of the principal near-term objectives of the SERI Solar Thermal Research Program is the development of silver/polymer films for use in constructing durable, low-cost, lightweight concentrating collectors for solar thermal systems. The objective of the Silvered Polymer Reflector subtask is to study mechanisms to achieve light stabilization of polymers and hence develop durable, UV-resistant polymers for silver mirrors. Loss in specular reflectance from a variety of causes is currently a principal barrier in the widespread use of silver/polymer films for solar thermal application.

This report documents the work accomplished during FY 1986. R. Goggin conducted the polymer mirror fabrication and measurement activities. Y. Shinton made the specular and hemispherical reflectance measurements, M. Steffeck and P. Gomez carried out the

chemical synthesis related to stabilized polymer films, and E. Tracy carried out the vacuum sputtering. The equipment and techniques for measuring mirror specularity were developed by I. Susemihl. The authors thank B. A. Benson, 3M Company, for supplying experimental polymeric sheets and silvered mirrors for our use, and Dr. R. B. Pettit, Sandia National Laboratories, for helpful technical discussion on optical measurements and for measurements on key mirror materials. We would like to express special thanks to Dr. G. Lensch of Nordische Universitat, West Germany, for valuable advice during preceding work, also critical reviews by B. A. Benson, J. A. Hutchison, and Dr. B. Butler are greatly appreciated.

Paul Schissel

Paul Schissel, Principal Scientist

Approved for

SOLAR ENERGY RESEARCH INSTITUTE

Daniel M. Blake, Manager
Materials Research Branch

Gerald G. Groff, Director
Solar Heat Research Division

SUMMARY

The long-term objectives of the Silvered Polymer Reflectors subtask within the SERI Solar Thermal Research Program are to develop silvered polymers that have a high specular reflectance and to develop modifications of polymers that will protect the silver and maintain the reflectance in outdoor environments for many years. Major progress has been made toward the specific long-term targets of a specularity resulting in 90% of the solar flux being contained within a cone angle of 4-10 mrad, and a useful life of at least 5 years.

This document reports the progress accomplished during FY 1986. We have used a dual approach by interacting with industrial fabricators to obtain and evaluate silver/polymer films, and by forming chemically modified silver/polymer mirrors at SERI to improve durability.

Earlier work in FY 1985 showed the need for improved optical measurements. We designed and constructed a state-of-the-art bidirectional reflectometer and used it to evaluate silvered polymers.

We have shown that silvered polymers can have an initial specular reflectance well over 90% into an acceptance angle of 1-2 mrad, significantly better than our long-range goals. It was further shown that these results could be obtained when the silvered polymer was mounted with an adhesive onto a smooth, flat substrate or stretched as a membrane without a firm support as in the membrane mirror configuration. Thus, the initial optics exceeds our goals, and the focus of our work is now directed to the durability of silvered polymers.

Durability studies using industrial silvered polymers are conducted at SERI in accelerated weathering devices and outdoors. Further data using accelerated weathering and outdoor exposure in Minnesota, Arizona, and Florida are provided by subcontracted work. Outdoor tests in Colorado show that silvered polymers can maintain reflectances in excess of our long-range goals (>90%, 4 mrad) for at least 48 weeks (18% of our durability goal) and the tests are continuing. Materials placed into test earlier, before we attained the full optical performance, are also providing encouraging results. Samples outdoors in Golden, Colo., for 2 1/2 years maintain reflectances near 90% at 12 mrad while other samples have avoided silver corrosion as determined by visual inspection for nearly 3 years.

Outdoor exposure data in Arizona and Florida demonstrate harsher exposure than in Colorado or Minnesota. Comparison of stabilizer systems in Arizona and Florida has identified the current best stabilizer system. There is evidence from a small sample set in Arizona that the durability of the current best stabilizer system may not yet reach our long-range durability goal in contrast to the continuing excellent performance in Colorado.

Polymer films scratch more easily than glass, so the polymer films may not be easily cleaned by methods that are adequate for glass. Industrial silvered polymer films have been coated with a harder coat to facilitate cleaning. Laboratory tests demonstrate that initial optical performance with the overcoat is good and the abrasion resistance is greatly improved. Laboratory and outdoor tests are in progress and they show that polymer optical performance is not affected for at least 13 months. Tests to evaluate the effectiveness of the hard coats during anticipated cleaning procedures are being planned.

The durability tests on industrially silvered films are augmented by a broader study of stabilizers in films fabricated at SERI. Mirrors made at SERI to test advanced stabilizer systems used Corning 7809 glass as a substrate onto which a thin silver film is deposited, and the modified polymeric films are then cast from solution onto the silver. The glass substrate is used simply to simulate a collector substrate of smooth surface quality. The mirrors are characterized by measuring the hemispherical reflectance as a function of wavelength and the specular reflectance at one wavelength (660 nm). The mirrors are exposed to environmental degradation using accelerated weathering devices and outdoor exposure.

We have shown conclusively that stabilizers are needed in the polymer films to aid in protecting the silver and have identified and/or prepared a series of representative examples within the different groups of UV stabilizers and incorporated them into polymethyl methacrylate (PMMA) to enhance its effectiveness.

We have also demonstrated the extra effectiveness of placing UV light absorbers near the polymer/air interface. Evidence is accumulating that the permanence of the stabilizers may limit mirror durability and that the stabilizer performance slowly diminishes because of photolysis and/or leaching and removal from the host polymer. To attack this problem, we have synthesized polymeric stabilizers on the basis that polymeric stabilizers will not leach from the host. Various synthetic chemistry approaches have been successfully used to prepare polymerizable stabilizer monomers of the hydroxy-benzophenone, hydroxy-benzotriazole and hindered amine classes. These monomers were copolymerized with methyl methacrylate using various feed ratios. The SERI synthesized polymer materials, along with polymeric stabilizers from other sources, are being tested to evaluate their performance over time. Using accelerated extraction tests, we have shown that the polymeric stabilizers are more permanent in contrast to their low molecular weight counterparts.

Because physical and chemical aspects of the silver surface (bulk and surface plasmon absorption, silver surface degradation) interfere with the direct evaluation of stabilized polymeric films on silver mirrors, we started to evaluate changes in the polymer through studies of transparent, nonmetallized PMMA films.

Despite the high inherent UV stability of the UV absorbers tested, we find that their concentrations in thin films do fall steadily during accelerated UV irradiation. The deactivation of stabilizers depends on the weathering mode and may be explained by cleavage and/or modifications of the pendant stabilizer groups. Deactivation is slow enough not to limit outdoor lifetimes of mirrors for at least several years; however, it may become a factor after more prolonged use.

Solvent residues may accelerate optical degradation of solution-cast films. However, optical losses and molecular weight degradation in these films are considerably diminished by the presence of the stabilizers. Any optical losses due to light absorption of chromophores are limited mainly to wavelengths less than 400 nm and thus do not affect the solar performance of these films to a great degree. However, surface crazing in incompletely protected surface layers can cause considerable light scattering during the later stages of accelerated weathering.

TABLE OF CONTENTS

TABLE OF CONTENTS (Concluded)

LIST OF FIGURES

LIST OF FIGURES (Continued)

LIST OF FIGURES (Continued)

Page

LIST OF FIGURES (Concluded)

LIST OF TABLES

LIST OF TABLES (Continued)

LIST OF TABLES (Concluded)

1.0 INTRODUCTION

Current glass/metal heliostats for central receiver systems use silver/glass mirrors to reflect solar radiation onto a target receiver that may be several hundred meters away [1]. Silver is preferred because it reflects about 97% of radiation in the 300-2600 nm wavelength range. Central receiver systems require mirrors of high specularity, which is currently met by silver/glass mirrors, and performance durability for up to 20 years. The long-term durability for currently available silver/glass mirrors, which has been discussed in depth [2], is affected by some fundamental mechanisms of degradation [3]. Silver mirrors are also used in dish and parabolic trough collectors, but the specularity requirements are less stringent for troughs than for central receiver and dish collector systems. Glass, because of its brittle nature and its own weight, requires a stiff supporting structure. To reduce weight and cost of structures and allow design flexibility, the use of silvered/ polymer materials as the mirror and a thin polymer film to protect the silver is envisioned as a possibility. In addition to lower cost, concentrators must have adequate durability while maintaining high optical performance. These silver/ polymer mirrors could then be used for constructing durable, low-cost, lightweight concentrating collectors such as advanced stretched membrane heliostats and dishes.

Although some polymer-protected silver mirrors have excellent optical properties, increased durability and specularity to meet the needs of solar thermal systems require new polymers. Among the desired properties of the silver/polymer films, as identified by system studies [4], are a specularity resulting in 90% of the solar flux being contained within a solid cone with apex angle of a few milliradians, a useful life of at least 5 years, and resistance to UV, pollutants, and environmental degradation. System studies are now defining the required specularity that will depend on the system and application. For stringent applications, we are using the specularity goals of 90% of the solar radiation captured within the solid angle defined by a right circular cone whose full apex angle is 4 mrad. These are long-term programmatic goals that have been accomplished, and in this report we present the progress in our investigations on the specularity and durability of a number of silver/polymer combinations as a first step toward the long-term, 5-year life goals. In this report, all specular reflectances will refer to a measurement within the quoted full apex angle.

The specific goals for this subtask are (1) to evaluate industrially available silvered polymers and polymer films in terms of the long-range goals, and (2) to identify or develop polymers that can be used with silver as the reflecting surface of films, coatings, or structural elements and that will be fully effective for at least 5 years in solar thermal applications. These goals establish the following specific research objectives for polymer/silver mirrors: establish the degradation effects of UV radiation on polymer/ silver mirrors, determine the most effective means of blocking such effects by modifying the polymer, and prepare UV-resistant polymers or laminates that provide a basis for durable silver mirrors.

To achieve the long-term goals, test specimens are fabricated in two principal configurations (Figure 1-1). Extruded polymeric films are metallized and mounted on a substrate with an acrylic adhesive. It is likely, but not certain, that this will be the method for commercial fabrication. Results of our tests of silvered polymers with this configuration are discussed in Sections 3.1 and 3.2. Alternatively, polymeric films are cast from solution onto a metallized substrate, usually glass. The alternative process is used mainly as a practical means for altering the polymers for laboratory testing, and results are discussed in Section 3.3. Insight into degradation mechanisms has come from both fabrication methods, so both fabrication methods do require separate consideration.

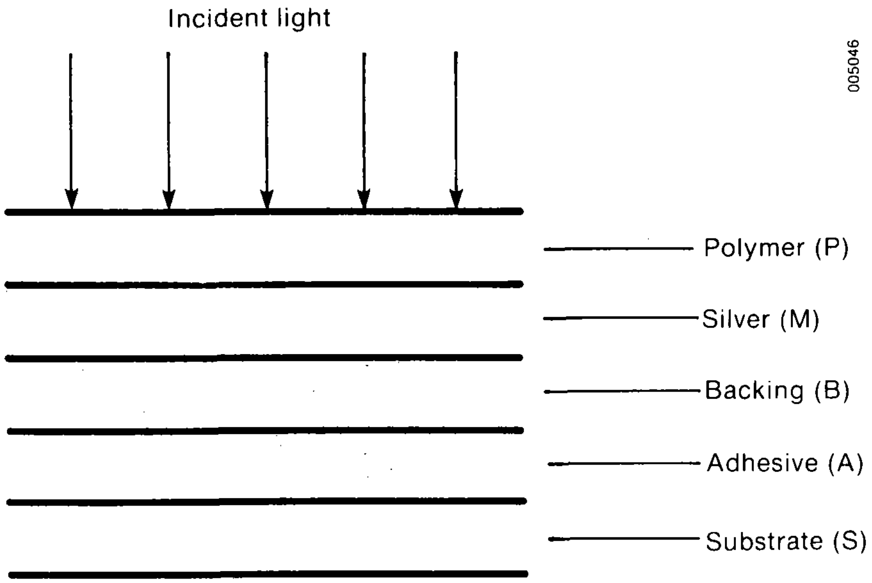

Figure 1-1. Test Mirror Configurations

Either configuration can be represented by variations of Figure 1-1. For cast films, the backing (B) and adhesive (A) would be absent. For extruded films, as might be used in membrane heliostats, the test samples would consist of the four or five layers as shown. In some cases, the backing, adhesive, and substrate are all identical (e.g., silver deposited onto glass), and in other cases, the backing and adhesive are identical (e.g., using Scotch brand tape to affix the silvered polymethyl methacrylate to a support). In all cases in this report, the host polymer is poly methylmethacrylate (PMMA). Empirical evidence has shown that PMMA is a stable polymer in a terrestrial environment and that it can protect aluminum in that environment. Also, it is relatively inexpensive and has excellent optical characteristics. We have chosen to emphasize PMMA for silver mirrors, recognizing that unaltered PMMA will not protect silver for a sufficiently long time [5]. The silver may be deposited in different ways (e.g., vacuum deposited or by the wet-chemical electroless process). Various backing materials and adhesives have been used to attach the silvered PMMA, with or without a backing, to glass or stainless steel supports. The backing and adhesive have been found to affect the optical performance.

This SERI in-house research is aided by subcontracted research. Researchers at the University of Denver are studying the photo and thermal degradation of polyacrylonitrile (PAN) films on silver using the Fourier transform infrared (FT-IR) method. They are emphasizing measurements of the chemical changes in the polymer, the results of which will guide the polymer modification effort. The PAN work serves as a research path parallel to the PMMA effort since both chemical types are commonly used in industry and have been found suitable as a baseline polymer for this purpose. The principal observations of the research are given in Appendix A. Work on several aspects of silvered polymers (durability, fabrication, abrasion-resistant surface coats) is being conducted in cooperation with the 3M Company, and the University of Akron has initiated the study of the influence of processing variables and film type on the mechanical and optical properties of membrane mirrors. The 3M work is summarized in Appendix B.

2.0 EXPERIMENTAL PROCEDURE

The experimental work consisted of preparing or securing silver/polymer multilayer combinations for optical characterization and durability testing. The combinations were either secured from commercially available sources or prepared as described in Section 2.3. The optical characterization and testing consisted primarily of measuring the reflectance of samples after preparation and at various stages of durability testing.

2.1 Optical Measurements

Our work in FY 1985 [6] identified the need for improved optical measurements. We had used portable instrumentation that performed well within its design range but was inadequate for specularity measurements that are compatible with our long-range goals. This problem is now solved and we have designed, constructed, and used two new reflectometers [7,8]. One, the "Specularometer," is used as a research tool for the complete evaluation of reflectors; the other, Reflectometer II, is of simplified design for use in routine measurements.

The optical performance of a solar mirror is determined by the absolute reflectance (ratio of reflected light to incident light) and its specularity, which describes the intensity distribution of the reflected light. The absolute reflectance depends mainly on the wavelength-dependent complex refractive indexes of the materials involved; the specularity is influenced by surface irregularities. Loss of specularity because of surface roughness can result from many causes. Theoretical models usually distinguish between roughness that is either large or small, in a direction perpendicular to the mean surface, when compared to the wavelength of the incident light. The distribution of the roughness over the surface is also important. While theoretically one can think of a continuum of spatial wavelengths representing the surface configuration, for purposes of discussion, it is convenient to think of local roughness (surface wavelengths small compared to the wavelength of the incident light), waviness (surface wavelengths large compared to the wavelength of the incident light), and curvature (macroscopic surface wavelengths). The topography of an actual surface is best described by the spectrum of spatial wavelengths existing on that surface; micro-roughness and large curvature then appear on the same diagram with a continuous scale of spatial wavelengths. Since every instrument that is capable of measuring the specularity of a mirror has a limited spatial wavelength bandwidth, it usually is necessary to combine different measurements when a mirror is to be described completely. The work reported here was related to the research for new mirror materials. Hence, the specularities of the materials themselves were of main interest.

The three kinds of surface irregularities are illustrated in Figure 2-1 in the cross section of a mirror. While roughness and waviness may be characteristic for a certain reflector material, the global curvature is due to the system design and may be desired if, for example, a mirror with a certain focal length were designed. Deviations from the ideal curvature are usually referred to as slope errors, and they may, in fact, be the largest component for a poor specularity of the system. A thorough description of the optical performance of a mirror is complete when the following is known as a function of wavelength and angle of incidence of the light:

a) specular reflectance: absolute ratio of reflected light to incident light as a function of the acceptance solid angle over the wavelengths of interest.

b) hemispherical reflectance: the maximum achievable specular reflectance with this material over the wavelengths of interest.

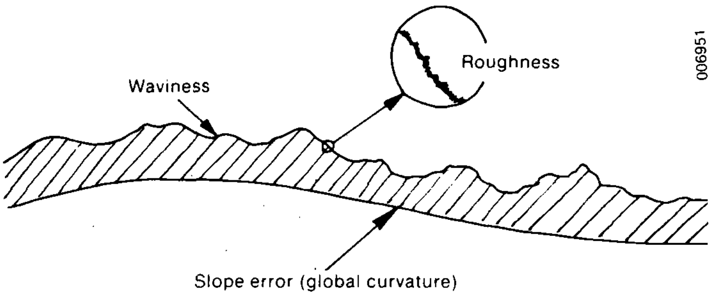

Figure 2-1. Schematic Cross Section of a Mirror Showing Three Scales of Roughness

2.1.1 Specularometer

A new reflectometer for specularity and specular reflectance measurements was designed that will be referred to as the "Specularometer." The block diagram of the Specularometer is shown in Figure 2-2. The instrument consists of a xenon arc light source (Oriel Model #7340) followed by a monochromator (Oriel Model #77250) and a chopper (EG&G Princeton Applied Research Model 192). The chopped input beam is collimated and is either reflected from the sample mirror or measured directly in the straight through configuration. In either case, collection optics directs the beam to the exit aperture and the UV-enhanced silicon detector (United Detector Technology UDT UV100). The silicon detector limits the observable wavelength range from 300 nm to 1100 nm. The detected signal is filtered by the lock-in amplifier (Stanford Research Systems Model SR510) and recorded by a Hewlett Packard HP 85 desktop computer, which also controls a stepper motor that drives the collection optics around the sample in a very accurate motion. Rotation of the collection optics also allows the angle of incidence to be varied from 20° to 70°. Comparison of the reflected beam to the straight through beam provides an absolute measurement of the reflectance of a sample mirror.

When the intensity distribution (specularity) of a beam is to be displayed, the source and collection apertures are adjustable slits perpendicular to the plane of incidence. The intensity distribution in the Fourier image plane of the collection lens is the Fourier transform of the reflection (or transmission) function of the sample convoluted with the beam divergence of the instrument. When the collection slit scans across the Fourier image plane of the collection lens, the detected signal is a convolution of the slit aperture and the actual intensity distribution in that plane [9].

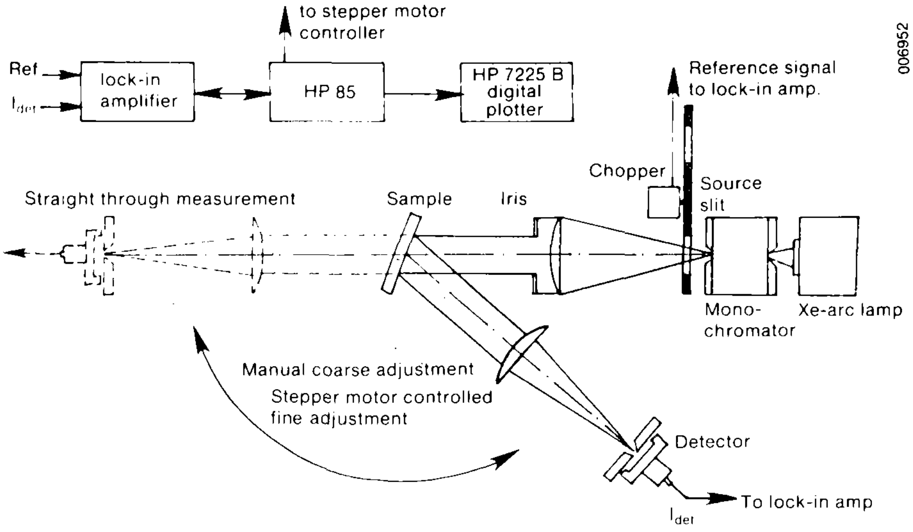

Figure 2-2. Schematic Diagram of the Specular Reflectometer

Figure 2-3 shows that the detected signal for a straight through measurement is less than 0.2 mrad broad. Because of this small beam divergence of the instrument, a deconvolution of the detected signal is not necessary for many applications and the detected signal can be referred to as the Fourier transform of the reflection function of the sample. Alternatively, a precision flat reflector (flatness better than $\lambda/20$) can be used for adjustment purposes; its reflection function is beyond the resolution limits of the Specularometer; hence, a more accurate calibration for determining the beam divergence of the instrument can be done with the instrument adjusted to the angle of incidence at which the sample is to be measured.

In Figure 2-3 and all following similar plots, a line is drawn at 13.5% of the maximum intensity, which corresponds to 95% of the area under the curve between the intersection points assuming a one-dimensional Gaussian distribution. Alternatively, the area under the curve can be numerically integrated and a given percentage width can be calculated for the actual one-dimensional distribution or for a two-dimensional distribution assuming rotational symmetry. Assuming rotational symmetry, the 95% width in one dimension corresponds approximately to that aperture required to capture 90% of the incident radiation in the related solid angle. The corresponding (planar) angle is denoted a_{90} and is given in milliradians. The instrument was designed to evaluate the intensity distribution of the specular beam. However, the collection optics can scan over 8° with a resolution of 0.014 mrad per step. This facilitates specularity measurements for a large variety of materials and scattering measurements in the vicinity of the specular beam. The latter is possible because of the large dynamic range of (>100,000) of the detection system.

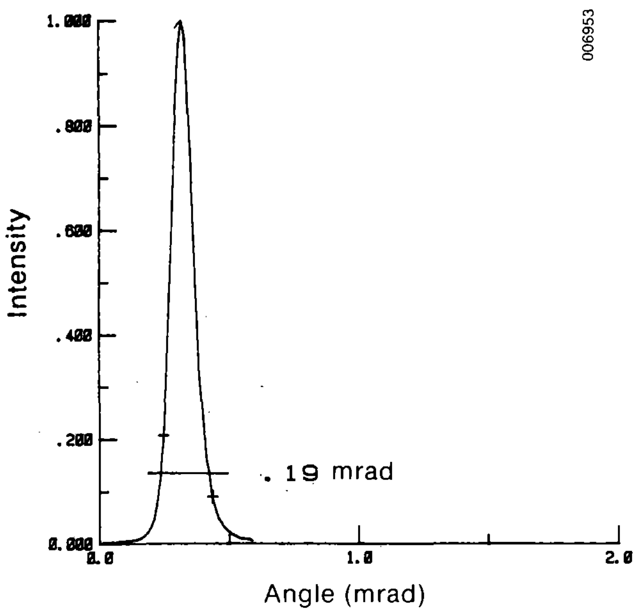

Figure 2-3. **The Input Beam Spread of the Specular Reflectometer (λ=630 nm).** The horizontal line defines the spread that corresponds to about 90% of the beam assuming a symmetrical, two-dimensional Gaussian distribution.

When numerical values of specular reflectance are to be determined, there are two possible procedures. The slit width of the collection slit can be varied to achieve a series of different apertures [10,11] or a set of circular apertures can be used. We usually use a circular source aperture of 0.7 mrad full-cone angle and a series of circular collection apertures of 4, 6, 8, 10, and 12 mrad.

To have as few parts in the optical path as possible, we omitted a beam splitter which, in combination with a second detector, would provide a signal that could automatically account for changes in the intensity from the light source. Instead, the computer takes 10-100 readings at each measurement point and calculates an average, which suppresses the short period noise level. In the absolute reflectance mode, an accuracy of about ±1% can be assumed as determined by comparison with a National Bureau of Standards (NBS) reflectance standard. The NBS standard is aluminized quartz for which the specular reflectance (λ=660 nm) is certified to be 86.2% using an acceptance aperture of 4°. We determined a value for the NBS standard of 85.9% (standard deviation of 0.3%) using our largest circular collection aperture of 12 mrad.

One of the possible applications of polymer mirrors is an ultralight free-standing membrane mirror where the silvered polymer membrane is clamped into a ring and the desired focal length of the system is adjusted with a vacuum system [12]. To facilitate the evaluation of the optical properties of a free standing membrane, we designed a special membrane sample holder as shown in Figure 2-4. The membrane is clamped with an outer ring, and a spring-loaded inner ring pushes against the membrane so that it becomes flat and taut. The membrane holder can be mounted onto the sample holder of the Specularometer.

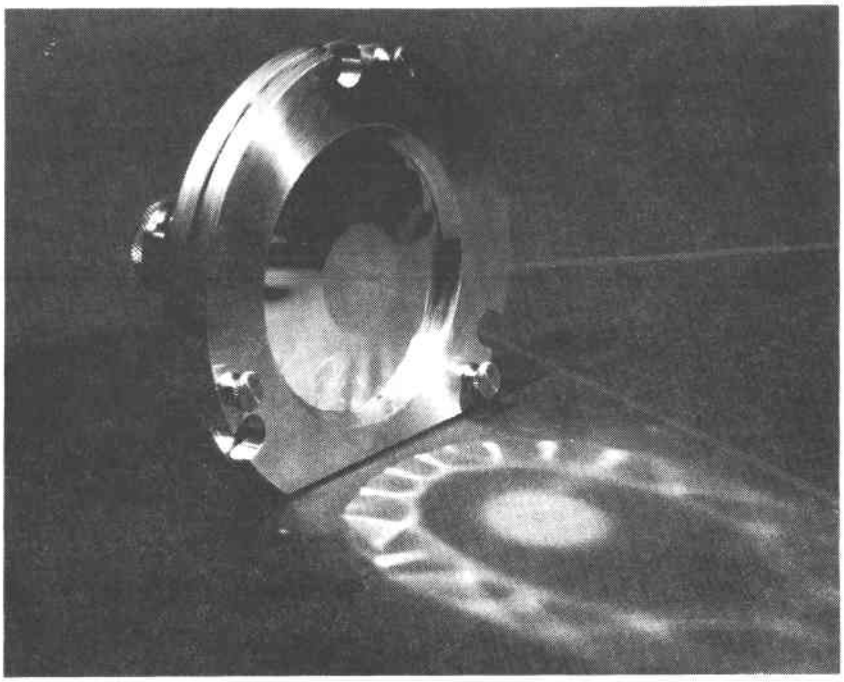

Figure 2-4. Mount for Thin Silvered Polymer Membrane Mirrors

2.1.2 Reflectometer II

Reflectometer II is a simplified version of the Specularometer, which is used mainly for the many mirror samples that are being tested for durability in accelerated weathering chambers and outdoors (Appendix C). It consists of:

- point light source
- chopper
- collimating lens
- reference detector
- sample
- collection lens
- detector
- lock-in amplifier
- HP85 desktop computer
- power supply for the point light source
- interferences filter (650 nm)
- iris
- aperture wheel.

The specifications of this bidirectional instrument are: angles of incidence variable between 20° and 80°; spectral response maximum at 650 nm; bandwidth 40 nm; beam diameter 10 mm; beam divergence 0.8 mrad full-cone angle; collection apertures 4, 8, 12 mrad full-cone angle; detector, two silicon photodiodes; lock-in amplifier for signal detector and reference detector; frequency 10 kHz. The source aperture as well as collection apertures are circular apertures [sizes are given in full-cone angles (mrad)] to obtain data on the two dimension beam distribution. Self calibration is possible with the straight through measurement and comparison with NBS standards shows the accuracy and precision are about ±1%.

2.1.3 Hemispherical Reflectance

Hemispherical reflectances were determined using a Perkin-Elmer 340 spectrophotometer and integrating sphere over the wavelength range of 200-2600 nm. These data were used to calculate the solar-weighted (air mass 1.5) hemispherical reflectance. To save time in obtaining preliminary data for polymer films that we have cast, we integrate, in most cases, from 300 to 1000 nm rather than from 200 to 2600 nm, and hence, H is somewhat lower than the solar value. Losses in H can result from physical (e.g., plasmons, agglomeration, diffusion) and chemical (e.g., corrosion) changes in the silver metallization of mirrors from a variety of causes.

2.1.4 Surface Profiles

A DEKTAK surface profile measuring instrument manufactured by SLOAN Technology Corporation and equipped with a fast leveling module, strip chart recorder, and multiaxial translation/rotation stage was used to record surface profiles of some samples. In these investigations, the waviness of the sample was of main interest, hence, long scanning lengths (30 mm) were used. The chart was digitized with an HP 7225B Digital Plotter in combination with an HP 85 computer for further data analysis.

2.1.5 Metallizing

Polymer sheets are metallized using a DC magnetron sputterer with a 4 in. × 6 in. silver target that facilitates a uniform deposition over an area of approximately 6 in. square. Four 2 in. × 2 in. specimens are mounted at the same time onto a water-cooled rotating sample holder, which maintains the polymer surface temperature at an acceptable level during the sputtering process.

2.2 Industrially Silvered Polymers

A few types of industrially available silvered polymers were obtained and tested. The related results are discussed in Sections 3.1 and 3.2.

2.3 Solution Cast Stabilized Polymer/Silver Glass Mirrors

Mirrors are made using Corning 7809 glass as a substrate onto which a thin, reflective silver film is deposited, and polymeric films are then cast from solution onto the silver. A Tencor Alpha-Step surface profiler, which has an effective sensitivity of 5 nm, was used to measure the thickness of the polymer films applied to the substrates.

There are several possible silvering processes. We have used mainly deposition by the wet-chemical process onto glass substrates or vacuum metallization by sputtering onto glass substrates as a precursor to casting polymeric films. Other metallization processes such as ion plating may be used if, for example, adhesion of the silver to contiguous materials is a limiting factor, but we have not yet used them.

When the polymer formulations are being altered to improve durability, it is convenient to use the solution-casting technique to make the polymeric films. In this case, we coat the polymer onto the silver in contrast to the use of extruded films where we deposit the silver onto the polymer. While solution casting may not be used in large-scale production, we have observed some factors that influence optical performance; the factors are all relevant for our tests, and they may be relevant where extruded films are used.

A series of additives (UV screens, quenchers, antioxidants, antipermeants) can enhance the effectiveness of PMMA. We have identified an initial series of commercially available additives (Table 2-1) with first emphasis on UV screens that have been and are being tested. These have been augmented with additional stabilizers specifically synthesized for protecting silvered polymers (Table 2-2). The details of the synthetic chemistry are given in Section 2.5. Generally, the stabilizers are incorporated in the polymers by dissolving PMMA (10 w% solids) with the stabilizers in toluene. Stabilizer concentrations are given in Tables D-1 and D-2 in Appendix D.

2.4 Solution Cast Stabilized Polymer Films

Free-standing PMMA films are prepared in a manner similar to the method described in Section 2.3 by casting toluene solutions (10 w% solids) of the polymer/stabilizer (98.5 w/1.5 w) combinations onto glass substrates. PMMA (Polysciences) was used in most cases as received without further purification. The solvent is slowly evaporated for 1 day in a drying box. Next, the films are vacuum dried for another day and stripped from the glass substrates.

2.5 Polymeric Light Stabilizers

Attention has been focused on the synthesis and characterization of polymeric UV-absorbing stabilizers of the 2-hydroxybenzophenone and 2-hydroxy phenylbenzotriazole classes, which are methacrylic, vinyl, or isopropenyl derivatives. Other work has concentrated on the synthesis and polymerization of polymerizable 2,2,6,6-tetramethylpiperidine derivatives, which can act as non-UV-absorbing stabilizers.

2.5.1 Materials

Most of the following chemicals were, if not otherwise noted, obtained from Aldrich Chemical Company o-Nitroaniline (Eastman Kodak Co.) was used as received. 2,4-Dihydroxyacetophenone was recrystallized from a dilute solution of hydrochloric acid (water/conc. hydrochloric acid, 12/1). Iodomethane, magnesium turnings, sodium borohydride, and zinc powder were used as received. Potassium hydrogen sulfate and zinc chloride were freshly fused before use. Picric acid was dried in small quantity in vacuum for 1 day.

Methyl methacrylate (MMA) monomer was distilled under nitrogen at reduced pressure. It was then stored under nitrogen in the freezer.

We used 4-methacryloxy-2-hydroxybenzophenone (MHB) (Polysciences), isocyanatoethylmethacrylate (IEM) (Dow Chemical), 4-amino-2,2,6,6-tetramethylpiperidine, 4-hydroxy-2,2,6,6-tetramethylpiperidine, methacryloylchloride, and triethylamine (Sigma) as received.

Azobisisobutyronitrile (AIBN) (Alfa) was recrystallized from absolute methanol and dried for 4 h at 25 mm Hg at room temperature.

Anhydrous diethyl ether was used from freshly opened cans. Tetrahydrofuran (THF) was heated to reflux over calcium hydride for 3 h, distilled, and kept over molecular sieves.

Solvents such as acetonitrile, toluene, benzene, dimethoxyethane (DME), dichloromethane, methanol, and hexane were dried when necessary and used without distillation.

Table 2-1. Commercially Available Stabilizers

Structure[a]	Symbol	Product	Supplier	Mechanism of Action[b]
I	Tin-P	Tinuvin P 2 (2'-hydroxy-5'-methylphenyl) benzotriazole	Ciba-Geigy	UVA, CB-D(Q)
II	UV	Uvinul 408 2-hydroxy-4-n-octoxybenzophenone	BASF-Wyandotte	UVA, CB-D(Q)
III	MHB	4-Methacryloxy-2-hydroxybenzophenone	Aldrich	UVA, CB-D(Q)
IV	NS	National Starch 78-6121 developmental copolymer of a 2-hydroxybenzophenone	National Starch	UVA, CB-D(Q)
V	TIN-2	Tinuvin 292 bis (1,2,2,6,6 pentamethyl -4-piperidinyl) sebacate	Ciba-Geigy	CB-A/CB-D
VI	IRG	Irganox 1010 tetrakis [methylene (3,5-di-tert-butyl-4-hydroxyhydrocinnamate] urethane	Ciba-Geigy	CB-D Synergist only with UVA
VII	G-30	Goodrite UV 3034 1,1'-(1,2-ethanedioyl) bis (3,3,5,5-tetra-methylpiperazinone)	Goodrich	CB-A/CB-D
VIII	G-31	Goodrite UV 3125 3,5-di-tert-butyl-5-hydroxy hydrocinnamic acid triester with 1,3,5-tris(2-hydroxyethyl)-S-triazine-2, 4,6 (1H,3H,5H)-trione	Goodrich	CB-D Synergist only with UVA
IX	IST	Irgastab 2002 Nickel bis [O-ethyl(3,5 di-tert-butyl-4-hydroxybenzyl)] phosphonate	Ciba-Geigy	CB-D, UVA(Q)
X	CH	Chimasorb 944 polymeric HALS	Ciba-Geigy	CB-A/CB-D
XI	SP	Spinuvex A36 polymeric HALS	Borg-Warner	CB-A/CB-D

[a] Structures tabulated below.
[b] UVA = ultraviolet absorber.
Q = Quencher.
CB-A = Chain-breaking acceptor antioxidant.
CB-D = Chain-breaking donor antioxidant.

Table 2-1. Commercially Available Stabilizers (Continued)

I

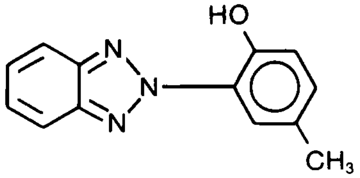

II

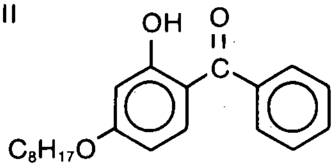

III

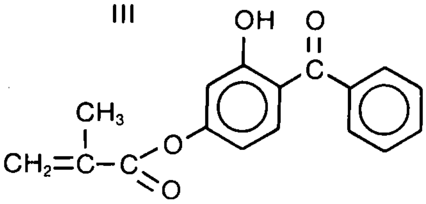

IV

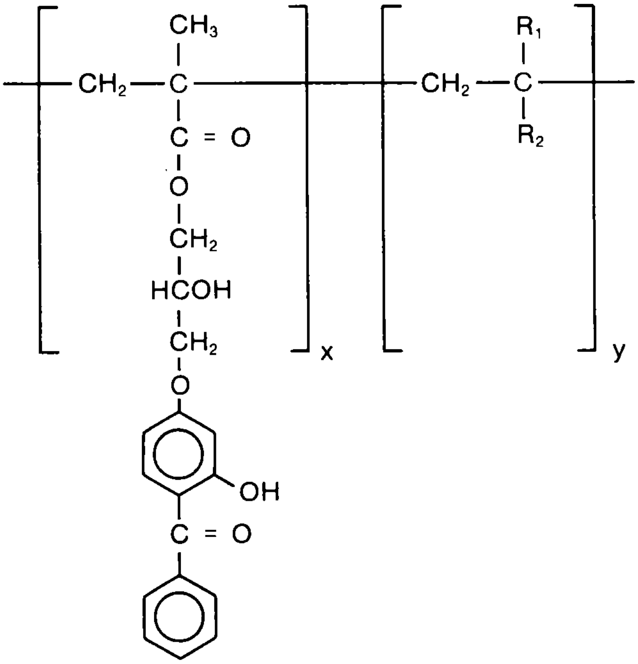

V

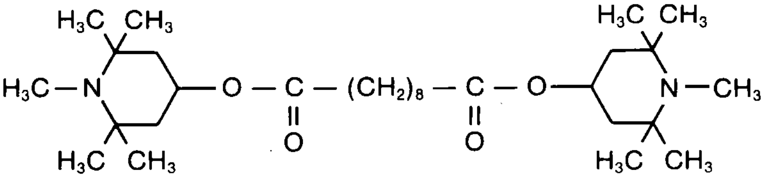

Table 2-1. Commercially Available Stabilizers (Continued)

VI

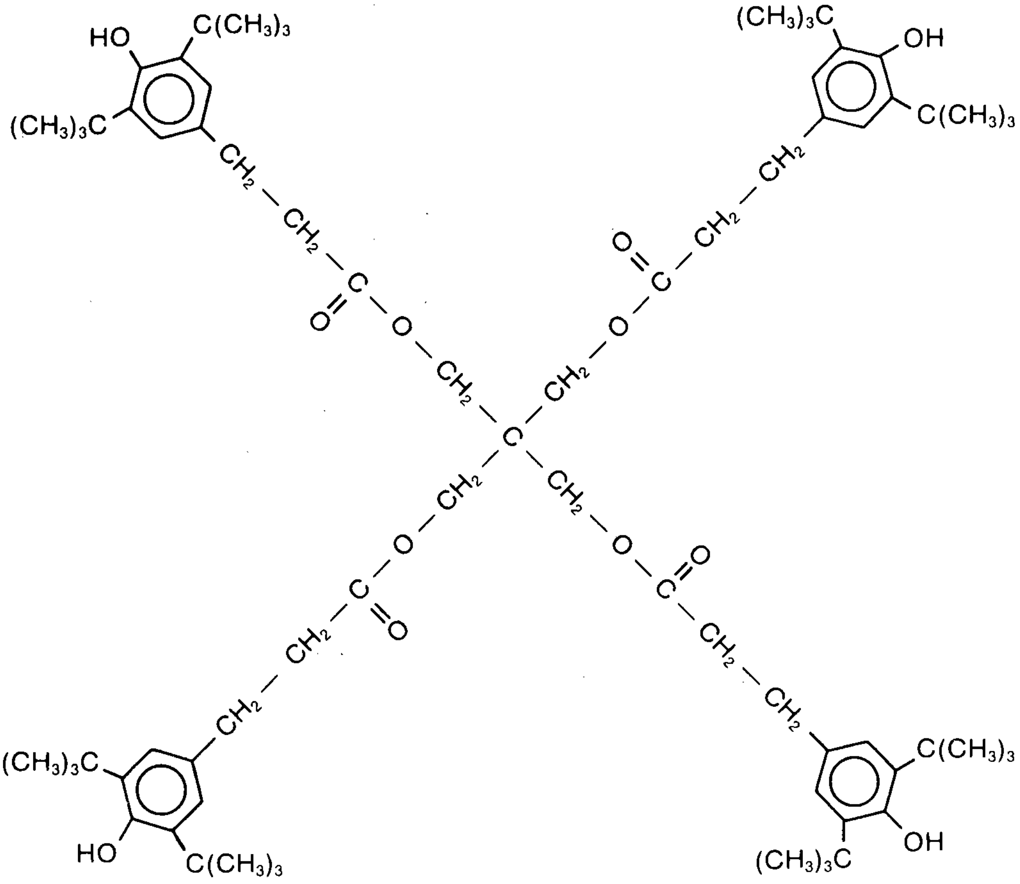

VII

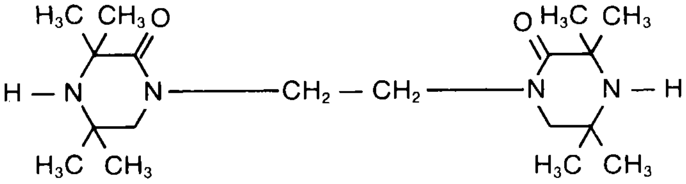

Table 2-1. Commercially Available Stabilizers (Continued)

VIII

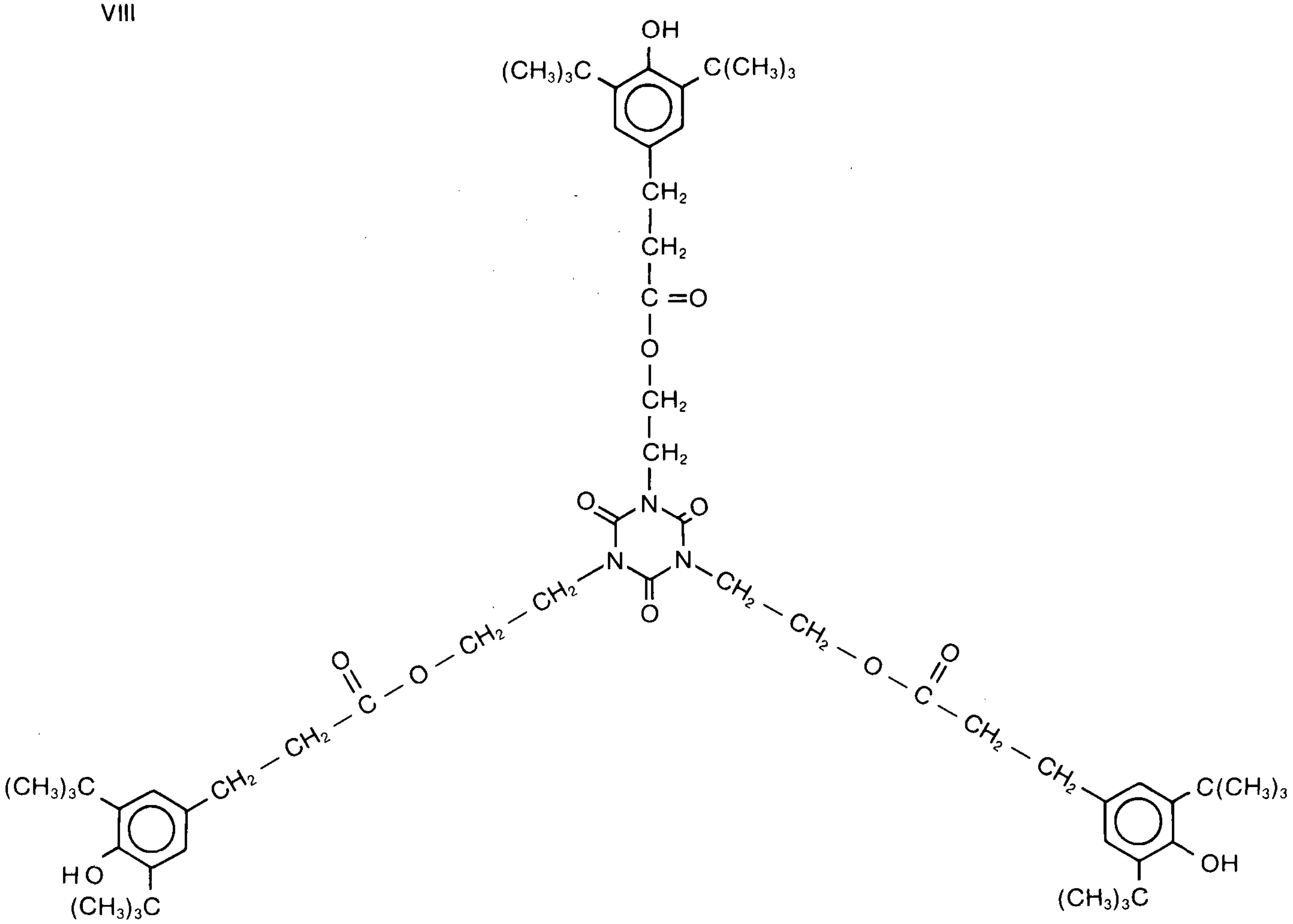

Table 2-1. Commercially Available Stabilizers (Concluded)

IX

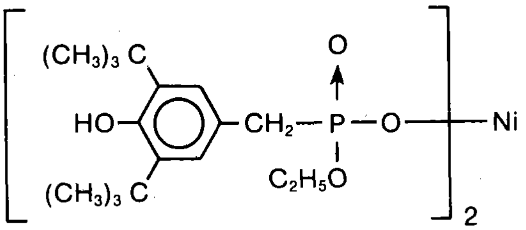

X

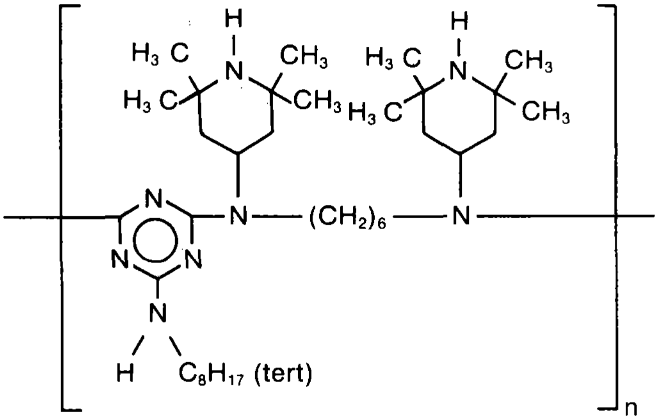

XI Proprietary

Table 2-2. Polymeric SERI Stabilizers

Structure[a]	Product	Mechanism of Action[b]
XII	p-MMA-co-MHB (Table 3-8) Copolymers of methyl methacrylate and 4-methacryloxy-2-hydroxybenzophenone	UVA, CB-D(Q)
XIII	p-MMA-co-2H5V [6] Copolymers of methyl methacrylate and 2-hydroxy-5-vinylphenylbenzotriazole	UVA, CB-D(Q)
XIV	p-MMA-co-DBDH-5V (Table 2-5) Copolymers of methyl methacrylate and 2(2,4-dihydroxy-5-vinylphenyl)1,3-2H-dibenzotriazole	UVA, CB-D(Q)
XV	p-MMA-co-DBDH-5P (Table 2-5) Copolymers of methyl methacrylate and 2(2,4-dihydroxy, 5-isopropenylphenyl) 1,3-2H-dibenzotriazole	UVA, CB-D(Q)
XVI	p-MMA-co-BDHM (Table 2-5) Copolymers of methyl methacrylate and 2(2-hydroxy-4-methacryloxyphenyl)2H-benzotriazole	UVA, CB-D(Q)
XVII	p-MMA-co-MAP (Table 2-6) Copolymers of methyl methacrylate and 4-methacrylamido-2,2,6,6-tetramethyl-piperidine	CB-A/CB-D
XVIII	p-MMA-co-MAP-E (Table 2-6) Copolymers of methyl methacrylate and N-methacryloxyethyl, N'-(2,2,6,6-tetramethyl-4-piperidyl) urea	CB-A/CB-D

[a] Structures tabulated below.

[b] UVA = ultraviolet absorber.
Q = Quencher.
CB-A = Chain-breaking acceptor antioxidant.
CB-D = Chain-breaking donor antioxidant.

Table 2-2. Polymeric SERI Stabilizers (Continued)

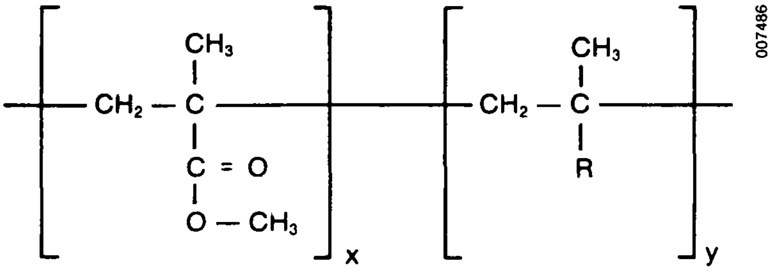

XII

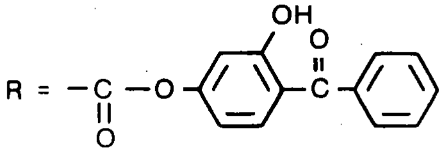

XV

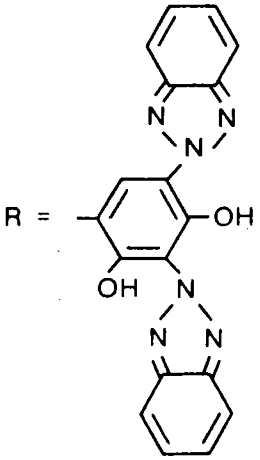

XVI

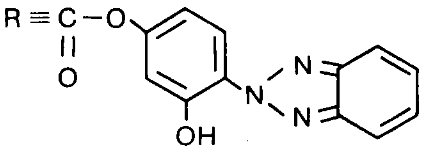

XVII

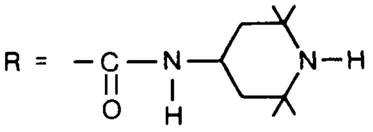

XVIII

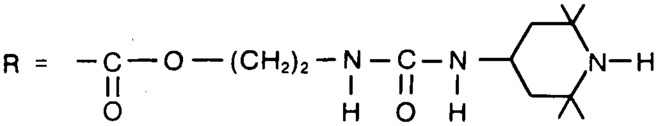

Table 2-2. **Polymeric SERI Stabilizers** (Concluded)

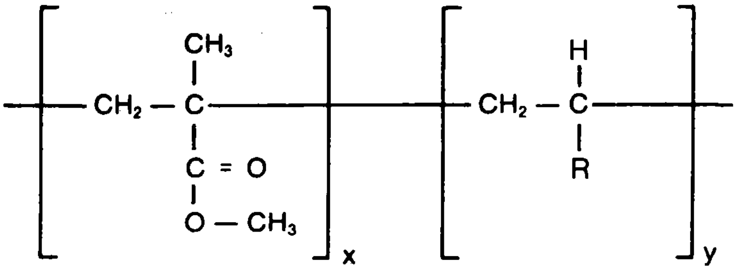

XIII R =

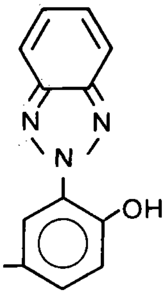

XIV R =

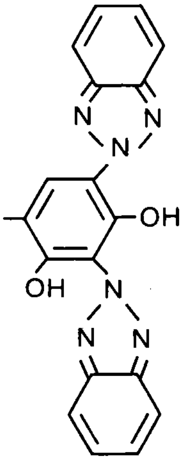

2.5.2 Characterization Measurements

Ultraviolet spectra were measured in dichloromethane solution (Spectrograde, Malinkrodt) with a Hewlett-Packard HP 8450 rapid-scanning spectrometer using 1-cm quartz cuvettes. The instrument covers a 200 to 800 nm range with a resolution capability of 0.5 nm.

^{1}H NMR spectra were recorded on a Joel FX 90Q FT NMR spectrometer using deuterated $CDCl_3$ solutions.

Infrared spectra were recorded on a Nicolet 7199 FTIR spectrometer using KBr pellets.

Micro-analyses (C,H,O,N) were carried out at the Huffman Laboratories, Wheat Ridge, Colo.

Molecular weights and molecular weight distributions (MWD) of the polymers were determined in tetrahydrofuran solution using gel permeation chromatography [Varian Model 5030 liquid chromatograph equipped with a high resolution column (IBM, 8635755)]. A variable wavelength UV detector (Varian Model VUV-10) equipped with a constant temperature bath was used to measure the absorbance of the polymer fractions eluted from the GPC column. These data were plotted and stored as a function of elution time by a Hewlett-Packard Model 3388A integrator. The latter device was programmed in BASIC to calculate the MWD of the samples from the stored calibration data of a set of monodisperse polystyrene and polymethyl methacrylate standards of known molecular weight.

Melting points were determined on a Thomas Hoover capillary melting point apparatus at a heating rate of 2°C/min and are uncorrected.

2.5.3 Procedures

2.5.3.1 Monomer Syntheses

3,5[Di(2H-benzotriazole-2-yl)]2,4-dihydroxyacetophenone (DBAP). The synthesis of the common precursor DBAP for the monomers DBDH-5V and DBDH-5P followed essentially the procedure described by Vogl and his associates [13] using o-nitroaniline and 2,4-dihydroxyacetophenone as starting materials. The first step, the azo dye formation, proceeded smoothly in high yields. However, we encountered some difficulty in isolating the crude product DBAP from the zinc residue after reductive cyclization to form benzotriazole rings. We therefore slightly modified the work-up procedure with purification performed by repeated recrystallization from chloroform/methanol solutions. A yield of 30%-40% was obtained. DBAP has been characterized by its melting point (265°-267°C), IR spectrum (-OH, 3420 cm^{-1}; C=0, 1625 cm^{-1}), and by thin layer chromatography.

2(2,4-Dihydroxy-5-vinylphenyl)1,3-2H-dibenzotriazole (DBDH-5V). The procedure for the preparation of DBDH-5V was essentially the same as that described by Ref. [13]. A solution of zinc borohydride in DME (35 ml of 0.5 M solution) was slowly added by syringe over a period of 8 h to a cooled (-5°C) stirred mixture of DBAP (3.1 g, 8 mmol) in chloroform (100 mL) and DME (50 mL). (Zinc borohydride was prepared by the reaction of sodium borohydride with freshly fused zinc chloride in DME at 0°-5°C). The reaction was followed by TLC. After 18 h, no starting material remained. Dilute HCl was then added to decompose excess zinc borohydride and the mixture was stirred for an additional hour. The organic layer was separated and the aqueous layer was extracted twice with chloroform. The combined organic layers were washed with water and dried over $MgSO_4$ before evaporation of the solvents to a small volume to precipitate a light yellow solid 2[2,4-dihydroxy-5(1-hydroxyethyl)phenyl]1,3-2H-dibenzotriazole (DBDH-5HE) (2.5 g, 78%).

DBDH-5HE (2.0 g, 5.2 mmol) was dissolved in toluene (100 mL) and potassium hydrogen sulphate (1.0 g), and picric acid (~60 mg) was added and the mixture refluxed for 18 h under a nitrogen atmosphere. The toluene was then evaporated and the residue taken up in methylene chloride. The solution was then washed with 5% aq. $NaHCO_3$, then dilute HCl, and twice with water before drying over $MgSO_4$ and evaporation. A crude yield of DBDH-5V (1.7 g, 85%) was precipitated as a light yellow solid, which was recrystallized from chloroform/hexane (1:1), m.p. 194°-195°C.

The ultraviolet absorption data are presented in Table 2-3 and the spectrum in Figure 2-5. IR (KBr): 890 cm^{-1} ($C=CH_2$,C-H bending).

Table 2-3. Ultraviolet Spectral Data for DBDH-5V, DBDH-5P, BDHM, BDHAO, BDHPBr, p-MMA-co-DBDH-5V, and p-MMA-co-DBDH-5P
(Absorption determined in chloroform solutions; concentration: 2×10^{-5} mol/L)

Compound	λmax (nm)	ε (L/mol cm x 10^{-4})
DBDH-5V	327	3.15
p-MMA-co-DBDH-5V		
PG1-35-1	327	3.18
PG1-35-2	327	3.15
PG1-35-3	327	3.03
DBDH-5P	332	3.80
p-MMA-co-DBDH-5P		
PG1-27-1	332	3.93
PG1-27-2	332	4.03
PG1-27-3	332	4.01
BDHM	335	2.50
BDHAO	344	2.72
BDHPBr	345	2.30

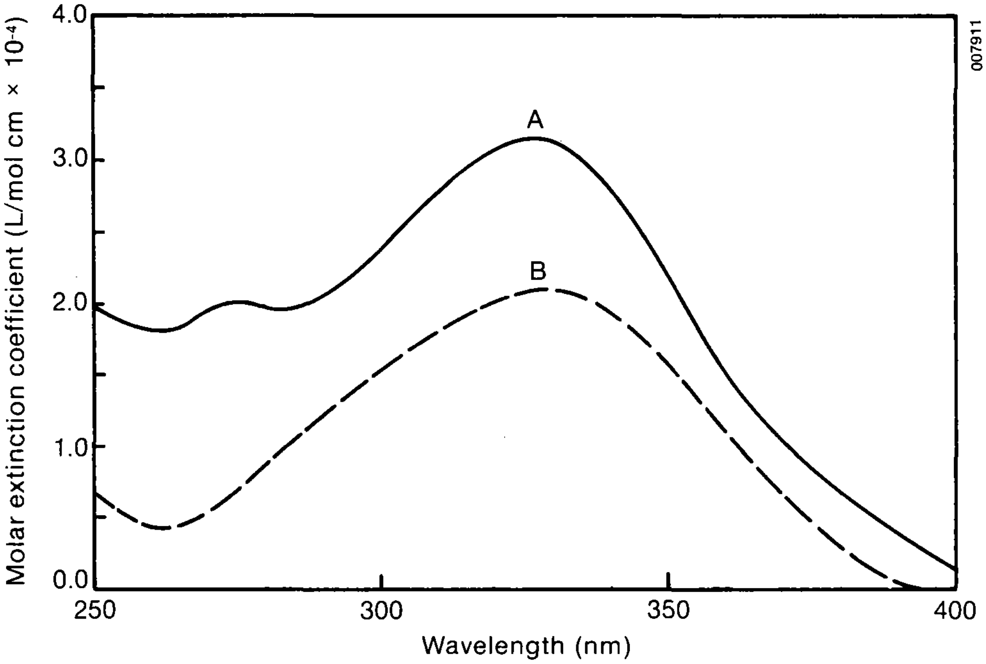

Figure 2-5. Ultraviolet Spectra of DBDH-5V (A) and p-MMA-co-DBDH-5V (B)

2(2,4-Dihydroxy, 5-isopropenylphenyl) 1,3-2H-dibenzotriazole (DBDH-5P). A Grignard reaction was prepared by adding MeI (17 g, 8 ml) in THF (15 ml) to magnesium turnings (3.0 g). DBAP (5.0 g, 13 mmol) was dissolved in 250 mL toluene (dried by distillation off NaOH) and THF (100 mL) (distilled off $LiAlH_4$) and added dropwise to the Grignard mixture. The mixture was stirred for an additional 4 h after complete addition, then treated with a mixture of ammonium chloride (50 g), conc. H_2SO_4 (10 mL) in water (150 mL). The organic layer was separated and the aqueous layer extracted with ether (3X). The combined organic solutions were dried over $MgSO_4$ and evaporated to leave a light pink solid. This solid was placed in a vacuum oven at ~100°C for 5 h and the resulting reddish solid recrystallized from a mixture of methylene chloride-petroleum ether to give 3.5 g of DBDH-5P, m.p. 174°-176°C.

The ultraviolet absorption data are presented in Table 2-3 and the spectrum in Figure 2-6. IR (KBr): 890^{-1}cm ($C=CH_2$, C-H bending).

^1H NMR ($CDCl_3$): δ = 7.6-6.5 (Bzt, phenolic); 4.8 ($=CH_2$,2H); 1.6 ($-CH_3$,3H).

2(2,4-Dihydroxyphenyl)2H-benzotriazole (BDH). The synthesis of the common precursor BDH for the monomers BDHM, BDHAO, and BDHPBr followed essentially the procedure described by Vogl and his associates [14] using o-nitroaniline and resorcinol as starting materials. BDH (50% yield) was recrystallized from ethanol/water (1/1) and gave white needles, m.p. 199°-200°C.

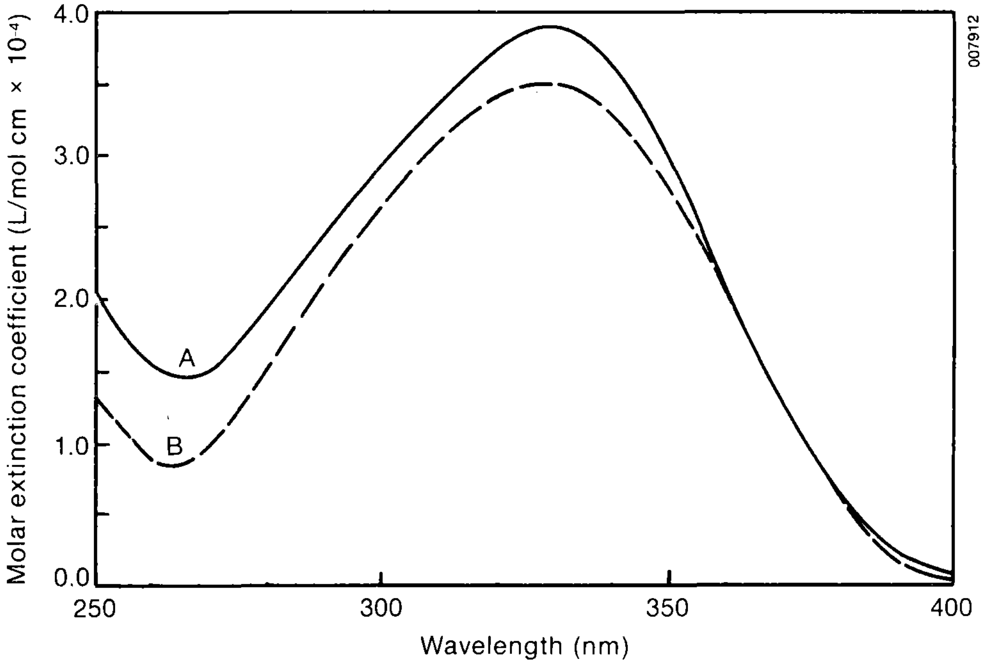

Figure 2-6. Ultraviolet Spectra of DBDH-5P (A) and p-MMA-co-DBDH-5P (B)

2(2-Hydroxy-4-methacryloxyphenyl)2H-benzotriazole (BDHM). The synthesis of BDHM followed essentially the same procedure as described in Ref. [14].

The ultraviolet absorption data are presented in Table 2-3 and the spectrum in Figure 3-43. IR (KBr): 1740 cm^{-1} (C=O stretching).

^1H NMR ($CDCl_3$): δ = 8.5-6.7 (Bzt, phenolic); 5.8 and 6.4 (=CH_2, 2H); 2.1 (-CH_3, 3H).

2(2-Hydroxy-4-allyloxyphenyl)2H-benzotriazole (BDHAO). BDH (5g, 16.9 mmol) was dissolved in DME (20 mL) and the solution added dropwise to a stirred slurry of allyl bromide (60 mmol, 7.25 g, 5.22 mL) and sodium hydride (20 mmol, 0.48 g, 0.6 g of 80% suspension in oil washed out with dry hexane). After 48 h of stirring at room temperature, TLC showed only traces of starting material. The solution was then diluted with chloroform and acidified with dilute HCl. The organic layer was separated and washed with water (2X) then dried over $MgSO_4$ and concentrated before addition of methanol to precipitate a cream-colored solid which was filtered and dried (3.2 g, 55%).

The ultraviolet absorption data are presented in Table 2-3 and the spectrum in Figure 2-7.

2[2-Hydroxy-4-(3-bromopropoxy)phenyl] 2H-benzotriazole (BDHPBr). BDH (4.4 g, 19.38 mmol) was dissolved in 50 mL DME and potassium-t-butoxide (20 mmol, 2.24 g) and dibromopropane (0.1 mol, 20.1 g, 10.1 mL) added. The solution was refluxed for 4 h then cooled and diluted with chloroform. The organic solution was washed with water before

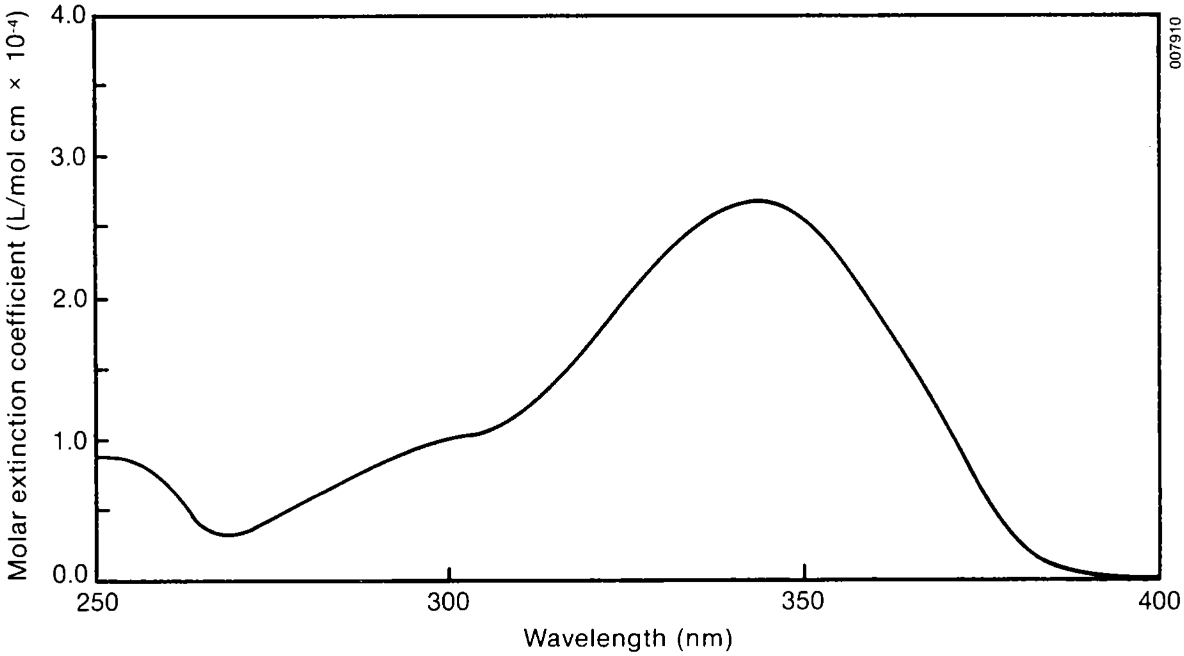

Figure 2-7. Ultraviolet Spectrum of BDHAO

drying ($MgSO_4$) and evaporation of the solvent to a small volume. Ethanol was added to precipitate a white solid, which was filtered and recrystallized from $CHCl_3$/EtOH. Yield 4.0 g (61%), m.p. 116°-118°C.

The ultraviolet absorption data are presented in Table 2-3 and the spectrum in Figure 3-45.

4-Methacrylamido-2,2,6,6-tetramethylpiperidine (MAP). The synthesis and characterization of MAP followed essentially the same procedure as described earlier [6]. A solution of methacryloylchloride (5.2 g) in dried benzene (50 mL) was added dropwise to a cooled (0°-5°C) stirred mixture of 4- amino-2,2,6,6-tetramethylpiperidine (7.8 g), triethylamine (2.7 g), and dried benzene (150 mL). After the addition, the reaction mixture was stirred continually for approximately 4 h at room temperature. The cloudy reaction mixture was washed with a 5% aqueous sodium hydroxide solution and then water, and dried over anhydrous potassium carbonate. After the benzene was removed by vacuum distillation, the remaining product was recrystallized from hexane and stored in the refrigerator. White needle crystals (m.p. 119°-120°C) were obtained with a yield of 40.2%.

4-Methacryloxy-2,2,6,6-tetramethylpiperidine (MOP). The synthesis of MOP followed essentially the same procedure as described for the synthesis of MAP. A solution of methacryloylchloride (5.2 g) in dried benzene (70 mL) was added to a cooled, stirred mixture of 4-hydroxy-2,2,6,6-tetramethylpiperidine (7.8 g), triethylamine (15 g), and dried benzene (100 mL). The reaction mixture was then stirred continually for approximately 6 h at 40°-45°C. The precipitate formed (triethylamine hydrochloride) was filtered out of the reaction mixture, and the filtrate was washed with saturated sodium bicarbonate solution and then water, and dried over anhydrous magnesium sulfate. After the benzene was removed by vacuum distillation, an oily substance remained, which was distilled at 75°C and 0.5 mm Hg. The colorless distillate crystallized after cooling to room temperature and was further purified by vacuum sublimation (15% yield).

N-methacryloxyethyl, N'-(2,2,6,6-tetramethyl-4-piperidyl)urea (MAP-E). Isocyanatoethylmethacrylate (IEM) (5 mL, 35.3 mmol) was dissolved in dried toluene (150 mL) and the solution added dropwise under nitrogen to a stirred solution of 4-amino-2,2,6,6-tetramethylpiperidine (7 mL, 40.9 mmol) in toluene (150 mL). The reaction mixture was stirred for 2 h at room temperature and then for 4 h at 60°C. After evaporation of the solvent to a small volume, the viscous solution was left standing overnight during which time a solid crystallized. This solid was recrystallized from a mixture of toluene and petroleum ether to give white needle crystals, m.p. 68°C.

IR(KBr): 3340 (NH), 1720 (C=O, ester), 1660 (NH-CO-NH, urea), 1630 (C=C), and 1560 (NH bending) cm^{-1}.

N-methacryloxyethyl, 0-(2,2,6,6-tetramethyl-4-piperidyl) urethane (MOP-E). IEM (5 mL) was dissolved in dried toluene (100 mL) and the solution added dropwise under nitrogen to a stirred solution of 4-hydroxy-2,2, 6,6-tetramethylpiperidine (5.55 g) and dibutyltindilaurate (1 mL) in toluene (200 mL). The reaction mixture was stirred for 1 h at room temperature and then for 18 h at 60°C. After evaporation of the solvent to a small volume, a clear yellow liquid remained that crystallized upon standing. The solid was recrystallized from cyclohexane to give 7.1 g (70%) MOP-E.

IR(KBr):3340 (NH), 1720 (C=O, ester), 1700 (O-CO-N, urethane), 1640 (C=C), and 1530 (NH bending) cm^{-1}.

^{1}H NMR ($CDCl_3$):δ=6.14 (s,H^a); 5.59 (s,H^b); 4.5 (m,H^c); 4.25 (m,H^d); 3.53 (m,H^e); 1.95 (s,CH_3^f); 1.86 (dd,H^g); 1.38 (s,H^h); 1.24 and 1.11 (2s,$CH_3^i$and CH_3^j) 0.99 (m, H^k); 0.84 (s,NH^l). Intensity ratios are: 1:1: 1:2: 2:3: 2:1: 6:6: 2:1. [s = singlet, d = doublet, dd = doublet of a doublet, m = multiplet).

2.5.3.2 Polymerizations

Polymethylmethacrylate-co-4-methacryloxy-2-hydroxybenzophenone (p-MMA-co-MHB). MHB was copolymerized with MMA with AIBN as initiator (Table 2-4). Typical copolymerization experiments were carried out as follows: A solution of MHB (1.5 g), MMA (9.4 g), and AIBN (0.25 g) in acetonitrile (30 mL) was placed in a 250-mL round bottom flask, immersed in a liquid nitrogen Dewar bottle, and degassed. The freeze-degassing was repeated twice, and nitrogen gas was introduced. The reaction vessel was heated to 65°-70°C under a positive pressure of nitrogen, and the polymerizations were carried out for an appropriate polymerization time (16-20 h). The contents of the reaction flask were then precipitated slowly under stirring into methanol and collected by filtration. The polymer was further purified by dissolution in dichloromethane followed by precipitation into methanol. The purification procedure was repeated, and the yellowish, powdery polymer was dried at room temperature under vacuum for 48 h, yield was 79%. A representative UV spectrum is reproduced in Figure 2-8.

Polymethylmethacrylate-co-2(2,4-dihydroxy, 5-isopropenylphenyl) 1,3-2H-dibenzotriazole (p-MMA-co-DBDH-5P). DBDH-5P was copolymerized with MMA with AIBN as initiator. Typical copolymerization experiments were carried out as follows: A 100 ml pear-shaped flask equipped with magnetic stirrer and side-arm with stopcock was charged with DBDH-5P (0.5 g, 1.3 mmol) and recrystallized AIBN (50 mg). The flask was capped with a rubber septum and purged with nitrogen. Toluene (10 mL) and DMAc (5 mL) was added to dissolve the solid completely and methylmethyacrylate (10.1 mL, 9.5 g of freshly distilled MMA) was then added via a syringe. After three freeze-thaw cycles at ~0.05 mmHg pressure to degas the homogeneous polymerization mixture, the flask was placed in an oil bath at ~60°-65°C under a positive pressure of dry nitrogen. The solution was left stirring for 48 h at an average temperature of 65°-68°C. The polymer solution was then dissolved in chloroform (100 mL) and added dropwise to a rapidly stirred beaker of methanol (600 mL) to precipitate a white fluffy polymer. The sample was dried overnight in a vacuum oven. The amount of materials used for the polymerizations and the results of all polymerizations are presented in Table 2-5. The ultraviolet absorption data are presented in Table 2-3.

Polymethylmethacrylate-co-2(2,4-dihydroxy-5-vinylphenyl) 1,3-2H-dibenzotriazole (p-MMA-co-DBDH-5V). DBDH-5V was copolymerized with MMA with AIBN as initiator. The procedure was essentially the same as that described for the copolymerization of DBDH-5P. The amount of materials used for the polymerization and the results of all polymerizations are presented in Table 2-5. The ultraviolet absorption data are presented in Table 2-3.

Polymethylmethacrylate-co-2(2-hydroxy-4-methacryloxyphenyl) 2H-benzotriazole (p-MMA-co-BDHM). BDHM was copolymerized with MMA with AIBN as initiator. Typical copolymerization experiments were carried out as follows: BDHM, MMA, and AIBN were dissolved in DMAc and placed in Schlenk tubes sealed with a rubber septum. After three freeze-thaw cycles, the tubes were placed in an oil bath with a positive pressure of nitrogen at 65°-70°C for 48 h with stirring. A viscous liquid/gel formed after 24 h. The contents of the tube was then dissolved in chloroform and added dropwise to a rapidly

Table 2-4. Reaction Parameters for the Copolymerization of Methylmethacrylate (MMA) with 4-Methacryloxy-2-hydroxybenzophenone (MHB) at 65°-70°C

Sample #	MMA		MHB		Initiator (AIBN)		Solvent	Time (h)	Conversion (%)
	g	mol %	g	mol %	g	mol %			
MS1-13-2	9.5	99.0	0.29	1.0	0.003[a]	0.01[a]	benzene	16	--
MS1-11-5	23.4	93.0	4.0	6.0	0.50	1.0	benzene	20	--
MS1-30-1	9.4	94.6	1.5	5.3	0.01	0.03	benzene	14	--
MS1-30-2	9.4	94.6	1.5	5.3	0.03	0.1	benzene	1	--
MS1-35-1	9.4	93.2	1.5	5.3	0.25	1.5	acetonitrile	20	79
MS1-35-2	9.4	93.8	1.5	5.3	0.15	0.9	acetonitrile	20	76
MS1-35-3	9.4	94.1	1.5	5.3	0.10	0.6	acetonitrile	20	70
MS1-49-1	9.4	98.0	0.1	0.4	0.25	1.6	acetonitrile	20	69
MS1-49-2	9.4	96.6	0.5	1.8	0.25	1.6	acetonitrile	20	66
MS1-49-3	9.4	94.9	1.0	3.6	0.25	1.5	acetonitrile	20	61
MS1-49-4	9.4	90.0	2.5	8.5	0.25	1.5	acetonitrile	20	77

[a] Dibenzoylperoxide

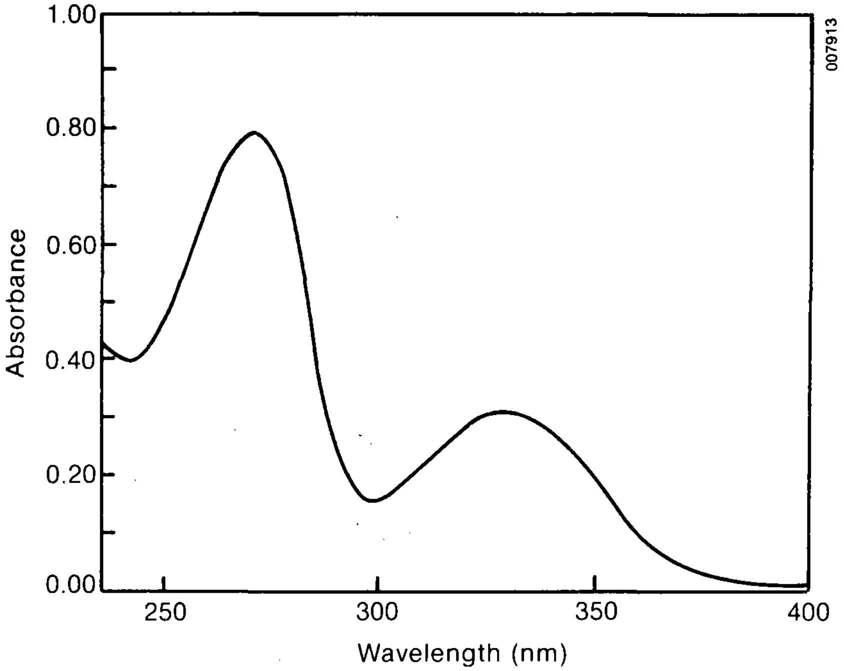

Figure 2-8. Ultraviolet Spectrum of p-MMA-co-MHB

stirred beaker of methanol to precipitate a white solid polymer. The polymer was further purified by redissolving and reprecipitating it once again. The sample was dried for 24 h at 50°C in a vacuum oven (0.1 mmHg). The amount of materials used for the polymerizations are presented in Table 2-5. The ultraviolet absorption data are presented in Table 2-3.

Polymethylmethacrylate-co-4-methacrylamido-2,2,6,6-tetramethylpiperidine (p-MMA-co-MAP). A radical copolymerization was performed under similar conditions as described for the p-MMA-co-MHB. However, hexane was used as precipitant. The amount of materials used for the polymerization and the results of all polymerizations are presented in Table 2-6.

Polymethylmethacrylate-co-N-methacryloxyethyl, N'-(2,2,6,6-tetramethyl-4-piperidyl) urea (p-MMA-co-MAP-E). MAP-E was copolymerized with MMA with AIBN as initiator. The procedure was essentially the same as that described for the copolymerization of MHB except for toluene as solvent and the polymerization time/temperature: 4 h at 70°C followed by 4 h at 100°C. The amount of materials used for the polymerization and the results of all polymerizations are presented in Table 2-6.

Polymethylmethacrylate by Group Transfer Polymerization (GTP). GTP reactions were carried out under a positive dry argon atmosphere at room temperature using glassware previously dried at 175°C for 24 h. THF (dried by distillation from $LiAlH_4$) was used as the solvent with 1-methoxy-1-(trimethylsiloxy)2-methyl-1-propene (Aldrich) as the initiator and tris(dimethylamino) sulphonium difluoride ($TASHF_2$) (Aldrich) as the catalyst. MMA (Aldrich) was washed with sodium hydroxide solution to remove the inhibitor then dried by stirring over CaH_2 powder for 24 h prior to distillation under reduced pressure before use.

Polymerizations were carried out by dropwise addition of the monomer to a stirred solution of the initiator and catalyst in THF. The formed polymers were isolated by

Table 2-5. **Reaction Parameters for the Copolymerization of Methylmethacrylate (MMA) with DBDH-5P, DBDH-5V, and BDHM and Resulting Copolymer Composition** (Polymerization conditions: temperature: 60°-65°C; time: 48 h; initiator: AIBN, 0.3 mol%)

Sample #	M_1 (MMA)		M_2					Solvent		Conversion	Composition (M_2)	
	g	mmol	Type	g	wt %	mmol	mol%	type	mL	(%)	wt%	mol%
PG1-27-1	9.5	95	DBDH-5P	0.50	5	1.3	1.3	DMAc	5	92	4.5	1.2
PG1-27-2	4.5	45	DBDH-5P	0.50	10	1.3	2.8	DMAc	5	90	8.0	2.2
PG1-27-3	4.0	40	DBDH-5P	1.00	20	2.6	6.1	DMAc	7	98	15.0	4.6
PG1-35-1	4.75	47.5	DBDH-5V	0.25	5	0.7	1.4	DMAc Toluene	5 5	76	3.3	0.9
PG1-35-2	4.5	45	DBDH-5V	0.50	10	1.4	2.9	DMAc Toluene	5 5	72	6.7	1.9
PG1-35-3	4.0	40	DBDH-5V	1.00	20	2.7	6.3	DMAc Toluene	5 5	72	12.6	4.0
PG1-59-1	3.99	40	BDHM	0.74	15.6	2.5	5.9	DMAc Toluene	5 4	89	12.4	4.7
PG1-59-2	3.78	38	BDHM	1.48	28.1	5.0	11.9	DMAc Toluene	9 4	87	21.7	9.2
PG1-59-3	3.36	34	BDHM	2.95	46.7	10.0	22.7	DMAc Toluene	12 4	80	30.4	14.8

Table 2-6. Reaction Parameters for the Copolymerization of Methyl Methacrylate (MMA) with MAP and MAP-E and Resulting Copolymer Composition

Sample #	M_1 (MMA)		Type	M_2				Initiator (AIBN)		Solvent	Conversion (%)	Composition (M_2)	
	g	mol %		g	wt %	mmol	mol%	g	mol%			wt%	mol%
MS1-48-1	9.4	94	MAP	1.5	13.8	6.7	6.7	0.15	0.90	benzene	53	10.2	4.8
MS1-50-1	9.4	94	MAP	0.5	5.1	2.2	2.3	0.15	0.95	benzene	56	5.4	2.4
MS1-81-1	9.4	94	MAP-E	0.1	1.1	0.3	0.3	0.10	0.6	toluene	69	c	c
MS1-81-2	9.4	94	MAP-E	0.6	6.0	1.8	1.9	0.10	0.6	toluene	62	c	c
MS1-81-3	9.4	94	MAP-E	1.1	10.5	3.5	3.6	0.10	0.6	toluene	54	c	c
MS1-81-4	9.4	94	MAP-E	2.7	22.3	8.7	8.6	0.10	0.6	toluene	25[a]	c	c
MS1-81-5	9.4	94	MAP-E	5.5	36.9	17.7	15.8	0.10	0.5	toluene	b	--	--

[a] Conversion to soluble copolymer, rest cross-linked.
[b] Cross-linked.
[c] Analysis in progress.

precipitation into methanol or hexane and the procedure repeated from a chlorinated solvent.

2.6 Outdoor and Simulated Weather Tests

After initial reflectance measurements, mirrors are exposed to environmental degradation using three techniques. Weather-Ometers* and QUV‡ accelerated weathering devices provide data for comparison with data from real-time, outdoor exposure (racks facing south with 45° tilt).

The Weather-Ometer specimens, as illustrated in Figure 1-1, are being subjected to UV or no UV, 60°C, and air at 80% relative humidity. A xenon arc lamp with filter cutoff to match the terrestrial solar spectrum supplies the UV light. The QUV test cyclically uses 4 h of UV exposure (from fluorescent lamps) at 60°C and 4 h of condensed water exposure at 40°C (ASTM, G53-77). The accelerated weathering devices are used for comparison only; it is not possible to state, *a priori*, which device provides the harsher test for any particular mirror material or how the accelerated tests compare with outdoor weathering. The spectral distribution for the irradiation in the three weathering modes is given in Figure 2-9.

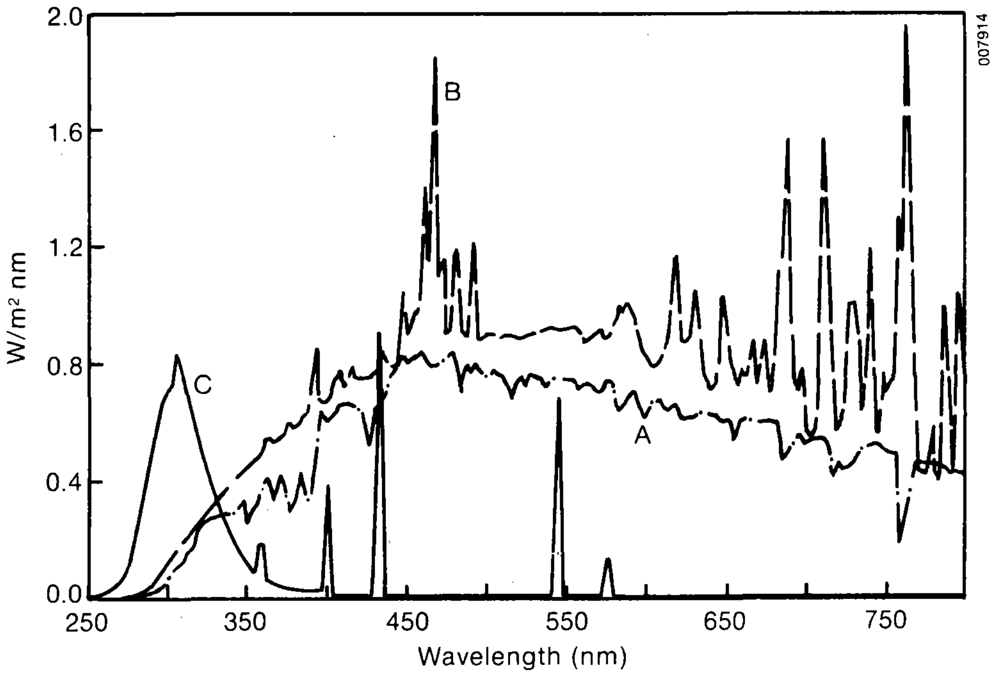

Figure 2-9. **A Comparison of Relative Spectral Energy Distribution of Sunlight (A), WOM (B), and QUV (C) Artificial Light Sources**

---

*Weather-Ometer is a registered trademark of the Atlas Electric Devices Company, Chicago, Ill.

‡QUV is a registered trademark of the Q-Panel Company, Cleveland, Ohio.

3.0 RESULTS AND DISCUSSION

3.1 Initial Optical Performance

The Specularometer has been used to demonstrate that silvered polymers can attain specular reflectances in excess of our long-range goals. This has been demonstrated for membrane configurations and for mirrors mounted on stiff substrates.

3.1.1 Transparent and Metallized Polymers, Transmission and Reflection

When the polymer sheets or polymer mirrors mounted on stiff substrates were mounted onto the sample holder, great care had to be taken because these samples bend easily. This caused some variations in the results; however, poor specularity of these samples could always be explained with curvature that was measured with an interferometer that was adjacent to the Specularometer. In this way the sample could be mounted onto the sample holder and the curvature of the front surface or the wedge angle for nonparallel surfaces could be determined interferometrically and, without moving the sample, specularity data could be taken. For transparent samples, the secondary reflection could be suppressed by a factor of < 0.02 by changing the optical uniformity of the second surface when it was taped with 3M Scotch tape.

Various clear samples, including glass and different polymeric materials, have been evaluated in transmission with the Specularometer set to its highest resolution (beam divergence about 0.15 mrad). In no instance could an appreciable beam spread be found, which means that the transmission function of these samples is beyond the resolution limit of the instrument.

Transparent cast polymer sheet materials and one type of extruded polymer film, which is the basic polymer material for the ECP 300 reflector that is manufactured by the 3M Company, have been investigated in reflectance. We measured the specularity of each of these transparent samples and compared the data with the specularity data of the silvered material. We silvered the polymer sheets with a sputtering technique in our laboratories, and compared the bare ECP 300 film with the silvered ECP 300 reflector material as supplied by the 3M Company. For each material, the specularity before and after silvering was essentially the same.

For example, in Figure 3-1a, the specularity data from the front and back surfaces of an Acrylite (CYRO Industries) sample (thickness 1.7 mm) are shown where no significant curvature could be detected with the interferometer. Good specularity can be seen, which is only possible when the sample is very flat (at a beam diameter of 10 mm, a curvature $1/R$ of 10^{-2} m^{-1} causes a 0.2 mrad beam spread). The beam divergence of the instrument was adjusted in both cases to 0.4 mrad to have a higher light throughput, to achieve a sufficient signal-to-noise level for reflected signals from the transparent material.

Figure 3-1b shows the specularity of the same sample after silvering. We measured the sample as a second-surface mirror, hence, one can see two side reflections. It is helpful that the different reflections due to the nonparallel surfaces could be resolved because a beam spread due to overlapping reflections can mislead data evaluation.

These data show that polymer surfaces are smooth enough to be used for mirrors of optical quality and that the metallization does not influence the optical performance. The main limitation is the lack of stiffness of the material so that it bends and loses surface figure, which strongly degrades the specularity.

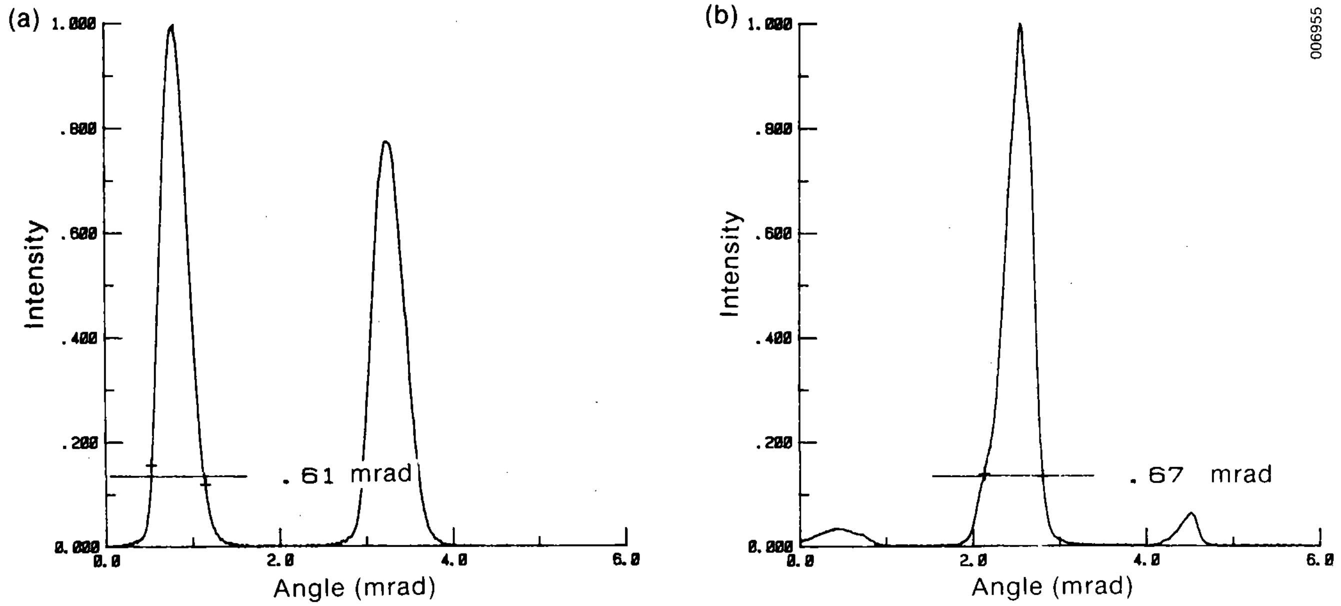

Figure 3-1. **Specularly Reflected Beam from a) the First and Second Surface of the Transparent Polymer Sheet Before Silvering and b) After Silvering Measured as a Second Surface Mirror** (Wavelength 492 nm, angle of incidence 20°)

3.1.2 Silvered Polymer Films on Various Substrates

The optical performance of silvered, thin polymer films has been determined when the polymers are applied to flat float glass substrates, to bare or painted aluminum substrates with an adhesive, or suspended as membranes. We have used glass substrates because the specularity of float glass is excellent and glass allows us to approach the intrinsic specularity of the silvered polymer. In practice, substrates such as aluminum or stainless steel would be used and a paint layer applied to the metal may smooth it to improve mirror optics.

The 3M Company supplied us with a series of 32 samples, where 10 silvered polymer samples were mounted onto float glass, bare aluminum sheet, and painted aluminum sheet, respectively. Also two 1/2 in. thick aluminum substrates were obtained each with a #2 micro finish; one was covered with silvered polymer and the other was left bare aluminum.

The silvered polymer samples (ECP 300) mounted on float glass had excellent specularity (a_{90} values all near 1 mrad). One sample was characterized more completely and specularity measurements were performed at three different wavelengths (400 nm, 600 nm, 1000 nm), at three different angles of incidence (20°, 45°, 60°), and for three different beam diameters of 8, 10, and 12 mm. The beam diameter was varied because earlier experiments showed that the specularity may vary with the size of the illuminated area on the sample. When the angle of incidence is changed, a different size of the illuminated area results but this is partially compensated for by changing the beam diameter. The results are shown in Figure 3-2 for fixed angle of incidence (20°), and beam diameter

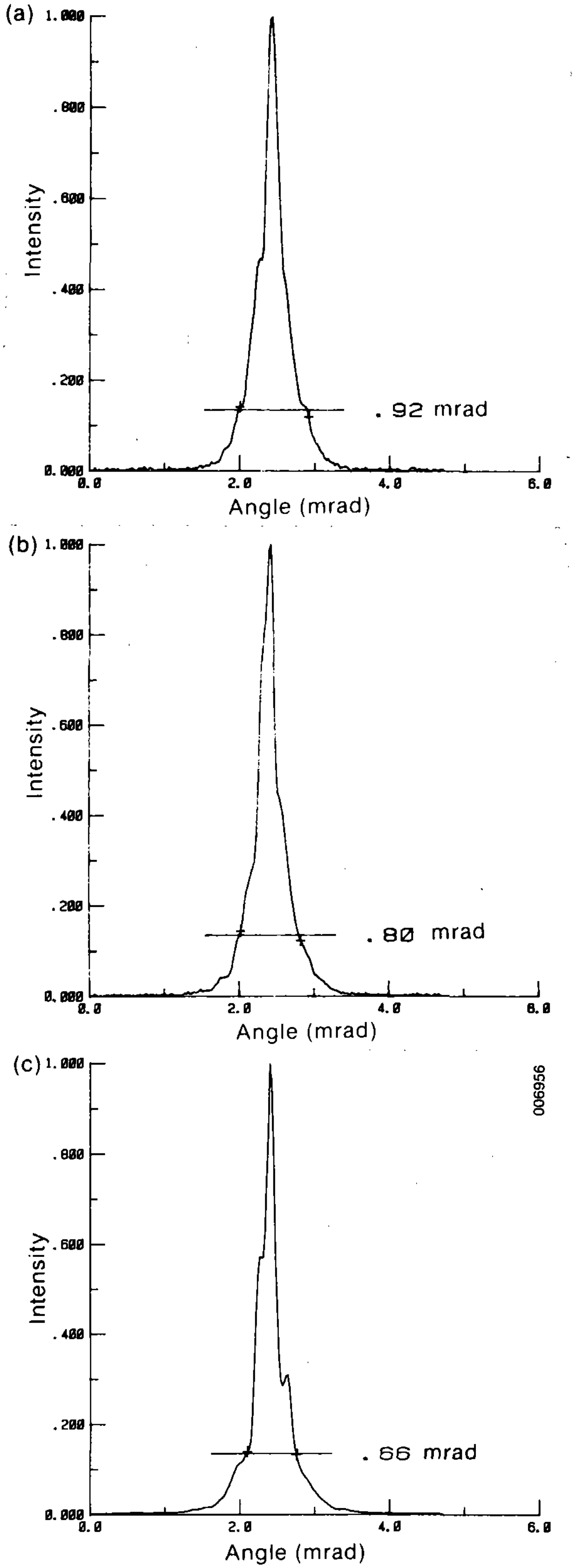

Figure 3-2. Specularly Reflected Beam from a Silvered Polymer Film Mounted on a Glass Substrate, for Fixed Angle of Incidence (20°) and Beam Diameter (10 mm), at a) 400 nm, b) 600 nm, and c) 1000 nm

(10 mm) and for three wavelengths. As Figure 3-2 shows, the a_{90} values or specularity are insensitive to wavelengths from 400 to 1000 nm.

Table 3-1 lists the beam width of the reflected beam (a_{90}-value) as a matrix determined by wavelength, by angle of incidence, and for three partially compensating beam areas at each angle of incidence. Also, the absolute reflectance (ρ) at 12 mrad is tabulated. At 400 nm, ρ is low (80%) because ultraviolet absorbers are intentionally added to the polymer so the specular reflectance is decreased but the specularity is not changed significantly. For practical purposes, the data of Table 3-1 show that mirror specularity is insensitive to wavelength, angle of incidence, and illuminated area. However, the measurements do show a slight trend with illuminated area. The diagrams in Figure 3-3 show the measured beam divergences for each wavelength as a function of the illuminated area on the sample independent of the angle of incidence. A linear regression line for each wavelength is included in the graph as well as the equation and correlation factor (R^2). For this particular sample, it was found that with increasing wavelength, the y axis intercept decreases and the slope increases. The intercept may be interpreted as the local specularity (zero illuminated area), whereas the slope indicates the sensitivity to the size of the illuminated area.

The main result is that silvered polymer can be used as a solar mirror with excellent optical performance when a good substrate is provided (like float glass). The variation in the a_{90} value over the wavelength range from 400 nm to 1000 nm and angles of incidence between 20° and 60° is relatively small.

We have compared silvered polymers mounted on float glass with the silvered polymers mounted on aluminum substrates and as stretched membranes without a substrate. The results of the measurements performed on the ECP 300 mounted

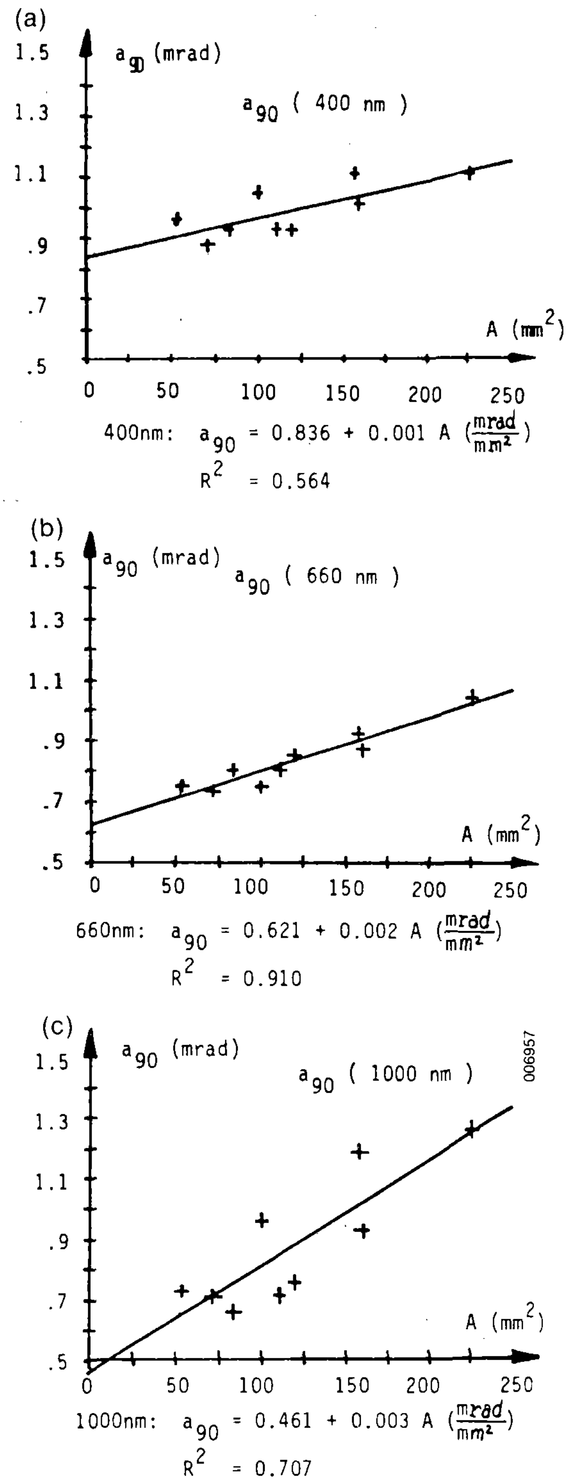

Figure 3-3. Beam Divergences from a Silvered Polymer Film Mounted on a Glass Substrate as a Function of Illuminated Area for a Fixed 20° Angle of Incidence: a) 400 nm, b) 600 nm, c) 1000 nm (see text)

on the aluminum sheets were quite variable since the curvature of the substrate varied from sample to sample. In contrast to the excellent specularity for silvered polymer mounted on glass (Figure 3-2), a typical result for the same type silvered polymer mounted on painted aluminum sheet is given in Figure 3-4. Table 3-2 contains the a_{90} values measured for the series of 30 samples on three different substrates as described above. The influence of the substrate on the specularity is evident.

The structure in the reflected beam shape (Figure 3-4) may be controlled by the long wavelengths of the aluminum substrate surface structure complemented by facets of relatively flat regions. The substrate structure is dominant so that painting has little effect on specularity. The results

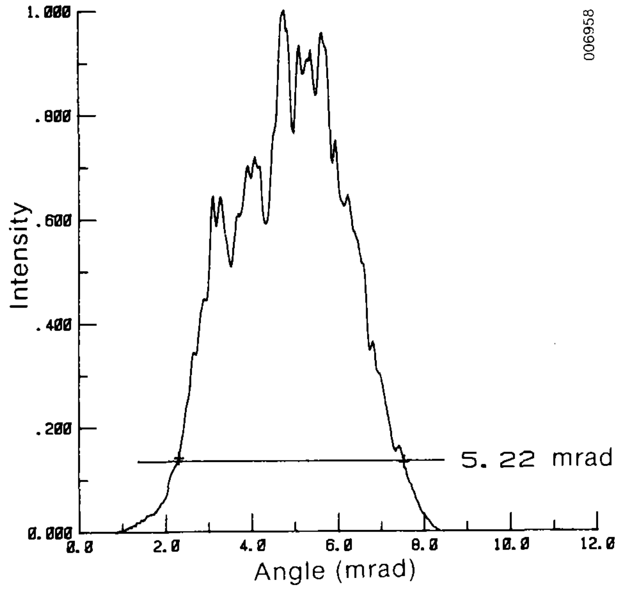

Figure 3-4. Specularly Reflected Beam from a Silvered Polymer Film Mounted on a Painted Aluminum Substrate (Angle of Incidence 20°, Wavelength 630 nm)

Table 3-1. Beam Widths Measured on One Sample Under Varying Conditions

	θ (deg)	20			45			60		
	A (mm^2)	54	84	120	71	111	160	100	158	226
λ (nm)	ρ(12 mrad) (%)									
400	80	0.96	0.92	0.92	0.87	0.92	1.01	1.04	1.11	1.11
660	96	0.75	0.80	0.85	0.73	0.80	0.87	0.75	0.92	1.04
1000	99	0.73	0.66	0.75	0.71	0.71	0.92	0.96	1.18	1.25

Table 3-2. Beam Widths of 30 Different Samples, Measured at 660 nm, 20° Angle of Incidence, and 10-mm Beam Diameter

	Sample No.										
Substrate	1	2	3	4	5	6	7	8	9	10	$a_{90} \pm \sigma_a$
Float Glass	1.04	1.06	1.25	1.18	1.15	1.25	1.04	1.13	1.06	1.01	1.12±0.09
Painted Al	6.30	4.61	4.48	5.22	4.50	3.34	3.34	4.02	3.60	4.12	4.35±0.91
Bare Al	8.54	10.26	10.33	10.00	8.38	4.00	8.89	7.22	4.40	5.65	7.77±2.36

for metal substrates are contrasted to those for glass substrates where substrate flatness is sufficient so that specularity at the 1-mrad level is limited by the polymer/silver/adhesive construction and not by the substrate.

Figure 3-5 shows the specularity typical for reflection from silvered and unsilvered polymers stretched as membrane mirrors. In this example, the specularity is comparable, but perhaps slightly less good than that obtained using a glass substrate. The specularity is superior to that using aluminum or painted aluminum substrates. The results using membrane mirrors or mirrors mounted on glass substrates demonstrate that a specularity of at least 1 mrad is attainable. In either case, the intrinsic specularity of silvered polymers may not have been reached. The adhesive may limit performance when the mirror is mounted on glass and the membrane test fixture may allow sufficient residual membrane curvature to limit membrane mirror performance.

Measurements on a thick (1/2 in.) polished aluminum sample and a similar sample covered with silvered polymer are represented in Figure 3-6 and Figure 3-7, respectively. Both substrates were machined the same way so that a similar topography of both substrates can be expected. The specularity was improved when the ECP 300 film was mounted onto one of these samples (Figure 3-7). The decrease in surface roughness suggests that the mounted film does not follow the micro-topography of the substrate.

3.1.3 Correlation Between Surface Topography and Specularity

Raether [15] has published a comprehensive review of the effects of roughness on scattering with and without excitation of surface plasmons. The theories frequently assume that the wavelength of the incident light is large compared to the roughness. For Raether's discussion 2-3 nm is considered a rather rough surface that represents about the largest roughness that some theoretical models can accommodate.

Other theories developed by radar scientists [16,17] may be more appropriate for application to silvered polymer mirrors in their current state of development where the roughness is much larger than 3 nm. The approach uses the tangent plane approximation where it is assumed that the reflective surface is composed of facets that reflect independently from one another according to the Fresnel coefficients for specular reflection. The facets are assumed to be nearly flat (radii of curvature large compared to the wavelength) and to be canted relative to a hypothetical reference plane. The facets are usually assumed to be isotropic, and multiple scattering and shadowing are neglected. The scattering cross sections can be expressed in terms of the Fourier transform of the joint probability density function of the surface-height random variables or in terms of a joint probability density function for the surface slopes where the characteristic correlation length is assumed to be small compared to the illuminated area. The distribution of surface heights is frequently assumed to be exponential or Gaussian and experiments [18,19] show that a Gaussian distribution is attained for some surfaces. Experiments [18] also show that the correlation between slopes is not Gaussian even for surfaces for which the distribution of slopes is Gaussian.

More recently, Elson and Bennett [20] reviewed scalar and vector scattering theories including those relevant to surfaces with roughness large compared to wavelength. Sung and co-workers [21-23] have used the tangent plane approximation, assuming that all plane segments are the same size, and the vectorial Kirchhoff integral method to calculate reflectances of very rough surfaces.

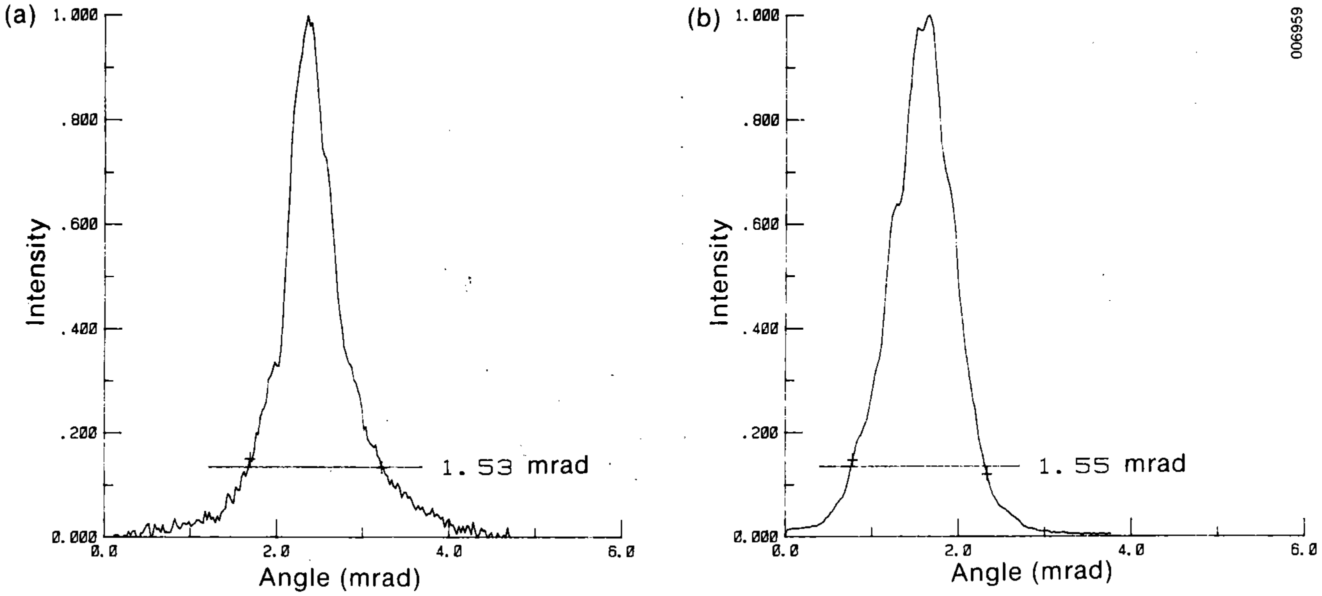

Figure 3-5. Specularly Reflected Beam from a) Silvered and b) Unsilvered Thin Polymer Films Stretched as Membranes

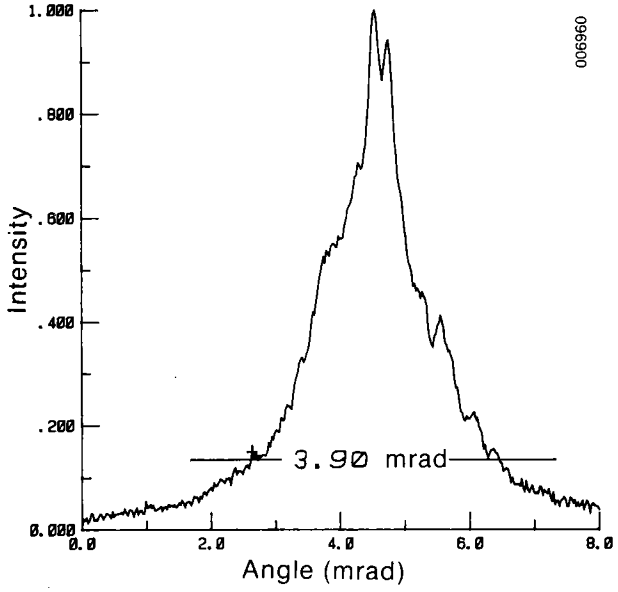

Figure 3-6. Specularly Reflected Beam from a 0.5-in.-thick, Polished Bare Aluminum Mirror

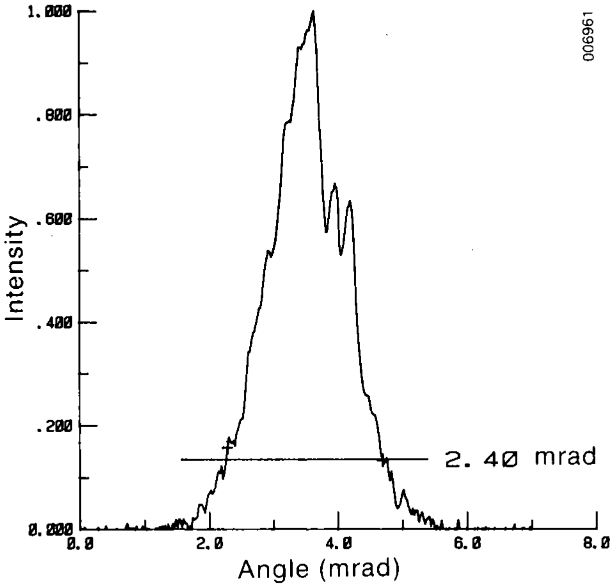

Figure 3-7. Specularly Reflected Beam from a 0.5-in.-thick Polished Aluminum Substrate Covered with a Thin Silvered Polymer Mirror

As a first experimental approach to correlate the surface topography with the optical performance of a silvered polymer mirror, surface profiles were measured and evaluated using geometrical optics. Figure 3-8a shows one of a series of surface profiles of the polymer/air interface that was measured on ECP 300 mounted on glass and was found to be representative for that material. Figure 3-8b shows the digitized form of the profile consisting of 79 flat segments, which is a very good approximation to the actual profile. Assuming that the silver contour replicated the polymer/air interface, the tilt of each segment, ϕ, was used to calculate the deviation of the reflected light from the specular direction. ΔX was used as a weighting factor for the intensity reflected into that direction with

$$\Delta X = X_{i+1} - X_i$$

for the i^{th} segment, and X_i being the x-coordinate of segment i.

Figure 3-9 shows the result, which is a prediction of the specularity for that sample. This simulated intensity distribution is similar to specularity curves measured for the same sample (see Figure 3-2).

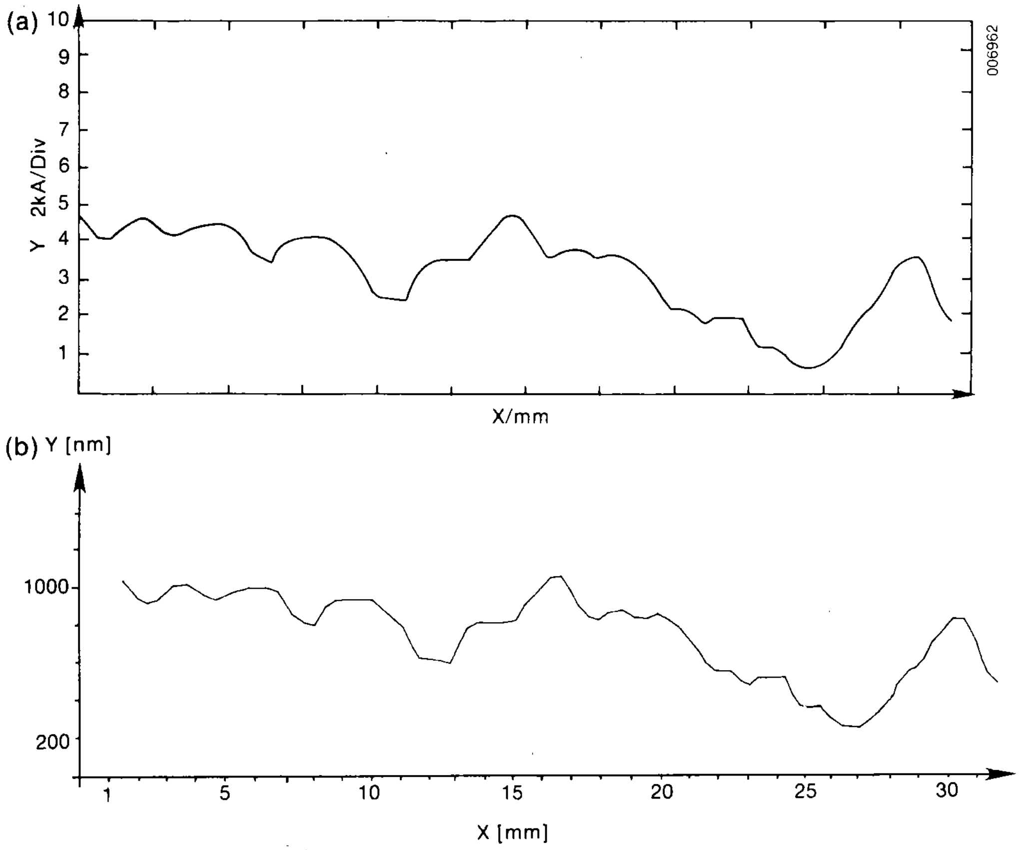

Figure 3-8. a) Surface Profile of the Polymer/Air Interface of a Thin Silvered Film Mounted on Glass and b) a Digitized Approximation of the Profile Consisting of 79 Flat Segments

3.1.4 Performance of a Polymer Mirror

In real applications, the sun with its beam divergence of 9.4 mrad full-cone angle has to be focused, which limits the image size on the receiver. In the case of a central receiver system, several additional factors further limit concentration:

a) tracking errors in the heliostat tracking system

b) slope errors either as a wavy mirror or as an improperly adjusted focal length of a heliostat

c) the reflection function of the mirror material (materials specularity)

d) dynamic misalignments caused by wind.

Terms b) and c) may be combined as one factor that may be called mirror system specularity [24].

Figure 3-10 shows two different cases. Figure 3-10a shows a convolution of the sun's intensity distribution (using a simple model [25]) with the reflection function of the ECP 300 material mounted on float glass (Figure 3-2), and Figure 3-10b shows the convolution with a reflection function that was shown in Figure 3-4. This comparison demonstrates that the contribution of the reflector material to an enlarged sun image at the receiver can be small compared to the effects of the curvature of the substrate and that goals for the reflector material should not be too stringent.

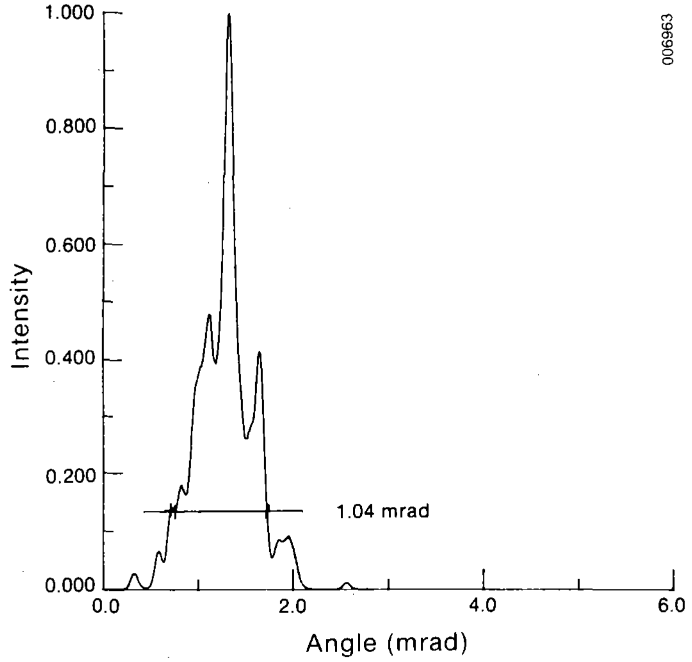

Figure 3-9. Simulated Specularly Reflected Beam from a Thin Silvered Polymer Film

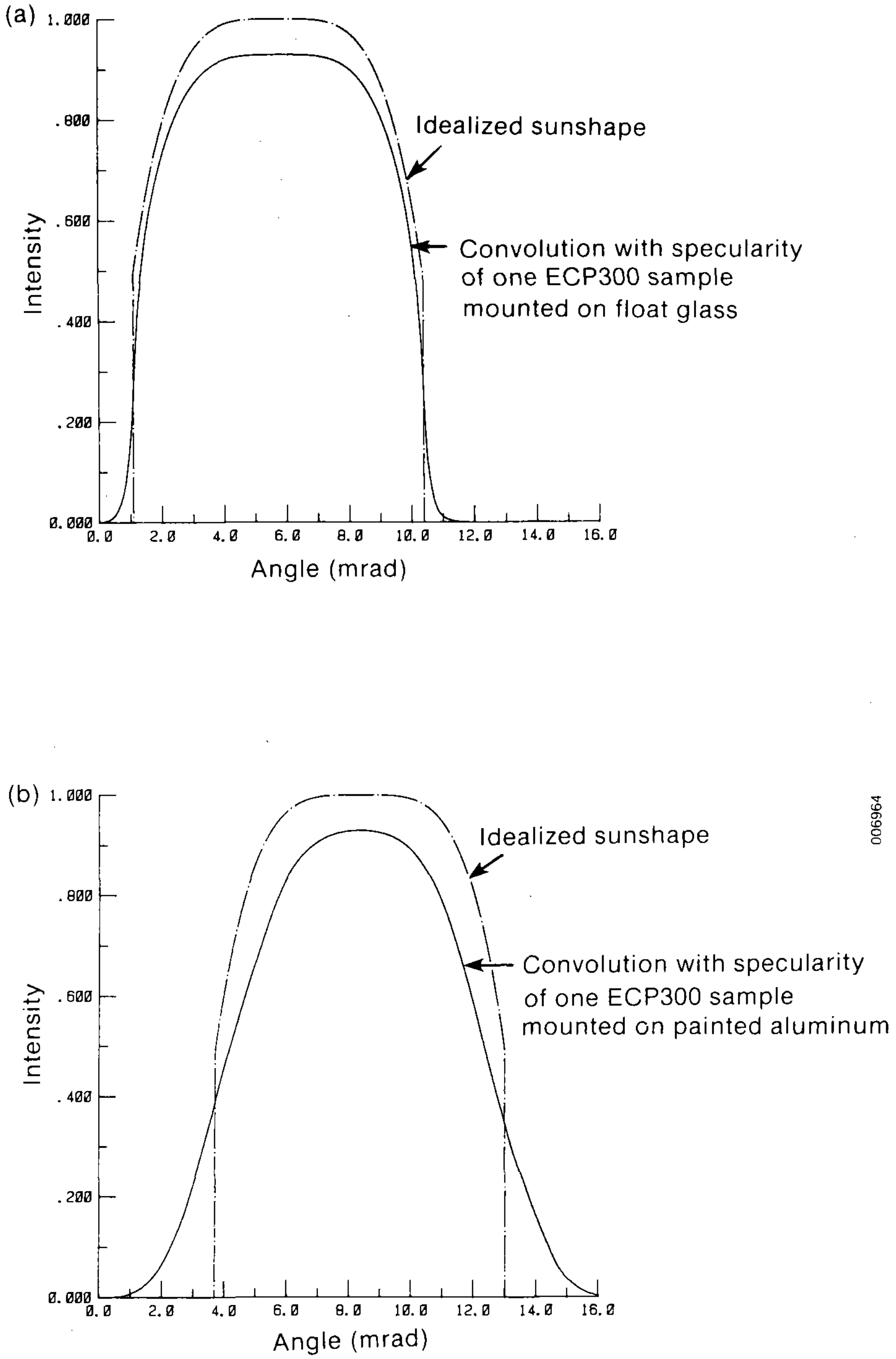

Figure 3-10. Convolution of the Sun's Intensity Distribution with (Curve a) the Reflection from a Silvered Polymer Film Mounted on Glass and (Curve b) the Reflection from a Silvered Polymer Mounted on Painted Aluminum. The heights of the convoluted curves include the absorption due to the silver.

3.1.5 Membrane Mirrors

The results presented in Figure 3-5 demonstrate the potential optical performance of the materials for stretched membrane mirrors. Applications will place requirements on the long-term mechanical properties as well as optical properties of the mirror constructions under weathering. System studies are defining the mechanical requirements and preliminary results suggested that thicker backing polymer films may be required. The 3M Company has supplied experimental films of silvered acrylic polymer laminated to a thick (7 mil) polyethylene terephthalate (PET) mechanical backing film. The initial optical performance of the mirrors (Table 3-3) is good.

Weathering studies on unsupported membrane mirrors are not yet in progress, but we anticipate data within the next few months from the University of Akron on the changes in mechanical properties (creep) of PET film under accelerated conditions. Initial mechanical properties are reported in Appendix B.

3.1.6 Effect of Structural Bulk Inhomogeneities on Specular Transmittance of Polymer Films

It has been recognized that light scattering from the bulk phase of a film contributes to a decrease in film specularity [26]. Evidence for a regular, equilibrium, amorphous structure with sizes of the order of the wavelengths of solar light is generally lacking for single phase polymers. However, light scattering, in many cases, may be caused by impurities, additives, and nonequilibrium structures associated with physical processes taking place during the fabrication and use of polymer films in various natural or artificial environments.

We have shown recently that practical transmittance measurements are greatly influenced by the angular width of the instrument receptor aperture. The choice of

Table 3-3. Specular Reflectance of Acrylic/Silver/7-mil PET Membrane Mirrors

Sample	Specular Reflectance (%) mrad 4	8	12
Sample #Y 1-100-1			
Measured through front acrylic	93.7	95.6	96.0
Measured through back PET	84.3	92.4	93.5
Sample #Y 1-100-2			
Measured through front acrylic	92.5	94.1	95.4
Measured through back PET	87.5	92.0	92.7

larger receptor apertures will tend to include some of the scattering at small angles because of large inhomogeneities in the measurement of specular transmittance. As a consequence, the transmittance measured is not necessarily increased by reducing the size of the inhomogeneities in the polymer films, but there is a critical size when the specular transmittance is a minimum. It is, therefore, of great importance to define the instrument receptor aperture when comparing transmission and visual measurements.

3.2 Industrially Silvered Polymers

The test results for these materials are given in Appendix C. Many of the test coupons provide data continuing from earlier reports [6, 27, 28]; however, all the optical data on durability presented in Appendix C are obtained using Reflectometer II (see Section 2.1.2) rather than the portable instrument that was available earlier [6]. Thus, data at 4 mrad are not now instrument limited. Reflectometer II has an accuracy and precision of about ± 1%, however, a current limitation of the data relates to the repositioning of the samples in the reflectometer after degradation exposure and to the fact that chance curvature of the substrates is limiting performance. Frequently, the mirror performance at small acceptance angles (4 mrad) is substrate limited and the polymer reflector performance is at least as good as the listed data. This is discussed further in Section 3.2.2. Most silvered polymers had been developed either for application to the space program or for reflectors used in interior lighting fixtures. For either application, outdoor terrestrial durability is not a key factor, and generally these materials have not been durable in harsh environments. In contrast, some of the materials that we are developing specifically for solar applications show considerably better performance.

3.2.1 QUV and Weather-Ometer Tests

The results of the environmental test chambers for industrial mirrors are given in Tables C-3 and C-4. We emphasize that these tests are used mainly for comparison purposes. **There is little scientific basis for predicting outdoor performance based on accelerated laboratory tests.** Nevertheless, for purposes of guiding research and development where decisions must be made with less than ideal information, these results are considered to yield a rough calibration that can be helpful.

Several modified constructions are in the early stages of testing as presented in Table C-3. They generally have different adhesive or stabilizer materials. Some are designated "Uncoated" meaning that the adhesive is mounted directly onto an aluminum substrate, while "Coated" identifies those materials that are mounted on an aluminum substrate that was first coil-coated with a white polyester paint. The paint potentially serves two functions: it can act as a leveling layer to effectively smooth the substrate, and it can influence degradation by separating the adhesive from the aluminum.

Other materials are further identified as coated with ARC Lot 2 or ARC Lot 1B, meaning that an abrasion-resistant coating is applied as an overcoat to the transparent acrylic polymer. Laboratory tests performed by 3M show the ARC coatings to be effective, but their longer-term effects on the optical properties of the mirrors are yet to be determined.

In earlier tests [6], the variation in performance of different films led to improved constructions. The improved materials are now showing more similar behavior in the harsh QUV test. In contrast to outdoor tests (Section 3.2.2) where the solar-weighted hemispherical reflectance (H) is affected very little, H decreases in QUV tests. This comparison can be made in Figures 3-11 and 3-12. Figure 3-11 shows the intensity of hemispherical reflectance as a function of wavelength for the 3M material, ECP 300

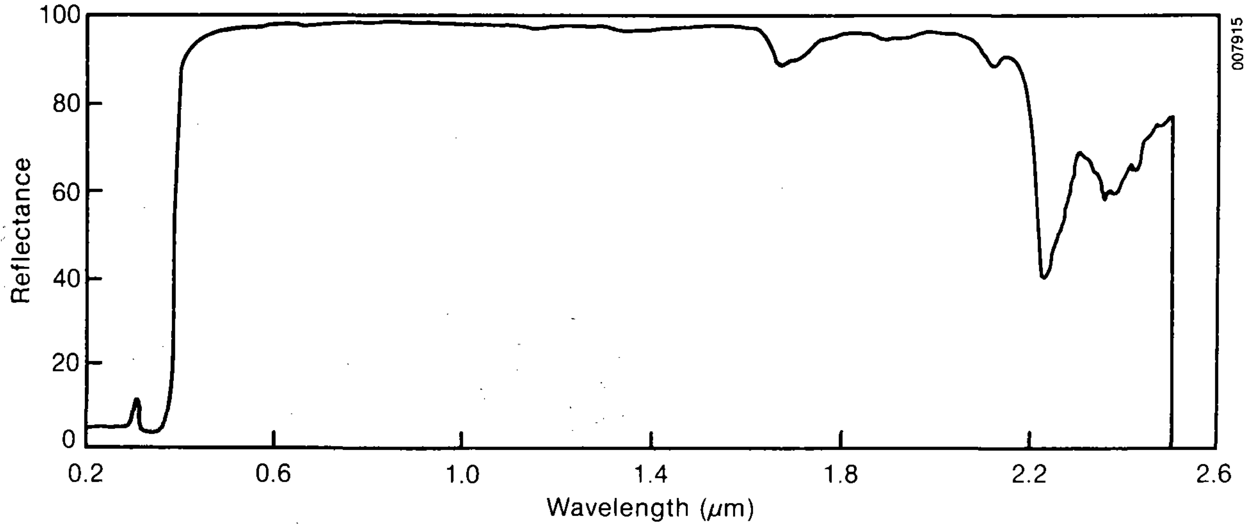

Figure 3-11. Hemispherical Reflectance of ECP 300 Lot 7 (Sample B4-152-3) After 7 Months Outdoors (Solar-weighted reflectance = 92.1%)

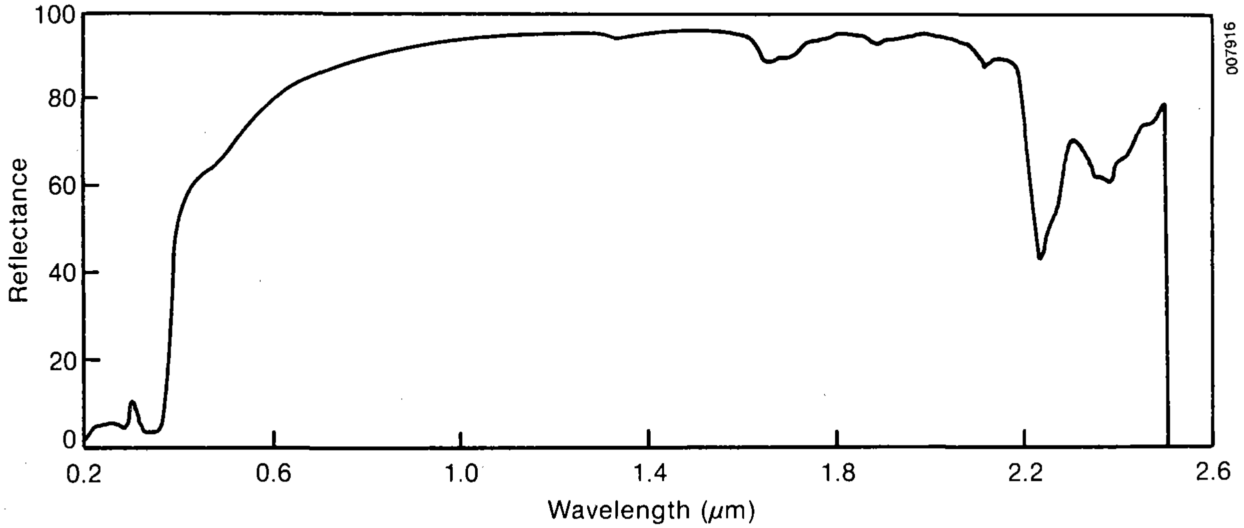

Figure 3-12. Hemispherical Reflectance of ECP 300 Lot 7 (Sample B4-153-7) After 5.5 Months in the QUV (Solar-Weighted Reflectance = 78.7%)

Lot 7, after 7 months of outdoor exposure; this curve is typical of unweathered films. After 5.5 months in the QUV, Figure 3-12, there is a significant decrease in reflectance for a similar material over a broad wavelength region; this curve is typical of behavior in the QUV.

The specular reflectances are also adversely affected. For example, note Table C-3, Group #2, sample B4-150-2, where between 5.5 and 6.5 months there was a marked, unusual change. We believe this change is due to an inadvertent temperature excursion (> 60°C) in the QUV. Prior to that event, there is little difference (at 12 mrad) between the various materials. In particular, there is no clear difference between painted aluminum and unpainted aluminum substrates, while in the Weather-Ometer (see Figures 3-13 and 3-14 below) there is a clear difference in performance for the two substrate types.

Three different edge seals have been used. An acrylic bead edge seal appears less reliable than tape edge seals. Two different edge seal tapes have been used, one was transparent and the other opaque white. Both tapes perform well under normal test conditions, but the white tape even survived the temperature excursion; we have not seen the white tape fail under any test.

There is some suggestion that Lot 2 ARC (abrasion or mar resistant coating on ECP 300) performs better than Lot 1B ARC (see Table C-3, Group #4) but further tests are needed.

The accelerated tests using the Weather-Ometer are given in Table C-4. In this test, there are two clear results. First, half of each sample mirror is shaded from the UV light while the complete sample is exposed to temperature and humidity. The mirror segments that are exposed to UV degrade more rapidly than the shaded parts. This result suggests that tests that do not include UV light as a means of degradation probably are not accelerated in a way consistent with outdoor exposures. Second, the performance of mirrors mounted on painted aluminum is better than that of mirrors mounted on bare aluminum. Note that in Table C-4, Group #4, ECP 300A Lot 9 on painted aluminum, performance is quite good even at 8 mrad (recall at smaller acceptance angles substrate curvature can limit performance).

The differences are striking in plots of hemispherical reflectance. Figures 3-13 and 3-14 show two extreme cases. In Figure 3-13, the UV-shaded and unshaded halves are compared for ECP 300 Lot 7 mounted on bare aluminum after 6 months of exposure. The effects of UV are marked and similar to those in the QUV, Figure 3-12. Figure 3-14 shows the marked improvement of ECP 300A Lot 9 mounted on painted aluminum in this test after 10 months of exposure.

3.2.2 Outdoor Tests

With reference to outdoor tests in Golden, Colo. (Table C-2), in general, the hemispherical reflectances are not much decreased after weeks of exposure, while the decreases in specular reflectance are more sensitive to weathering. Table C-2 of Appendix C lists results for all the ongoing tests. All data are taken with the new reflectometers and are accurate to about ± 1%. Data at 8 mrad are quite consistent, however, at 6 and 4 mrad, the data are limited by substrate curvature for either aluminum (Al) or painted aluminum (PAl) substrates and are not necessarily a true measure of the performance of the silvered polymer films. The polymer mirrors are at least as good as this data and we can identify the substrate quality as a problem for our tests and for engineering applications.

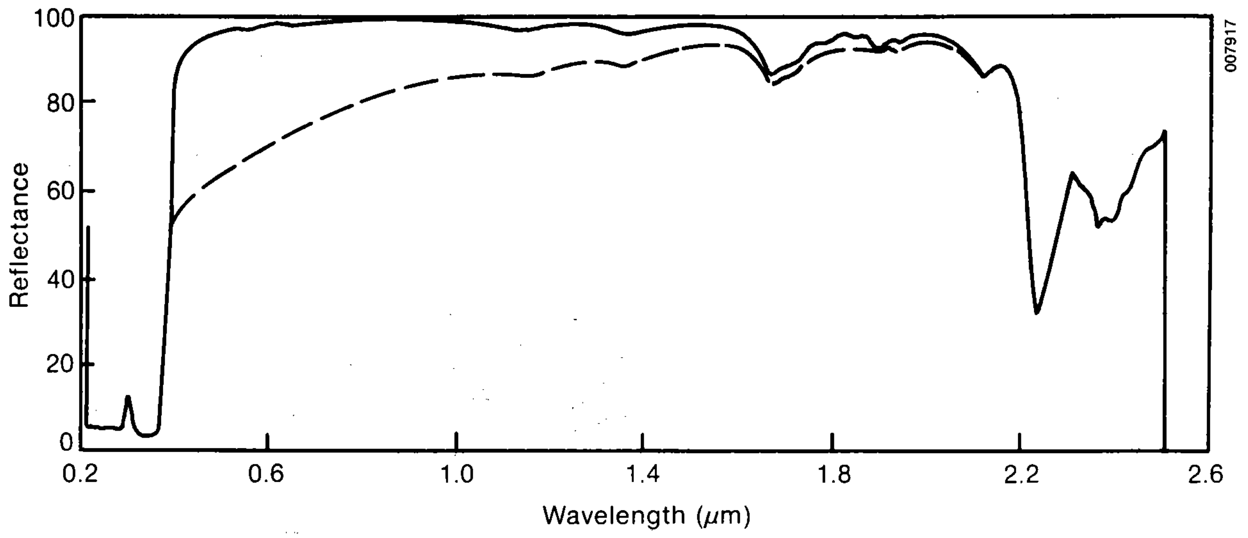

Figure 3-13. **Hemispherical Reflectance of ECP 300 Lot 7 (Sample B4-150-1), Mounted on Aluminum After 6 Months of Exposure in the Weather-Ometer.** Upper curve without UV exposure, solar-weighted hemispherical reflectance = 91.3%. Lower curve with UV exposure, solar-weighted hemispherical reflectance = 71.4%.

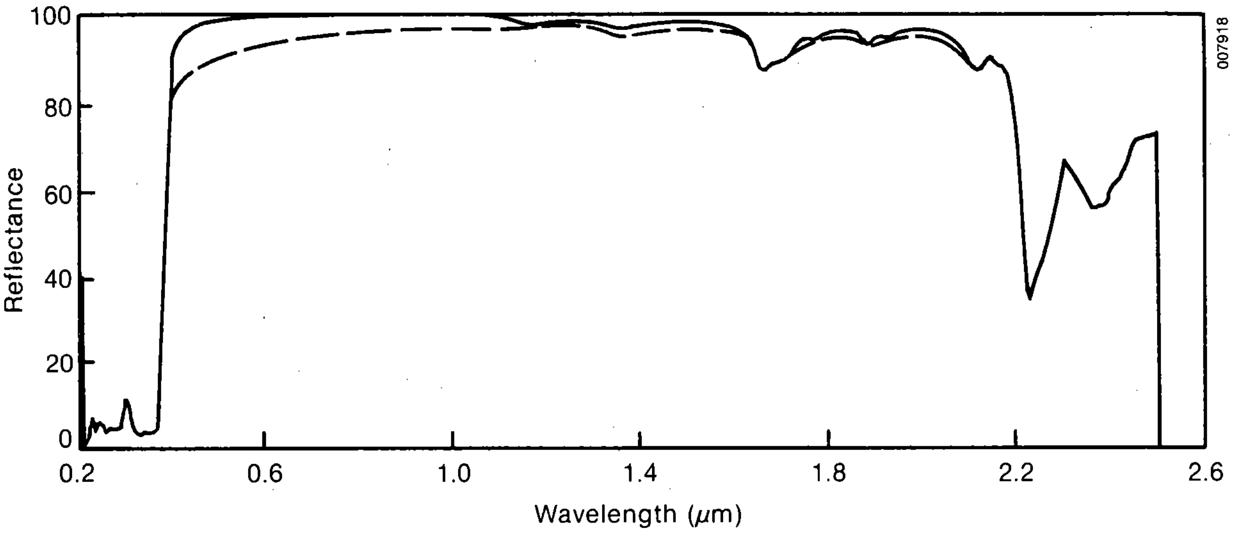

Figure 3-14. **Hemispherical Reflectance of ECP 300A (Sample Y1-30-13), Mounted on Painted Aluminum After 10 Months of Exposure in the Weather-Ometer.** Upper curve without UV exposure, solar-weighted hemispherical reflectance = 93.6%. Lower curve with UV exposure, solar-weighted hemispherical reflectance = 89.7%.

For exceptions to the substrate problem, note the data in Table C-2 under Group #6, ECP 300 Lot 7, where the substrate is glass. For these samples, the optics continues to be excellent even at 4 mrad.

The experimental samples (Group #1, Table C-2) are largely superseded by improved films, but the longest outdoor exposure data to date are in this group. For example, the B2-34-xx series is an experimental film that was a precursor to ECP 300, and after 142 weeks outdoors in Golden, Colo., the specular reflectances of several samples exceed 90% at 12 mrad. At lower acceptance angles, the curvature of the aluminum substrates limit performance.

The experimental B2-34-xx series is superseded by ECP 300. In Table C-2, Group #2 Lot 7, Group #3 Lot 8, and Group #4 Lot 7 are essentially the same structures. Performance up to 10 months outdoors at 8 mrad acceptance angle is excellent. At 6 and 4 mrad, substrate curvature again limits performance. In these data sets, there appears to be little difference between painted and unpainted substrates; however, one of our accelerated tests shows painted aluminum to be definitely superior and other outdoor data also suggest the same conclusion (see Appendix B).

At 10 months, five of six samples (Group #2, ECP 300 Lot 7), three on aluminum and three on painted aluminum substrates had a mottled appearance that did not wash off using our standard cleaning procedure, even though when they are wet during the cleaning process the mottling is much less apparent. The reflectance at 8 mrad is essentially unchanged and still good; at smaller acceptance angles the data are less significant because of substrate curvature. The mottled appearance of one sample was removed by a more vigorous cleaning procedure at the 3M Company. The mottled appearance for this sample group is the only negative indication for any of the ECP 300 material during outdoor exposure. Subsequent groups of ECP 300 Lot 7 (see Table C-2, Groups #4 and #6) are also in test on different time cycles, and these samples had not mottled at their last measurement.

Group #4, Table C-2 compares the standard ECP 300 Lot 7 with the same material with two types of mar resistant (MR) top coatings (Lot 2 ARC and Lot 1B ARC). The ARC-coated materials may be slightly poorer initially but all perform well at 8 mrad, and with little evidence of weathering differences. Other evidence (Appendix B) suggests that ARC-coated materials may weather less well.

Group #5, ECP 300A Lot 9, Acrylic Seal uses a different stabilizer system and it continues to perform well. Acrylic seal indicates that a different edge seal procedure was used.

Group #6, ECP 300 Lot 7 mirrors on glass substrates remain excellent and continue to meet our long-range goals for reflectance at 4 mrad in excess of 90%. Flat aluminum and stainless steel substrates are being fabricated with a high polish to determine whether metal/adhesive reactions may play a role that is not detected for these samples with glass substrates.

3.3 Solution Cast Stabilized Polymer/Silver/Glass Mirrors

The reflectance data of a series of stabilized silver/polymer mirrors, as a function of environmental degradation, are presented in Appendix D.

We observed earlier that the optical properties of PMMA cast onto Ag/glass are affected not only by the purity of PMMA and the PMMA/Ag interface, but also by additives to PMMA that serve as UV absorbers, excited state quenchers, or antioxidants. The optical properties are also influenced by the preparation methods of these polymeric mirrors and their degradation modes caused by the adverse effects of environmental parameters. The degradation modes have been addressed in prior publications [27,28].

In this report, we discuss the completed test results of a series of stabilized polymer mirrors started last FY 1985 and this FY 1986. Some of the stabilizers tested have been specifically synthesized for protecting silvered polymers, and the details of the synthetic chemistry and characterization are discussed in Section 3.4.4.

3.3.1 Effects of Polymer Additives

It has been known for many years that light has a deleterious effect on the properties of polymers. "Weathering," the technological term used to describe the deterioration of polymer properties in the outdoor environment, involves a complex interaction of physical and chemical processes, and photo-oxidation is recognized as the most important.

The characteristics of photodegradation permit application of stabilization methods to prevent such degradation by involving photon absorption, transfer of energy, and antioxidant mechanisms [29].

For the protection of solar reflectors, however, the stabilization of the polymer glazing is just one facet of the total problem, which also includes the stabilization of the polymer/silver interface, as well as the stabilization of a potential polymeric backing if no precautions are taken to eliminate the UV transparency of the silver layer. Since UV absorbers decrease the amount of solar light reflected from a mirror, the necessity of the presence of such additives to protect and extend the lifetime of the reflector is of high practical interest.

We have identified and prepared a series of representative examples with the different groups of UV stabilizers (Tables 2-1 and 2-2) and incorporated them into PMMA to enhance its effectiveness. Most known UV stabilizers do not act by a single mechanism, but by a combination of mechanisms. Commercial UV stabilizers are generally classified into UV absorbers (UVA), quenchers (Q), and antioxidants of the chain-breaking acceptor (CB-A) or chain-breaking donor (CB-D) type and synergists.

Most members of the UVA class (I-IV, XII-XVI) operate primarily by absorbing UV light and emitting it back as vibrational (thermal) energy, but they have been shown also to be able to scavenge radical species.

The term "quencher" for nickel complexes is still widely used in the industry to describe their ability to deactivate photo-excited species. This mechanism is not now believed to be very important in practice since, in all cases, their antioxidant function has been shown to be much more important. Compound IX is a UV-stable, CB-D antioxidant with UV-screening activity, but this is probably less important than its antioxidant properties.

The antioxidants VI and VIII are not normally considered very effective UV stabilizers alone, but they are very often included in a UV stabilizer formulation as synergists.

The hindered piperidine compounds V, VII, X, XI, XVII, and XVIII are not effective antioxidants, but their derived nitroxyl radicals have been shown to act by a CB-A/CB-D cycle, and their high activity is believed to be due to this species, formed either during processing or during photo-oxidation. They do not absorb UV light, so they are UV stable.

The initial emphasis in our studies has been on using light stabilizers in solution cast thin glazings (1-20 µm). Tests performed with these thin glazings are meant to guide later formulations for extruded, thicker films (ca 90 µm). Mirror samples with the stabilizers I-XIII incorporated in the polymer glazing have been tested in our accelerated testing devices QUV and WOM as well as outdoors.

In our earlier studies, we found that such modified thin glazings prevented or diminished the optical degradation of silver mirrors. However, mirror performance was found to depend on the weathering mode (i.e., WOM, QUV, outdoors). None of the tested mirror samples degraded significantly during short-term exposures outdoors (64 weeks) and in the accelerated QUV tests (52 weeks) as determined by comparing hemispherical reflectances (H). Accelerated Weather-Ometer tests, on the other hand, demonstrated an enhanced optical degradation of unstabilized PMMA/silver mirrors, while stabilizers added to PMMA impeded the degradation.

However, during this reporting period, we observed on another series of mirrors (R13-100-X, solution cast glazings, 11-20 µm thick) that the optical degradation is not due to increased absorption within the polymer glazing, but due to a photo-darkening of the wet-processed silver surface that is not yet completely understood (Tables D-2, and D-6 through D-12).

Although most stabilized mirror samples performed better optically than unstabilized samples over a 15-week testing period in the WOM (Figure 3-15), we noticed a decreased

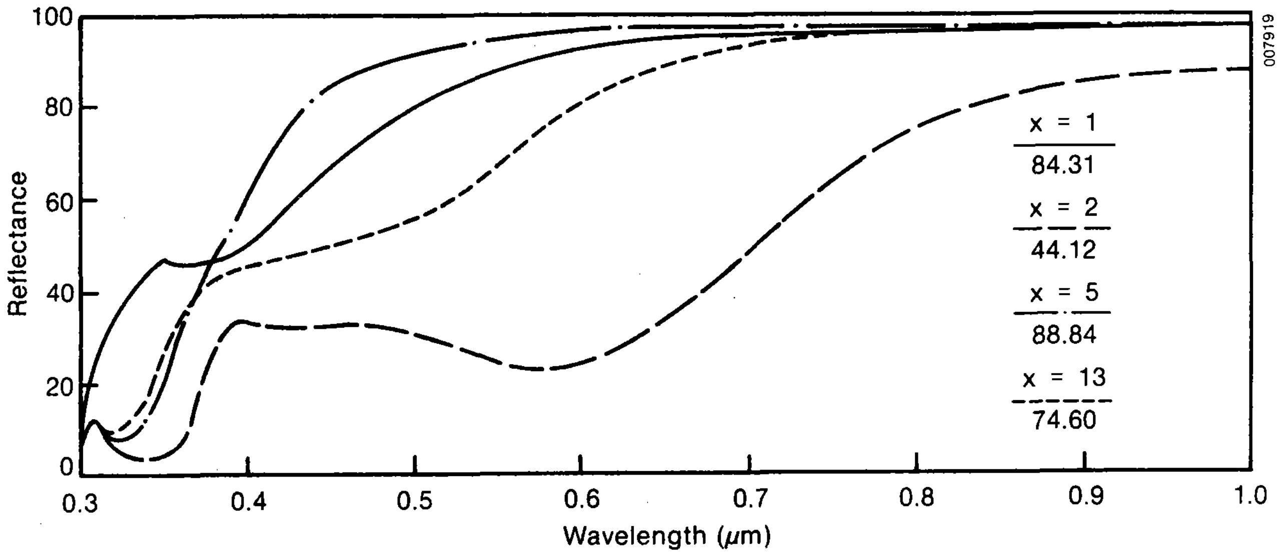

Figure 3-15. Change in Hemispherical Reflectance After 15 Weeks of WOM Exposure for Selected Mirrors of the R13-100-X Series

optical performance for mirror samples R13-100-2 and R13-100-13, which had the stabilizers TIN-P and MS1-11-5 incorporated, respectively. Similar results have been obtained with R13-100-X samples exposed to WOM irradiance filtered with polymeric UV-cut-off filters (Figure 3-16). Figure 3-17 demonstrates that the photo-darkening of sample R13-100-2 cannot be prevented through the use of such filters. Further, the darkening effect has also been observed for some wet-processed silver mirrors exposed to laboratory lighting. For example, mirror R13-100-5, which did not exhibit any optical changes during 15 weeks of WOM exposure (Figure 3-15), showed photo-darkening during an equivalent time under normal laboratory lighting conditions (Figure 3-18). In all of these cases, it could be noticed that the photo-darkening remained on the silver surface after solvent stripping and also that the transmittance of mechanically stripped polymer glazings did not change. As Figure 3-19 demonstrates, any residue of the photo products of the silver surface remaining on a stripped polymer film could be easily wiped off with an alcoholic solution.

Under the microscope, the darkened areas appeared more granular than lighter areas of the silver surface. These lighter areas appeared at the sample edges or in small, circular areas distributed over the silver surface. Each of these circular areas had a white, chloroform-insoluble, crystalline deposit at its center.

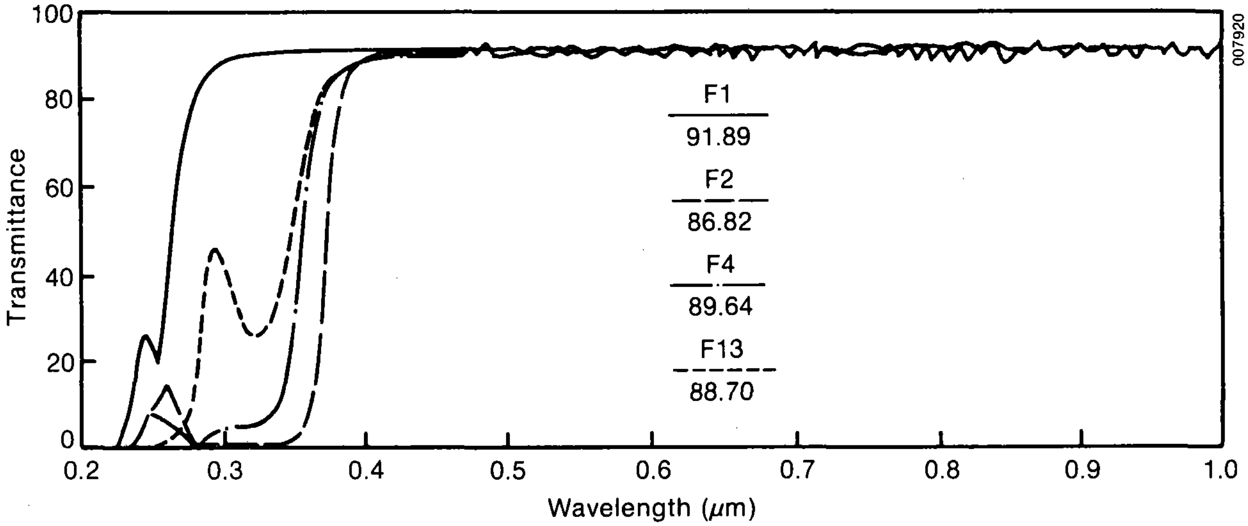

Figure 3-16. Transmittance Characteristics of Selected UV-Cut-Off Filters of the R13-100-X Series

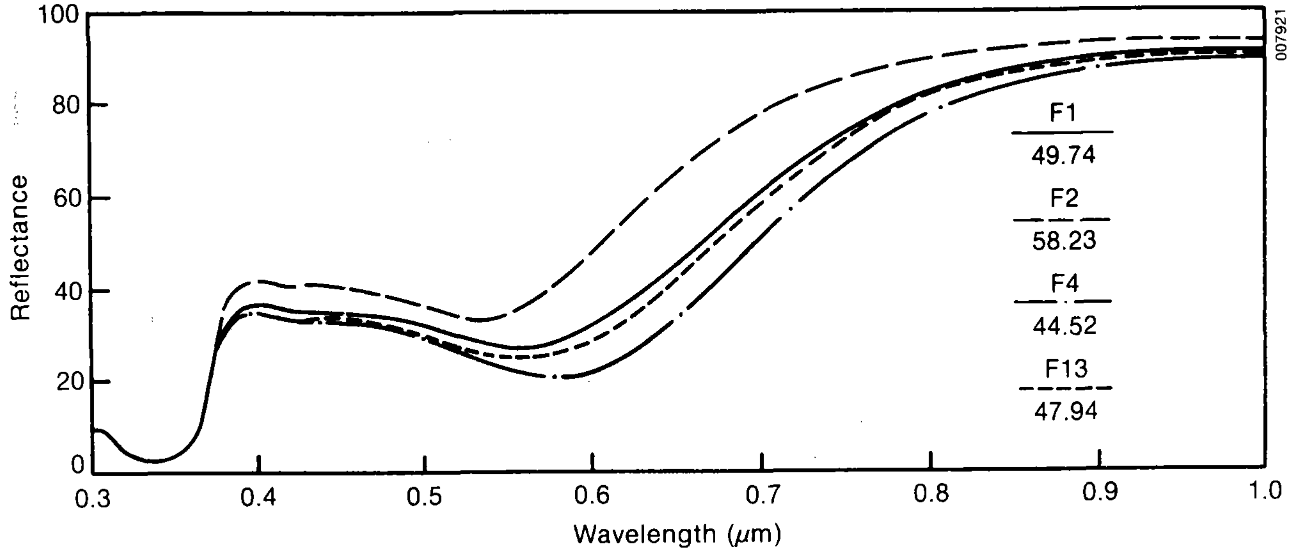

Figure 3-17. Change in Hemispherical Reflectance for Sample R13-100-2 After 15 Weeks of Filtered WOM-Exposure Using Filters F1, F2, F4, and F13

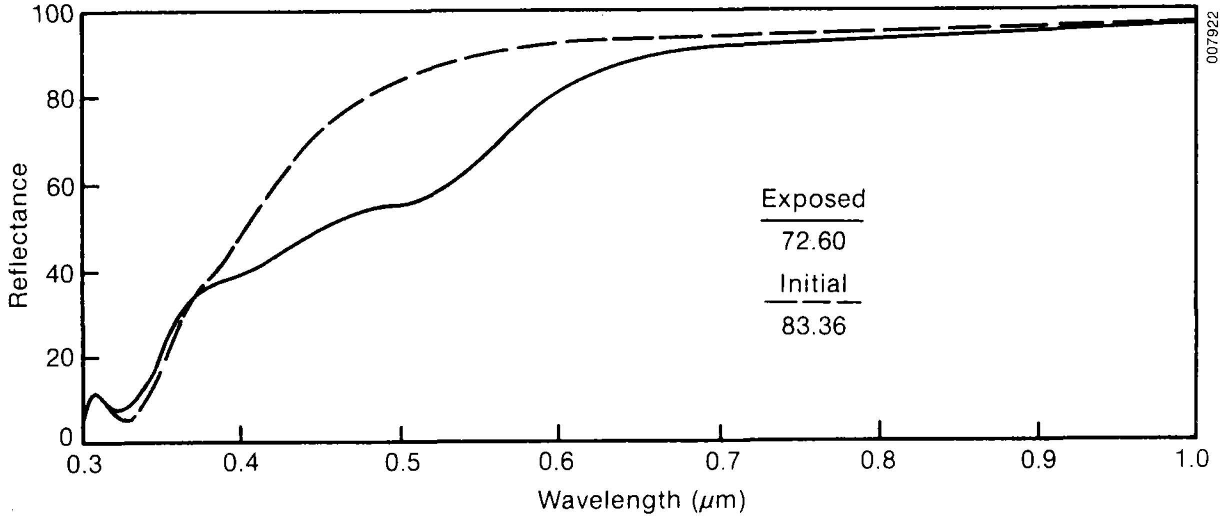

Figure 3-18. Change in Hemispherical Reflectance for Sample R13-100-5 After 12 Weeks of Laboratory Illumination

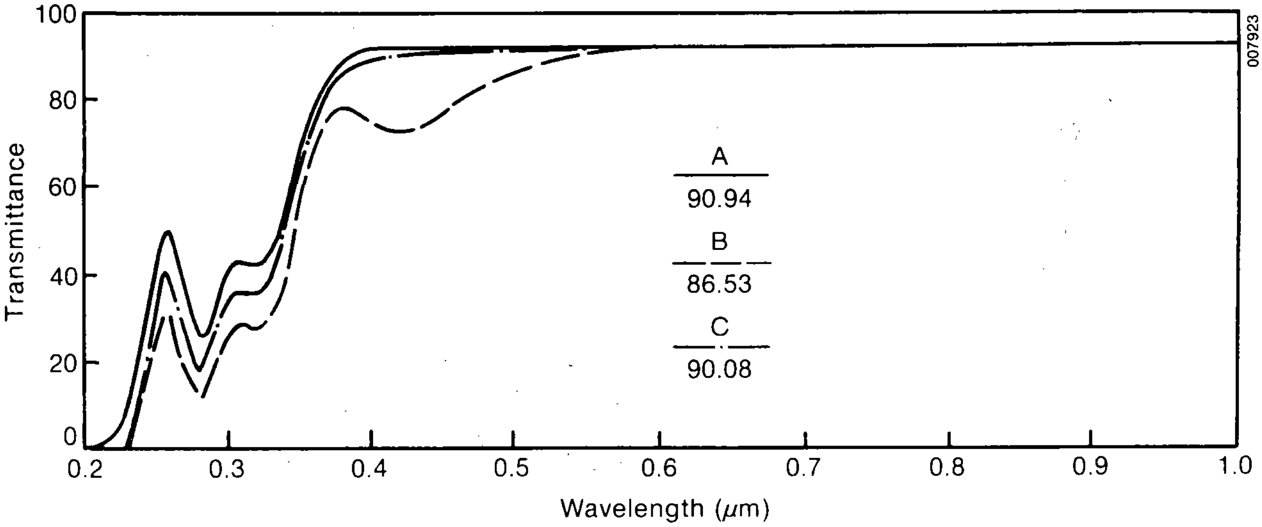

Figure 3-19. Transmittance Characteristics for Stripped Glazings of Sample R13-100-5 Before Exposure (A), After 12 Weeks of Laboratory Illumination (B), and After 12 Weeks of Laboratory Illumination and Surface Cleaning with Alcohol (C)

Some similarities were noted between the appearance of these samples and that of ozone oxidized silver samples prepared as part of another task. In the latter study, areas of the bare silver surface, which were not discolored after UV exposure, were found to contain high surface concentrations of chlorine. However, in the case of the WOM-exposed samples, it seems that oxidation of the Ag surface is proceeding by a different mechanism than ozonation, since ozone measurements in the WOM were negative (< 1 ppm). Also, no sulfides could be detected in the water reservoir of the WOM. FTIR reflection absorbance spectra of the darkened surfaces showed no silver oxide, carbonate, or sulfide bands. Surface analysis of the darkened samples might provide better information since IR-RA bands of oxidized metal surfaces are difficult to observe.

The possibility of passivating solar mirrors with adsorbed chlorine had been noted earlier [30]. To study the chlorine passivation phenomenon, we exposed freshly prepared wet-processed silver mirrors for various times (1, 5, and 15 min) to HCl vapor and dip-coated them afterwards with PMMA (R14-26-X). No darkening has been observed so far for these samples after 20 weeks of WOM exposure (Table D-14).

It is of additional interest to note that the photo-darkening effect is only observed with wet-processed silver surfaces and not with sputtered silver surfaces (Figure 3-20). Purity of the polymer glazing does not appear to be a factor in the process.

Darkening of mirrors is less or not at all noticeable on the samples that are exposed in the QUV mode or weathering outdoors. Corrosion of the silver layer below the thin polymer glazing because of water diffusion through the glazing and delamination of the glazing are factors of higher concern in these weathering modes. Specular reflectance measurements are more sensitive in detecting these changes than hemispherical reflectance measurements. Outdoor and QUV testing of these samples (R13-100-X) had to be

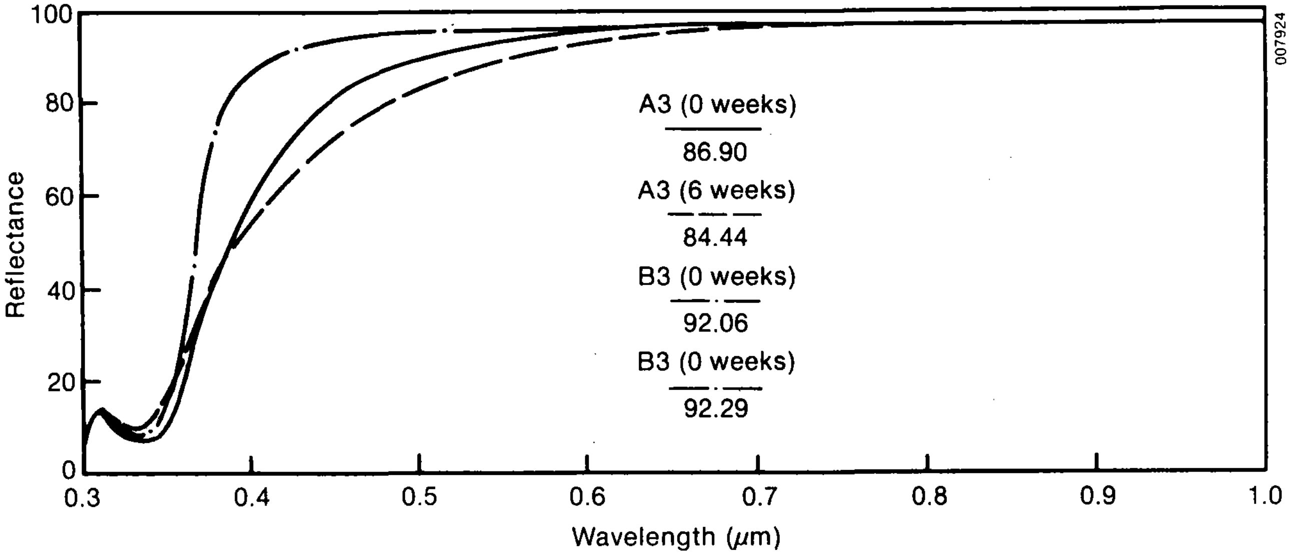

Figure 3-20. Change in Hemispherical Reflectance for Samples R14-74-A3 (Wet-Processed Silver) and R14-74-B3 (Sputtered Silver) After 6 Weeks of WOM Exposure

discontinued after 15 weeks because of delamination of the polymer films (Tables D-6 and D-7). Weathering trends observed for the R13-100-X series were essentially also confirmed by the results obtained for the dip-coated R12-178-X series (1-3 μm glazing thickness) (Tables D-1, and D-3 through D-5). However, samples of the latter series in the WOM tests were accidentally exposed to a saline environment for the initial first week of testing because of salt residues present in the instrument from an earlier experiment.

No photo-darkening of the wet-processed silver surface could be observed for any sample, which could be because of surface passivation (see above comments) by the salt. However, this initial salt exposure in the WOM caused severe corrosion of the silver layer and delamination at the silver-glass interface of the UV-exposed sections, which caused the specularity values to drop early.

QUV testing and outdoor weathering of this series did not affect reflectance values severely. Reflectance values were found, in general, to be comparable to the initial values. Specularity values, measured at all three acceptance angles, remained above the 90% mark after 2 months of testing. No optical degradation was observed for samples shielded from the UV light.

The R12-178-X series also included specimens where the incorporated stabilizers may contact the silver surface or be separated from it by an unstabilized layer of PMMA. No noticeable difference in the optical performance could be observed for the different specimens. The R12-178-X series was discontinued after 4.5 months of testing when delamination of the UV-exposed sections interfered with the measurements.

3.4 Solution Cast Stabilized Polymer Films

The physical aspects of the silver surface (bulk plasmon and surface plasmon absorption), in addition to silver surface degradation phenomena (photo-darkening and corrosion), interfere with the direct evaluation of thin polymer glazings on silver mirrors (Section 3.3). Therefore, to evaluate changes in the polymer, we are presently emphasizing studies with results obtained from transparent, nonmetallized PMMA films.

We have identified and/or prepared a series of representative examples within the different groups of UV stabilizers (Tables 2-1 and 2-2) and incorporated initially selective UV-absorbers into PMMA to enhance its effectiveness. Two series of films were prepared by solution casting techniques with one series having thicknesses comparable to the 3M ECP 300 films (ca. 3.5 mil ≡ 89 µm) and the other series being thinner (ca. 0.5-1.0 mil ≡ 13-25 µm). Because of the large number of samples tested, we used PMMA in most cases as received from the supplier (Polysciences) without further purification, realizing that impurities in the polymer may contribute to photodegradation in the polymer films. However, such impurities are expected to be normally present in the commercial materials used for film production, and we are interested in evaluating the effectiveness of stabilizer systems in such technical grade materials. Elimination of impurities in PMMA may lead, of course, to a more photostable product. The transmittance data of the stabilized PMMA films, as a function of accelerated weathering, are presented in Appendix E.

3.4.1 Effects of Polymer Additives on Weathering of PMMA films in QUV and WOM

3.4.1.1 Optical Properties

Figure 3-21 shows some representative changes in specular transmittance that have been observed during accelerated weathering for 6 weeks in the QUV and WOM for unstabilized PMMA and stabilized PMMA films. The irradiation of all samples causes some optical degradation during QUV exposure in comparison to the WOM-mode.

Figure 3-22 highlights this effect for unstabilized PMMA by comparing the different absorption spectra of PMMA after 6 weeks of exposure in the two accelerating weathering devices. Figure 3-23 displays the corresponding change in light absorbance of PMMA films at 275, 325, and 400 nm vs. exposure time. The monotonous increase in absorbance may be attributed to the formation of primary photoproducts. These curves subsequently level off, presumably because of competitive absorption of radiation by these products. The absorption bands are similar for the photoproducts generated in both weathering modes, indicating comparable degradation mechanisms, which are accelerated in the QUV mode. The band at 285 nm observed by Shultz [31] is also seen in these spectra and is the region usually associated with carbonyl chromophores. The band at 275 nm may be attributable to different carbonyl chromophores or to conjugated double bonds [32]. Photo-oxidation chromophores (hydroperoxides) may cause the band around 325 nm. The origin of these absorption bands is clearly connected with the polymer chain itself rather than with a low molecular weight photolysis product since gel permeation chromatography studies of the degraded polymers monitored at different wavelengths indicate the incorporation of these chromophores into the macromolecular chain.

The reason for increased absorbance changes during QUV weathering may be because of the severity of the QUV testing mode, where the UV lamps used emit a significant amount of UV in wavelengths shorter than the solar cut-off of 295 nm (Figure 2-9). (The crucial role of the UV component of the light on the photodegradation of the films tested

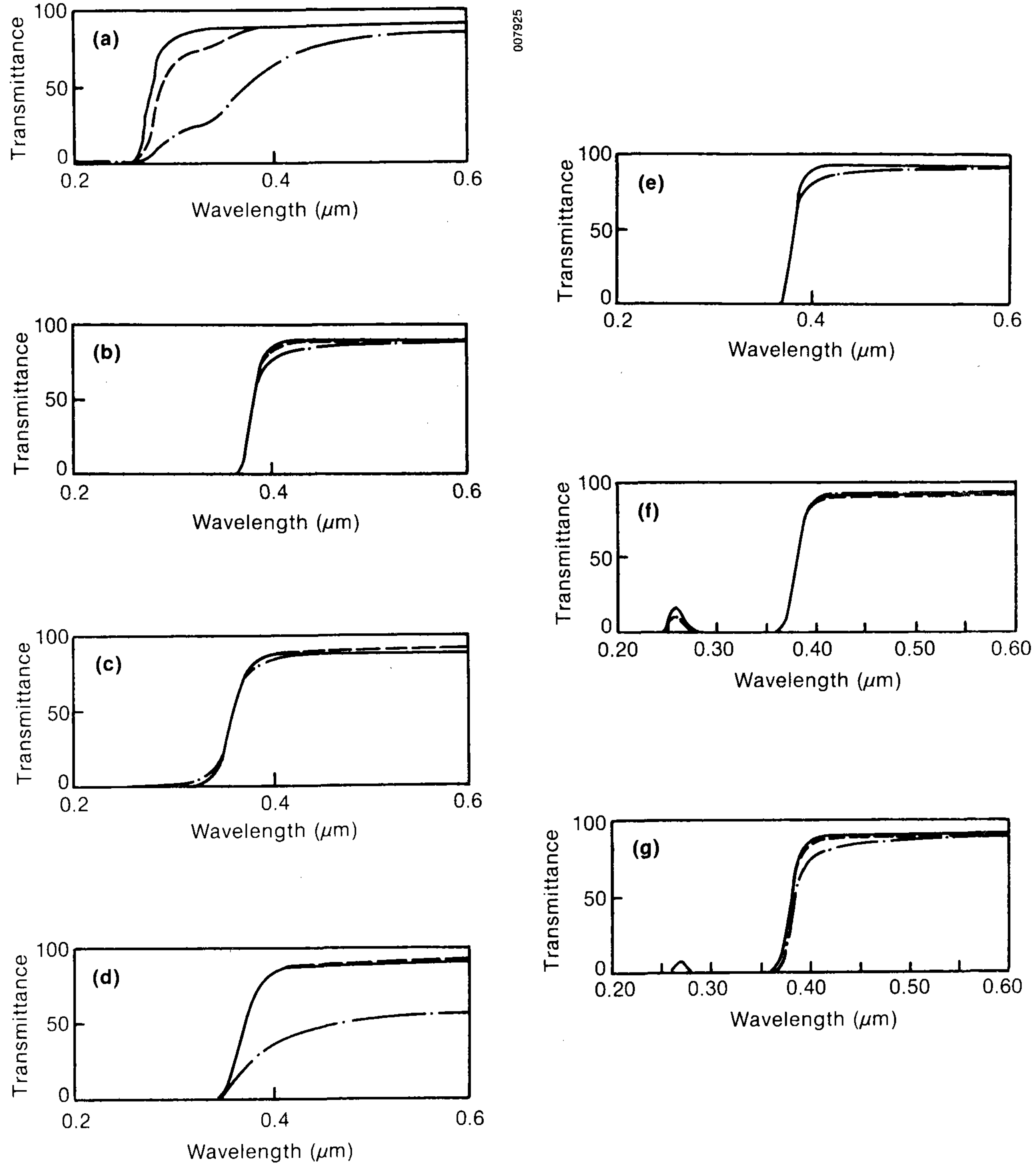

Figure 3-21. Changes in the Transmittance Spectrum Between 200 and 600 nm (initial—) After 6 Weeks of WOM (- - -) and QUV Exposure (– · –) for Unstabilized PMMA (a), Stabilized PMMA + TIN-P (b), Stabilized PMMA + NS (c), Stabilized PMMA + MS1-13-2 (d), Stabilized PMMA + PG1-27-3 (e), Nonmetallized Melt-Extruded ECP 300 Film (f), and ECP 300 Film Solution Cast (g)

is demonstrated because no optical degradation could be observed for samples shielded from the light.)

Optical losses and mechanical film failure in stabilized films are, however, considerably reduced in comparison to unstabilized PMMA, whose lifetime did not exceed 6 weeks of QUV exposure. As is evident from Figure 3-21, all stabilizers tested perform reasonably well in preventing optical degradation of the films except for stabilizer MS1-13-2, which could not prevent a considerable early surface crazing of this particular film during QUV testing.

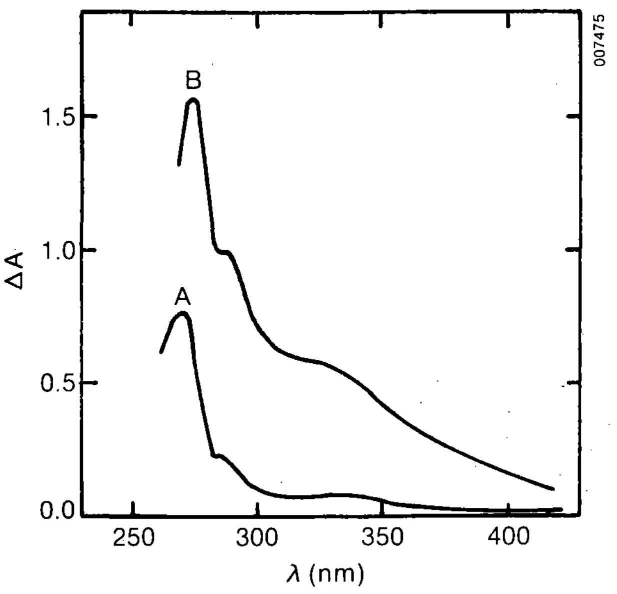

Figure 3-22. Changes in Absorbance of Unstabilized PMMA Films After 6 Weeks of WOM (A) and QUV (B) Exposure

Figure 3-24 summarizes the results by displaying the change in light absorbance of stabilized PMMA films at 400 nm vs. exposure time in a QUV. (Optical changes of these films during WOM exposure are negligible for the time tested.) The slight increase in absorbance for most of the stabilized films indicates that primary photoproducts are still formed in the films, although at a much reduced rate. Since the increase of light absorption because of the formation of photoproducts is limited mainly to wavelengths less than 400 nm, optical performance of these stabilized films is rather unaffected by it. However, main chain scission of PMMA (see Section 3.4.1.2), especially in the surface layer, causes a rapid decrease in molecular weight in unprotected or incompletely protected PMMA films, which subsequently is responsible for the formation of surface crazes that can cause considerable light scattering (see, for example, Figure 3-21d). These results also point out the need for arranging the UV stabilizer as close to the film/air surface as possible.

For comparison, we included the transparent ECP 300 film from 3M Company in our accelerated weathering tests. ΔA_{400} for this melt-extruded film is comparable to the absorbance change in most of our stabilized solution cast films (Figure 3-24). If the ECP 300 film is dissolved in toluene and solution cast, however, we observe a larger absorbance change after irradiation for this film in comparison to most SERI solution cast films.

It is conceivable that the different morphologies in biaxially stretched and solution cast PMMA films affect the rate of photodegradation. However, no studies known to us have addressed this effect. On the other hand, we have observed in our extraction studies (Section 3.4.2.2) that it is not practical to get the solution cast films toluene free in a reasonable amount of time. Therefore, it is possible that toluene residues in the films initiate or participate in the photo-oxidative degradation of the polymer. However, the presence of stabilizers considerably retards any such participation of the solvent in the photodegradation process.

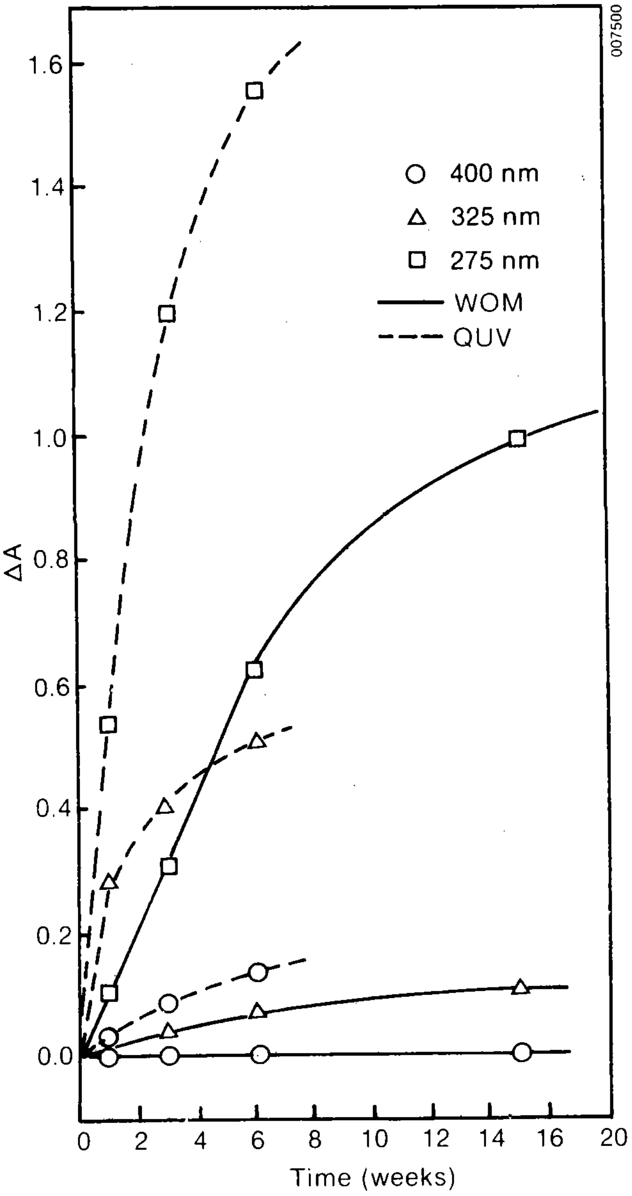

Figure 3-23. Changes in Absorbance of Unstabilized PMMA Films at 275, 325, and 400 nm versus Exposure Time in WOM and QUV

Another factor of concern with solution cast films relates to the potentially different solubilities of polymeric stabilizer and host during the drying process. This may cause distribution gradients of the stabilizer throughout the film with one surface being more protected than the other. Since photodegradation of the tested PMMA films proceeds from the surface of the film, where protection is incomplete, into the bulk, optical performance may be a function of which surface is exposed to the irradiation. An initial study on one sample (R13-100-3) indicates different weathering behavior depending on the surface exposed (see Section 3.4.2). Further studies of this phenomenon are in progress.

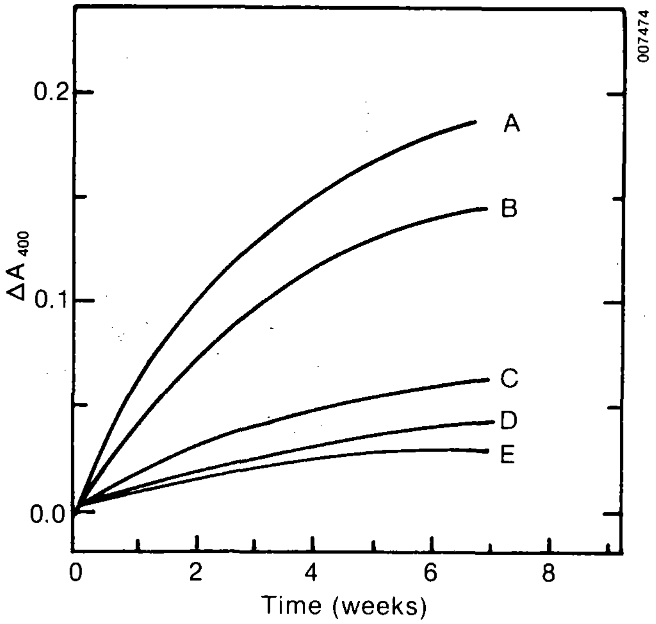

Figure 3-24. Changes in Absorbance of Stabilized PMMA Films at 400 nm versus Exposure Time in the QUV Mode: PMMA + MSI-13-2 (A), Unstabilized PMMA (B), Solution Cast ECP 300 Film (C), PMMA + TIN-P (D), PMMA + PGI-27-3 (D), PMMA + UV (E), PMMA + NS (E), Melt-Extruded ECP 300 Film (E).

3.4.1.2 Molecular Weight Changes

PMMA, if not unique, is unusual among polyalkylacrylates in that cross-linking does not occur during photolysis of films in air [33]. PMMA is unusual also in that the number of chain scissions per molecule tend to be linear with irradiation time. The effect of stabilizers on chain scission was studied by gel permeation chromatography (GPC) after irradiation. Values of M_n show a rapid decrease in the case of PMMA without stabilizer, more so during QUV exposure than during WOM exposure (Table 3-4).

Table 3-4. Representative Number-Average Molecular Weight and Chain Scission Data for Unstabilized and Stabilized PMMA After 100 h Exposure

Sample	Weathering Mode	$\bar{M}_n \times 10^{-3}$	Number of Scissions $S = ((\bar{M}_{n,o}/\bar{M}_n) - 1)$
PMMA	Initial	174.0	0
	QUV	7.5	22.2
	WOM	79.0	1.2
PMMA + 1.5 w% (TIN-P)	QUV	125.0	0.39
	WOM	129.0	0.35

This molecular weight decrease can be considerably retarded through the addition of UV stabilizers. Exact molecular weight changes for the systems stabilized with polymeric additives are difficult to elucidate from the GPC traces because of the superposition of guest and host traces (Figure 3-25). However, qualitative conclusions can be drawn: a noticeable increase of lower molecular weight fragments due to PMMA degradation can be observed for most films exposed in the QUV (Figure 3-25), whereas no noticeable degradation for the stabilized films can be noticed during WOM exposure.

Our GPC set-up provides us with the capability to monitor the eluant volume of the GPC at different wavelengths. This allows us to follow any molecular weight changes in the polymeric stabilizers by using the wavelength of their absorbance maxima. Changes in eluant volume (and thus molecular weight) after 6 weeks of exposure appear to be minor for the polymeric hydroxybenzophenone (Figure 3-26) and hydroxybenzotriazole stabilizers (Figure 3-27). High molecular weight appendices (retention time around 8 min) absorbing at 332 nm (Figure 3-26) may be due to the formation of chromophores in the PMMA chains that precedes chain scission and the subsequent formation of nonabsorbing (at 332 nm) chain fragments.

3.4.2 Permanence of Polymer Additives

3.4.2.1 Changes in Stabilizer Concentration During Accelerated Weathering

The permanence of the stabilizer in the PMMA film is another important factor for preventing long-term degradation of PMMA/silver mirrors and PMMA films. Despite the high inherent UV stability of the selected stabilizers, we noticed that their concentrations do fall steadily during UV irradiation. The change in the absorption maximum of UV-screening additives in thinner films (13-25 μm) was chosen to monitor this factor. [Thicker films (89 μm) have, normally, a complete UV cut-off and no changes are noticeable in their UV-absorbing characteristics during the testing time of 6 weeks.] As already observed earlier for dip-coated PMMA/silver mirrors [6], the consumption of stabilizers in PMMA films is also generally higher during QUV exposure and lower during WOM exposure. The reason for this behavior may be because of the severity of the QUV testing mode, where the UV lamps used emit a significant amount of UV in wavelengths shorter than the solar cut-off of 295 nm (Figure 2-9).

The UV stabilizing performance of the UV absorbers in test is attributed to a light-induced tautomeric isomerization involving an intra-molecular hydrogen bond, e.g., between the ortho-hydroxy group and the carbonyl group in hydroxybenzophenone, that causes a strong UV-absorbance around 330 nm. UV light below 295 nm, however, is predominately absorbed by the aromatic groups in the stabilizer that could participate in photo-oxidation reactions. The products of such reactions (e.g, aldehydes and ketones) may in turn sensitize photo-oxidation of PMMA. Since the QUV testing mode also involves a water condensation cycle on the samples, we checked if water could disturb the intra-molecular hydrogen bond by studying the UV absorbance of dilute aqueous solutions of 2-hydroxybenzophenone at varying pH-values.

No effect on the UV-absorbance spectra could be observed in aqueous solutions up to a pH of 11. However, at pH 12 and above, there is a dramatic shift in both absorbance peaks and in the ratio of the peak maxima. This indicates a pK-value for 2-hydroxybenzophenone somewhere between 11 and 12. Thus, the intra-molecular hydrogen bonding of this UV-absorber does not seem to be affected in water below a pH of 11. Above this value, equilibrium would be shifted to the salt form.

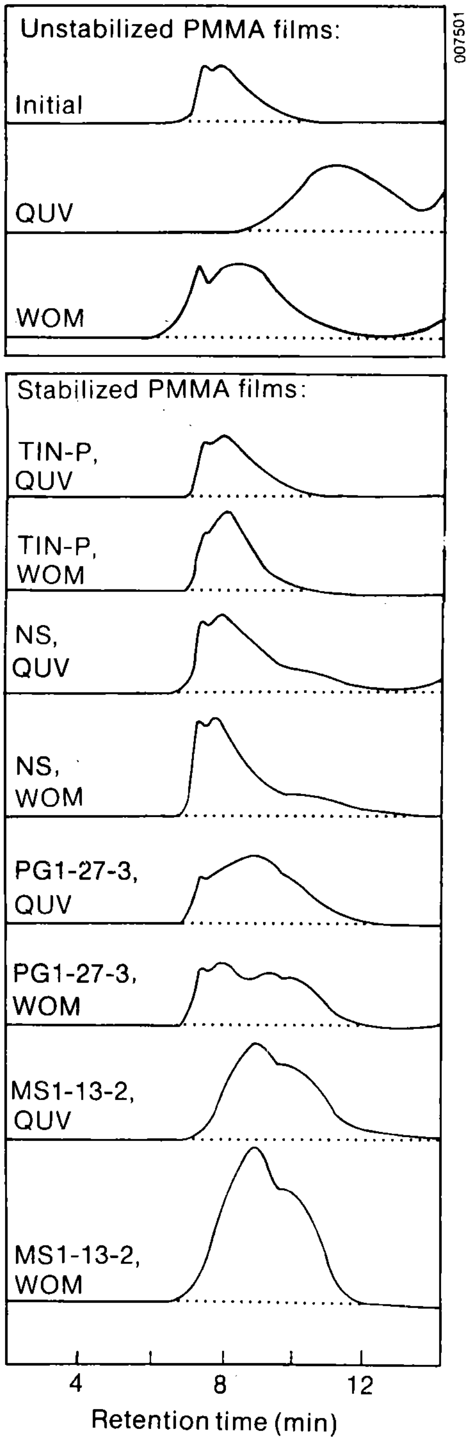

Figure 3-25. GPC Results for PMMA Films After 6 Weeks of Accelerated Weathering in WOM and QUV

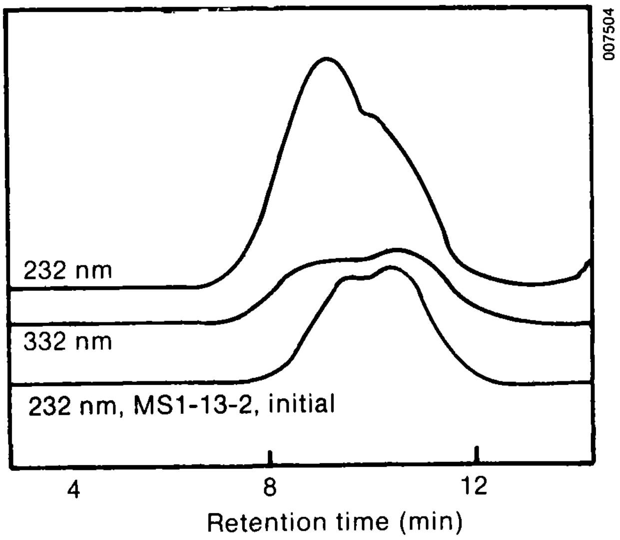

Figure 3-26. GPC Results for a MS1-13-2 Stabilized PMMA Film (R13-100-14) After 6 Weeks of WOM Exposure, Monitored at 232 and 332 nm

The additives tested in the QUV are normally consumed during irradiation according to linear kinetics (Figure 3-28). From the data (Figures 3-28 and 3-24), there is clearly an inverse correlation between the efficiency and consumption rate of the stabilizers. Polymeric stabilizers decompose, in general, in a fashion similar to their low molecular weight analogues, which is evident through losses in their characteristic absorption bands. The only exception is the polymeric stabilizer MS1-13-2 whose decomposition proceeds with a larger rate constant. However, no noticeable molecular weight changes of the polymeric stabilizers can be observed during their consumption (see, for example, Figures 3-26 and 3-27). This may indicate that only cleavage and/or modifications of the pendant stabilizer groups are involved in the consumption process. A detailed investigation of the reactions leading to stabilizer loss is required to indicate which reactions are an essential part of the protective process, and which are side reactions.

3.4.2.2 Extractability of Polymer Additives

To demonstrate the expected increase in physical permanence of the polymeric stabilizers in contrast to their low molecular weight analogues, we performed selected accelerated extraction experiments.

In the Soxhlet-extraction mode, the sample films are washed repetitively with a constant volume of warm water (~75°C) for one week. UV-spectroscopic analysis of the water extracts did not indicate any polymeric SERI stabilizer leaching in the samples tested (Figures 3-29 and 3-30). This is in contrast to a noticeable loss of the commercial polymeric stabilizer (NS) (Figure 3-31) and the low molecular weight stabilizers incorporated in ECP 300 (Figures 3-32 and 3-33).

We observed further that all film samples turned opaque after 1 day in the Soxhlet extractor. Similar opaqueness had been observed earlier on mirror samples taken out of the QUV weathering device during the dew cycle and was explained by the minute water sorption into the polymer films. Whereas the opaqueness in the latter case could be reversed by drying, the opaqueness of the film samples in the Soxhlet remained even after several days of vacuum drying. This opaqueness interfered with the direct monitoring of the stabilizer absorption in the film via transmittance measurements. It is of interest to note that the 3M ECP 300 films developed the highest turbidity of the samples tested and lost their dimensional shape early during the test, whereas the solution cast films retained their dimensions.

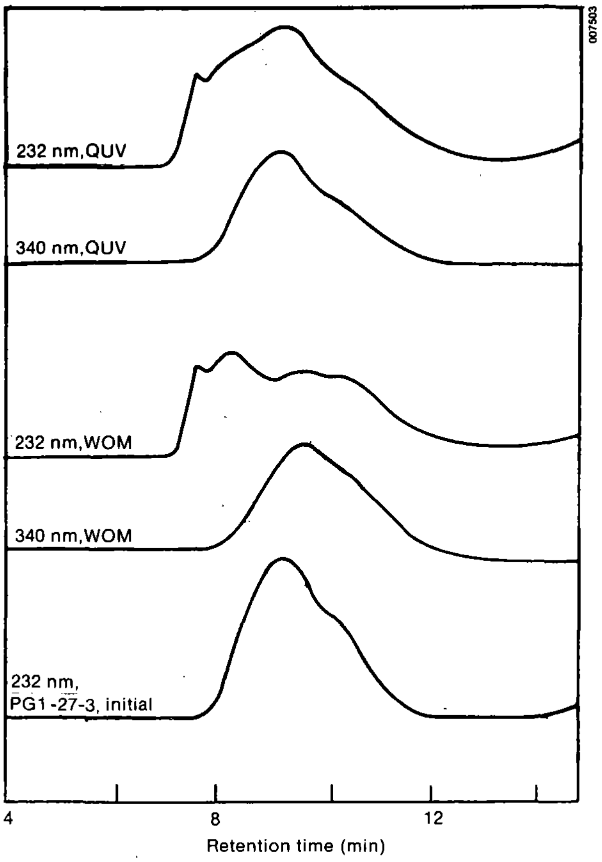

Figure 3-27. **GPC Results for PG1-27-3 Stabilized PMMA Films (R14-145-1) After 6 Weeks of QUV and WOM Exposure, Monitored at 232 and 340 nm**

Similar observations have been made in a more severe extraction test in ethanol at 75°C for 24 h. Although ethanol is a nonsolvent for PMMA, the ECP 300 film disintegrated early with the stabilizer being dissolved in the ethanol. All SERI solution cast PMMA films retained their shape under the same extraction conditions. We repeated the ethanol extraction test at a lower temperature (30°C) for 2 days. Still, the ECP 300 film shrank slightly under these conditions, whereas solution cast films retained their shape. UV-spectra of samples taken from the supernatant ethanol revealed, besides the extractability of all low molecular weight stabilizers (Figures 3-29 to 3-33), that residues of toluene and salts of benzoic acid were present in the solution cast films (characteristic absorbance bands of toluene and benzoic acid appear between 220 and 290 nm in Figures 3-29 and 3-30). It is especially noteworthy that none of the polymeric SERI stabilizers leached out of the films under these extreme conditions (Figures 3-29 and 3-30), whereas the stabilizers used in ECP 300 showed considerable leaching (Figures 3-32 and 3-33). The commercially available polymeric product (NS) exhibited an extractable component that may be attributable to residual monomers or oligomers in this sample (Figure 3-31).

3.4.3 UV and No-UV Effects

In the accelerated weathering studies, samples can be mounted so that a portion of each sample is shielded from UV light by an aluminum panel or an ECP 300 filter, while the whole sample is exposed to the temperature and humidity conditions. As described in

Section 3.4.1.1, the sample portions exposed to UV virtually always degrade optically more rapidly than the portions protected from UV. Since UV is known to degrade silver and PMMA, it is evident that the role of the stabilizer has been to diminish, if not eliminate, the problem. Of interest is the observation that UV screening by an ECP 300 filter is almost as effective as an aluminum panel shield in preventing PMMA and stabilizer degradation (Figures 3-34 and 3-35). The need for arranging a nonvolatile UV absorber as close to the film/air surface as possible is clearly recognized. Another challenge is the ability to incorporate a UV stabilizer that is also nondegradable without altering the desired transmittance properties of the PMMA. Encouraging in this regard is the good performance of polymer films with non-UV-absorbing hindered piperidine stabilizers during their first week of exposure time in the weathering devices (results of this series will be reported in the next annual report).

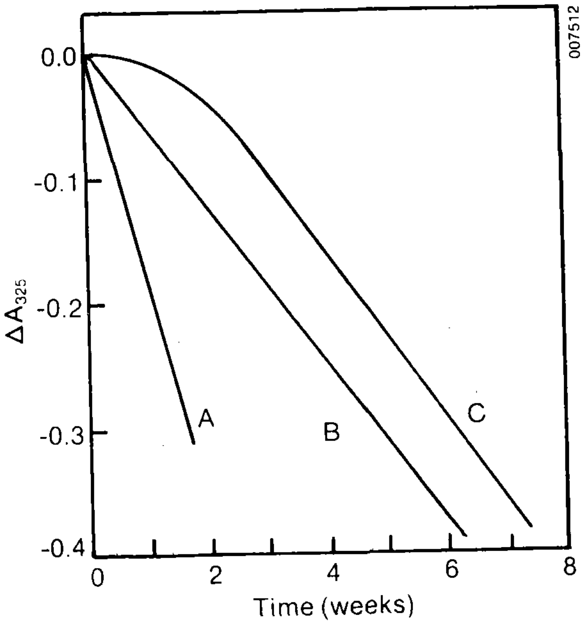

Figure 3-28. Changes in Absorbance of Stabilized PMMA Films at 325 nm After Exposure in a QUV: PMMA + MS1-13-2 (A), PMMA + PG1-27-3 (B), and PMMA + NS (C).

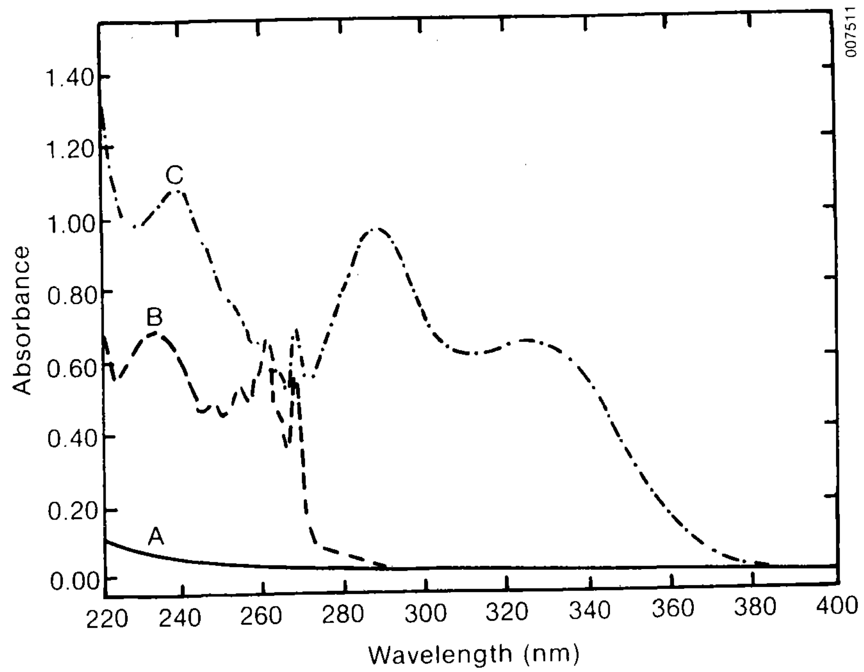

Figure 3-29. Ultraviolet Spectra from Extraction Studies of o-Hydroxybenzophenone Stabilized PMMA Films: Soxhlet Extract (water, 75°C) from PMMA/SERI MS1-35-2 (A), Ethanol Extract (30°C) from PMMA/SERI MS1-35-2 (B), and Ethanol Extract (30°C) from PMMA/Uvinul 408 (C)

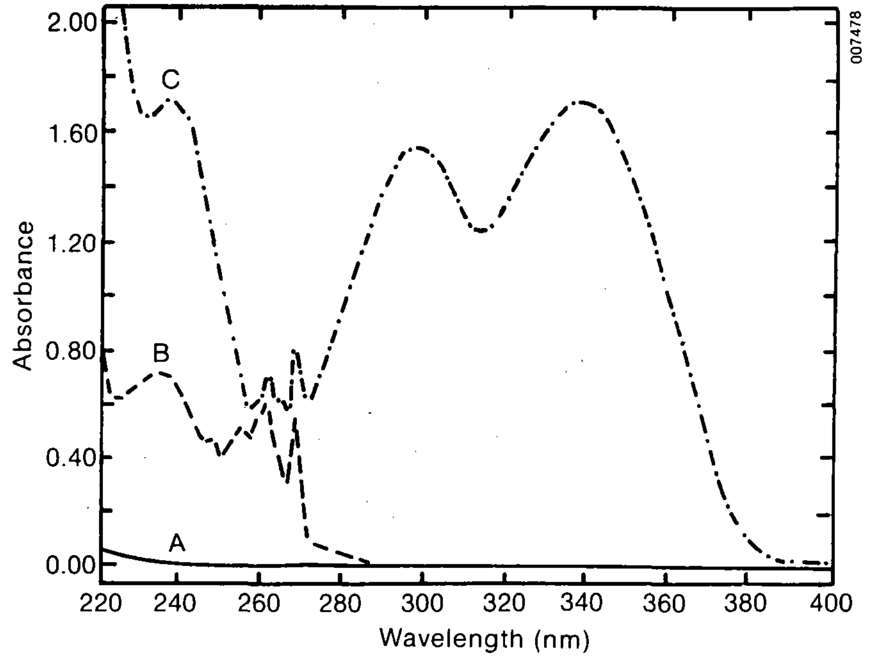

Figure 3-30. Ultraviolet Spectra from Extraction Studies of o-Hydroxybenzotriazole Stabilized PMMA Films: Soxhlet Extract (water, 75°C) from PMMA/SERI PG1-27-3 (A), Ethanol Extract (30°C) from PMMA/SERI PG1-27-3 (B), and Ethanol Extract (30°C) from PMMA/Tinuvin P (C)

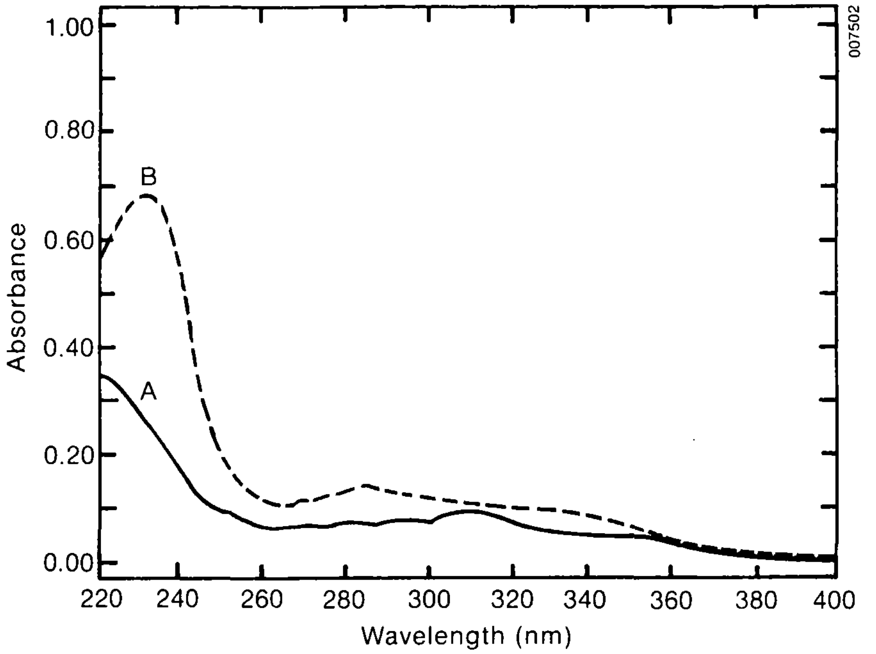

Figure 3-31. Ultraviolet Spectra from Extraction Studies of National Starch Stabilized PMMA Films: Soxhlet Extract (water, 75°C) (A), and Ethanol Extract (30°C) (B)

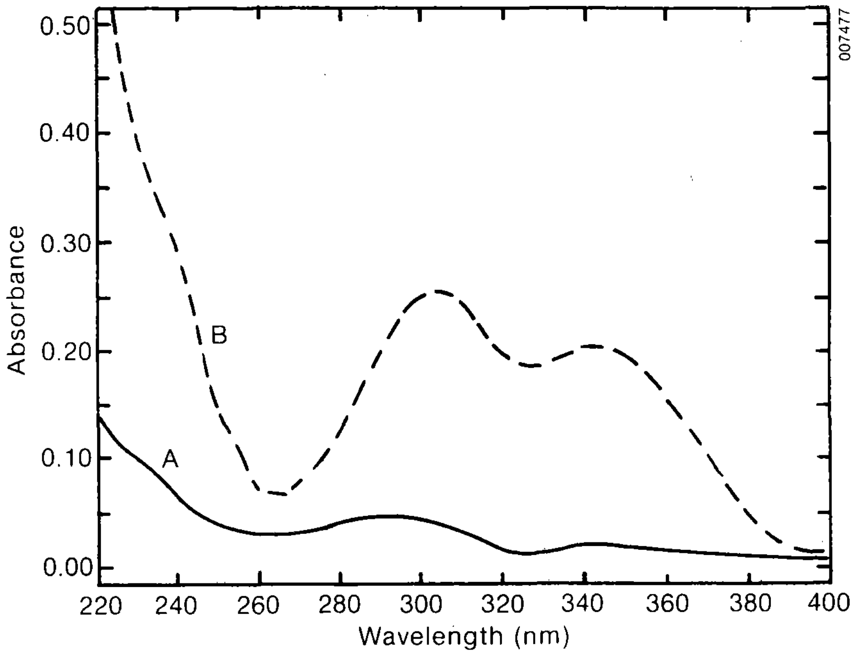

Figure 3-32. Ultraviolet Spectra from Extraction Studies of ECP 300 (Lot X09083): Soxhlet Extract (water, 75°C) (A), and Ethanol Extract (30°C) (B)

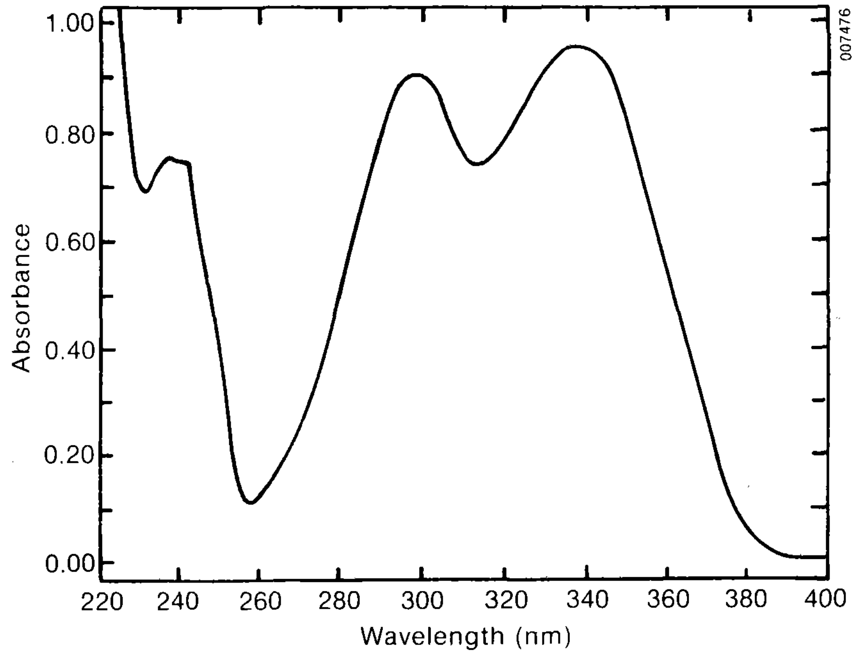

Figure 3-33. Ultraviolet Spectrum from Ethanol Extraction Study (30°C) of ECP 300 (Lot X09082)

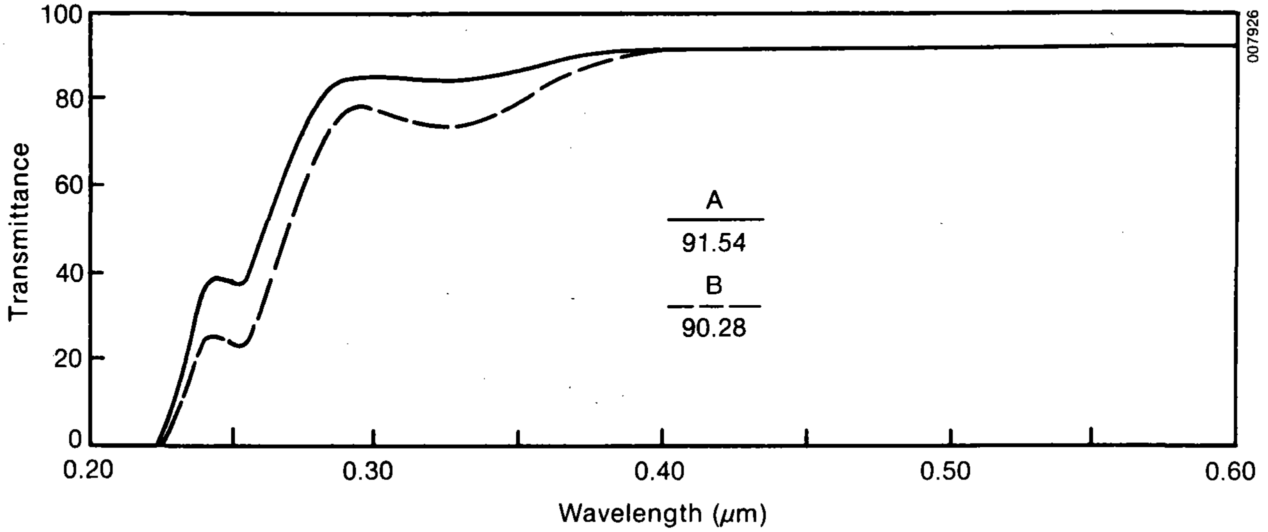

Figure 3-34. Changes in the Transmittance Spectrum Between 200 and 600 nm After 6 Weeks of QUV Exposure for Shielded (A) and Filter Screened (B) Unstabilized PMMA Films (13-25 μm thickness). (Unshielded PMMA films disintegrated after 3 weeks of QUV exposure.)

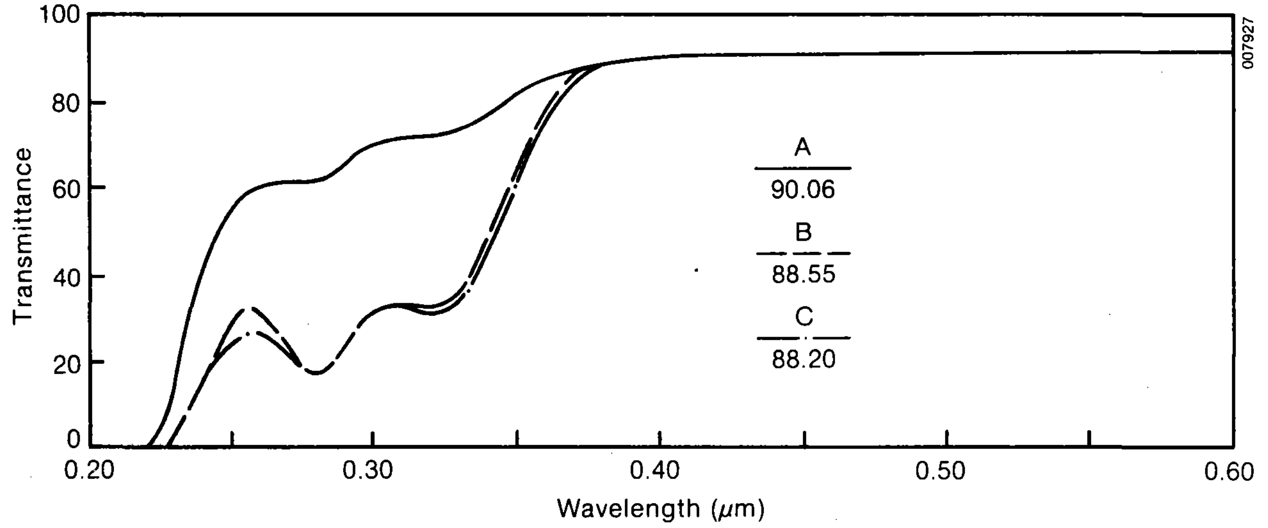

Figure 3-35. Changes in the Transmittance Spectrum Between 200 and 600 nm After 6 Weeks of QUV Exposure for Unshielded (A), Shielded (B), and Filter Screened (C) NS-Stabilized PMMA Films (13-25 μm thickness)

3.4.4 Preparation of Macromolecular Stabilizers

Polymerizable stabilizers have been copolymerized with methyl methacrylate (MMA) with the intention of increasing not only the light stability and permanence but also the compatibility of the stabilizer with the substrate PMMA.

3.4.4.1 Copolymers Involving MMA and Polymerizable 2-Hydroxybenzophenone UV Stabilizers

Copolymerization of 4-methacryloxy-2-hydroxybenzophenone (MHB) with MMA has been accomplished according to the general reaction in Figure 3-36 with AIBN as an initiator. The free phenolic hydroxyl group present in the polymerization mixture does not inhibit the polymerization if oxygen is rigorously excluded from the reaction mixtures. As a consequence, all our polymerizations had to be performed under nitrogen after thorough degassing by several freeze-thaw cycles.

Table 2-4 shows the conditions for some selected polymerization experiments. All polymers could be isolated as solid, white, and mostly powdery compounds.

Table 3-5 lists some characteristics of the resulting polymers. Molecular weights were determined by means of gel permeation chromatography. Under the polymerization conditions chosen, copolymers with average molecular weight values ($\bar{M}_n$) from 16,000 to above 100,000 could be synthesized.

The copolymerizations of MHB were carried out with feed ratios of 0.4 to 8.5 mol% of MHB in the mixtures. The obtained polymer yields ranged from 60% to 79% with incorporation of 0.4 to 9.4 mol% of MHB indicating that MHB is favorably incorporated into the copolymers. The composition of all copolymers was established by measurements of the ultraviolet spectra of the polymers (assuming no change in the extinction coefficient of 5.744×10^3 L/mol cm at $\lambda = 332$ nm during copolymerization).

The UV absorption spectrum of a representative p-MMA-co-MHB sample (MS1-49-3) is reproduced in Figure 2-8. All the spectra are characterized by two absorption bands, i.e., at $\lambda_{1,max}=270$ nm and $\lambda_{2,max}=332$ nm. The absorption band at the longer wavelength, which is attributed to the intramolecular hydrogen bond in the 2-hydroxybenzophenone molecule, remains preserved upon polymerization. The absorbance at 400 nm is practically zero. The spectra are, therefore, analogous to the spectra of low-molecular-weight 2-hydroxybenzophenone derivatives, although the absorption band at the shorter wavelength is shifted to shorter wavelengths (287→270 nm).

3.4.4.2 Copolymers Involving MMA and Polymerizable 2,2,6,6-Tetramethylpiperidine Light Stabilizers

Copolymerizations of 4-methacrylamido-2,2,6,6-tetramethylpiperidine (MAP) and N-methacryloxyethyl, N'-(2,2,6,6-tetramethyl-4-piperidyl) urea (MAP-E) with MMA were accomplished according to the general reaction shown in Figure 3-36 with AIBN as an initiator, although amino and imino groups can act as inhibiting or retarding substances in radical polymerizations. However, it is believed that the steric screening of the imino-nitrogen by the four methyls contributes to the polymerizability of this class of compounds.

Polymerization conditions are summarized in Table 2-6. The copolymerizations of MAP were carried out with feed ratios of 2.3 and 6.6 mol% of MAP in the mixtures. The resulting copolymers (yield about 55%) had 2.4 and 4.8 mol% MAP incorporated.

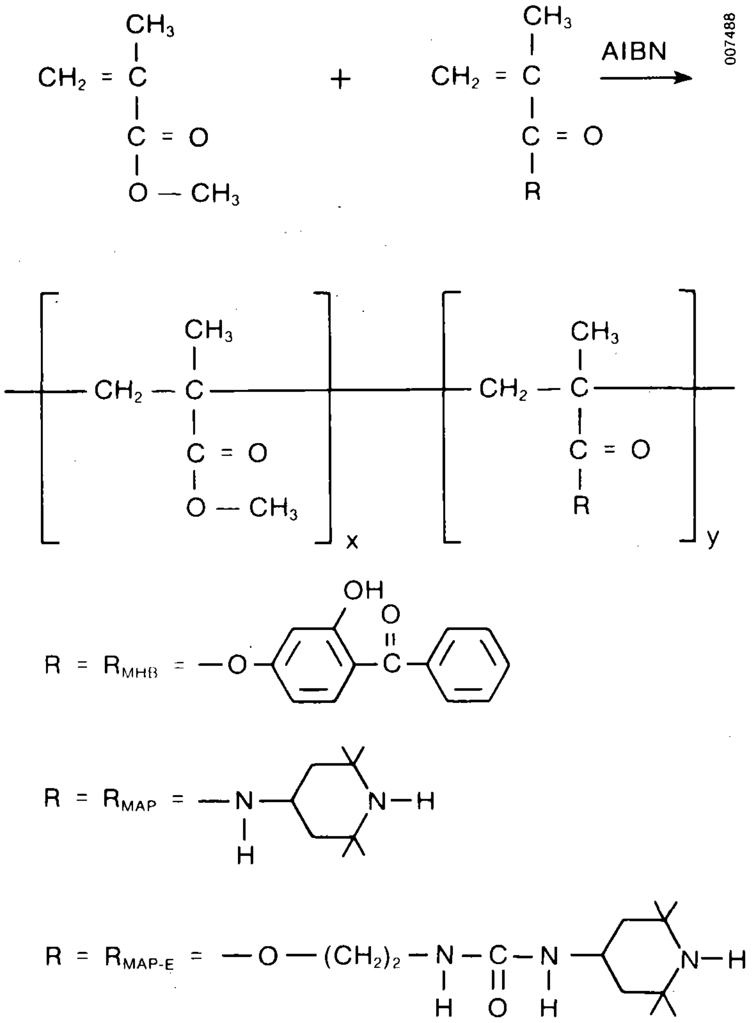

Figure 3-36. Copolymerization Reaction Scheme

The polymerizable stabilizer MAP-E contains a C_2-spacer group connected to the piperidine moiety via a urea group on one end and to a methacryloxy group on the other end. This is in contrast to the much shorter amide group connection in the MAP stabilizer. Copolymerizations of MAP-E with MMA (feed ratios from 0.3 to 15.8 mol% MAP-E) gave polymers with average molecular weight values ($\bar{M}_n$) of 5,400 and 6,700, respectively. There is evidence from the GPC-results that an oligomeric fraction is present in these samples. Further characterization of these copolymers is in progress. However, it could be observed that higher feed ratios (> 8 mol% MAP-E) lead to cross-linked products.

Table 3-5. Characteristics of Selected Copolymers of MMA and MHB

Sample #	$\overline{M}_w \times 10^{-3}$	$\overline{M}_n \times 10^{-3}$	$\overline{M}_w/\overline{M}_n$	MHB wt %	MHB mol %
MS1-132	38	19	2.0	12.3	4.7
MS1-11-5	50	29	1.7	16.2	6.4
MS1-30-1	131	48	2.7	17.0	6.8
MS1-30-2	239	151	1.6	16.9	6.7
MS1-35-1	44	25	1.8	15.9	6.3
MS1-35-2	72	38	1.9	14.5	5.7
MS1-35-3	124	56	2.2	15.0	5.9
MS1-49-1	33	22	1.5	1.1	0.4
MS1-49-2	35	23	1.5	6.1	2.2
MS1-49-3	26	17	1.5	11.0	4.2
MS1-49-4	49	26	1.9	22.7	9.4

3.4.4.3 Copolymers Involving MMA and Polymerizable 2-Hydroxybenzotriazole UV Stabilizers

3,5[di(2H-benzotriazole-2-yl)]2, 4-dihydroxy acetophenone (DBAP) has been synthesized in good yield and was transformed successfully in four steps to 2(2,4-dihydroxy-5-vinylphenyl)1,3-2H-dibenzotriazole (DBDH-5V) and 2(2,4-dihydroxy-5-isopropenylphenyl)1,3-2H-dibenzotriazole (DBDH-5P), respectively (Figure 3-37).

The synthesis route used followed essentially the procedure of Vogl and his associates [13]. However, some reaction solvents and conditions were modified to improve yields. The monomer (DBDH-5V) containing the vinyl group was found to spontaneously homopolymerize during the dehydration reaction in the absence of the radical scavenger, picric acid, normally added to the reaction mixture.

DBDH-5V and DBDH-5P were copolymerized with MMA in the presence of AIBN as initiator (0.3 mol%) in a mixture of toluene and dimethylacetamide as solvents. The reaction conditions for the copolymerizations are described in Table 2-5. A feed ratio of 5, 10, and 20 w% of each stabilizer monomer in MMA (corresponding to 1.3, 2.8, and 6.1 mol%, respectively) was used in the copolymerizations. Yields above 90% were obtained for the p-MMA-co-DBDH-5P series, and yields of 72%-76% were obtained for the p-MMA-co-DBDH-5V series. Incorporation of the functional monomers was normally below the amount present in the initial monomer feed, more so for DBDH-5V than for DBDH-5P. The composition of all copolymers was established by elemental analysis of nitrogen and was checked by measurements of the ultraviolet spectra of the polymers. The p-MMA-co-DBDH-5V series showed a λ_{max} of 327 nm (same as DBDH-5V) and extinction coefficients of 3.0-3.2 × 10^4 L/mol cm. The p-MMA-co-DBDH-5P series showed a λ_{max} of 332 nm (same as DBDH-5P) and extinction coefficients of 3.9-4.0 × 10^4 L/mol cm. The

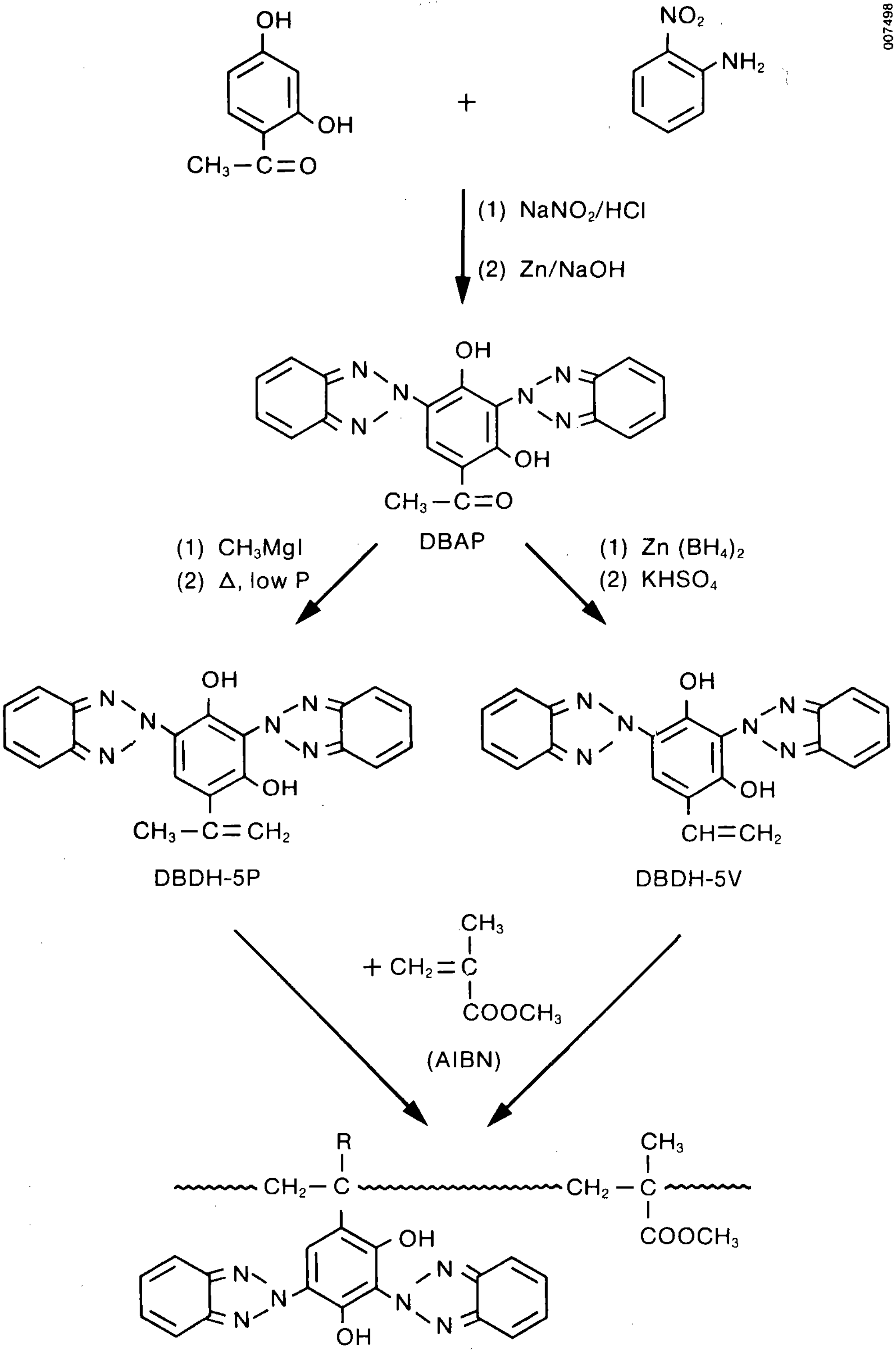

p - MMA - co - DBDH - 5P (R = CH_3)
p - MMA - co - DBDH - 5V (R = H)

Figure 3-37. Reaction Scheme for the Preparation of p-PMMA-co-DBDH-5P and p-MMA-co-DBDH-5V extinction coefficients of the copolymers did not differ very much from the ones of the corresponding monomers. The slight variations are not very significant and are within our experimental error limits.

The synthesis of the monosubstituted stabilizers 2(2-hydroxy-4-methacryloxyphenyl)2H-benzotriazole (BDHM) and its allyloxy analogue BDHAO were carried out according to Figure 3-38 [14].

These polymerizable stabilizers contain ester and ether linkages, respectively, as opposed to the vinyl and isopropenyl groups of DBDH-5V and DBDH-5P. The synthesis of BDHM and BDHAO proceeded in high yields (60%) in three steps from o-nitroaniline and resorcinol.

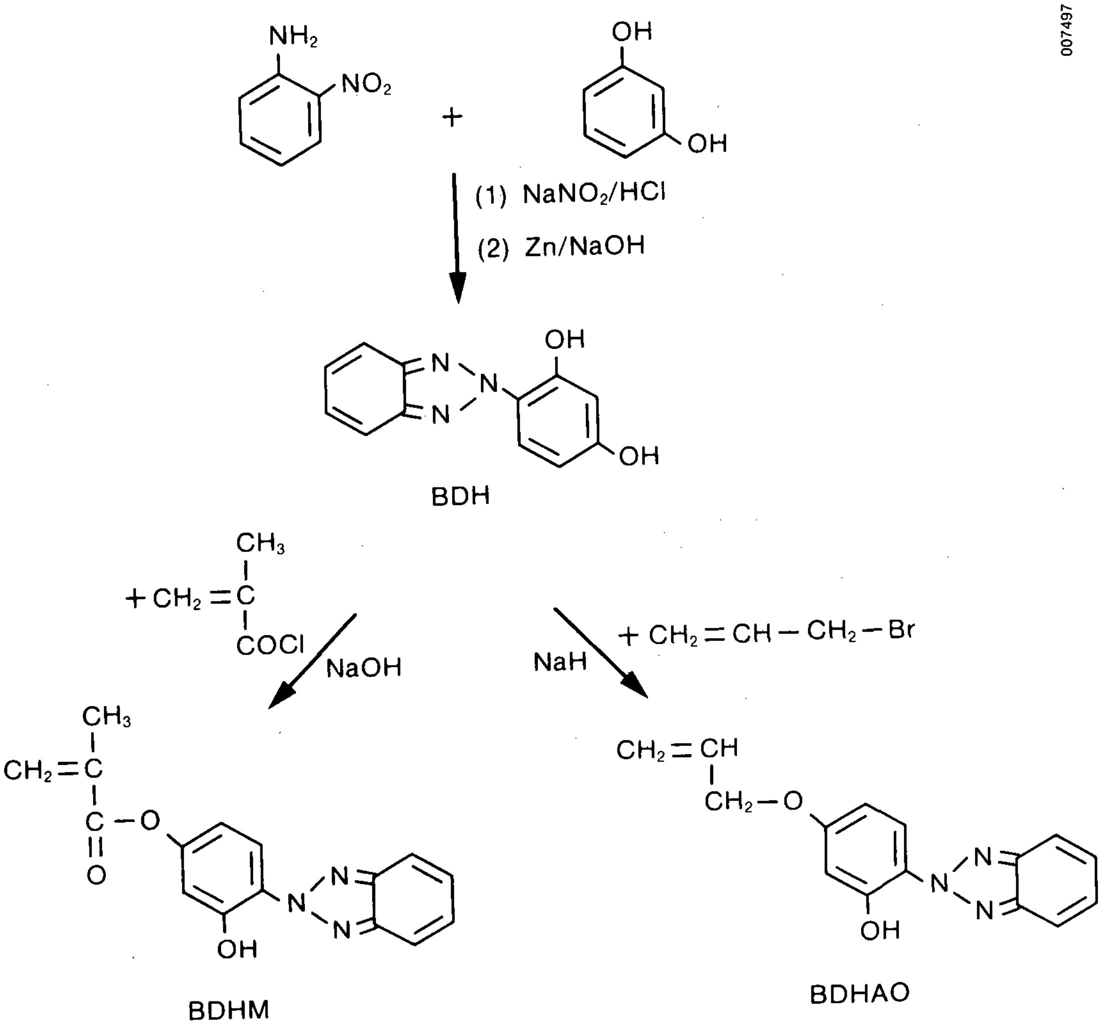

Figure 3-38. Reaction Scheme for the Preparation of BDHM and BDHAO

BDHM was copolymerized with MMA with AIBN as initiator with 5, 10, and 20 mol% in the feed ratio (corresponding to 16, 28, and 47 w%) (Table 2-5). The polymer yields were about 85%. The UV spectra of the copolymers showed incorporation of 4.7, 9.2, and 14.8 mol% BDHM, respectively, with λ_{max} at 335 nm.

BDHAO was copolymerized with MMA in a 5 mol% feed. Characterization of this polymer is in progress.

3.4.4.4 *Incorporation of Ultraviolet Light Stabilizers into PMMA Prepared by Group Transfer Polymerization*

A recently introduced technique [34-37] for the polymerization of acrylics, Group Transfer Polymerization (GTP), offers several advantages over conventional methods. Thus, well-defined low molecular weight (1000-20,000) acrylics of narrow molecular weight distribution can be prepared that may contain functional groups that are normally reactive in polymerization by free radical methods, such as vinyl or allyl moieties. In addition, functional end groups can be introduced either by incorporating them in the GTP initiator or by coupling of the silyl ketene acetal reactive end groups of the growing chain to a functionalized bromide or tosylate [38]. However, active hydrogen compounds, such as free hydroxyl groups, normally lead to termination of GTP. We attempted, during this reporting period, the introduction of UV stabilizers based on 2(2-hydroxyphenyl)2H-benzotriazole and 2-hydroxybenzophenone into GTP-prepared PMMA by copolymerization of their methacryloxy derivatives and by an endcapping reaction with 2[2-hydroxy-4-(3-bromopropoxy)phenyl]2H-benzotriazole.

The polymerizable UV light stabilizer 2(2-hydroxy-4-methacryloxyphenyl)2H-benzotriazole (BDHM) (Figure 3-39) was previously prepared by Vogl and his associates [39] and

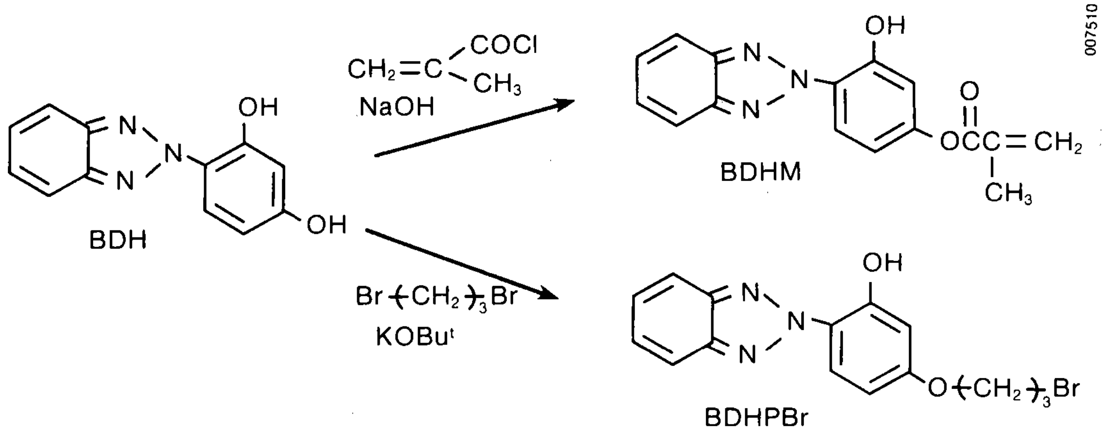

Figure 3-39. Reaction Scheme for the Preparation of BDHM and BDHPBr

successfully copolymerized by free radical methods with styrene and various acrylics. However, it was anticipated that introduction of BDHM into a living GTP mixture without prior masking of the 2-hydroxy group would lead to termination of the growing silyl ketene acetal end groups. Attempts at masking this hydroxyl as the trimethylsilyl ether by reaction of BDHM with common silylating agents such as trimethylsilyl chloride, hexamethyldisilazane and even bis(trimethylsilyl)acetamide proved to be unsuccessful. This was presumably because of the strong intramolecular hydrogen bonding present between the 2-hydroxyl and the nitrogen on the benzotriazole ring system (which is necessary for the structure to function as a UV stabilizer). This resistance of the 2-hydroxyl group to silylation led to an experiment in which 1 mole equivalent of the model compound 2(2-hydroxy-4-methylphenyl) 2H-benzotriazole (Tinuvin-P, Ciba Geigy) was introduced into a living PMMA GTP mixture followed by an additional amount of MMA after stirring for 15 min. GPC traces of the polymer sample before and after addition (see Figure 3-40) of the second batch of MMA showed virtual doubling of the MW from M_n = 1520 to M_n = 2940, as predicted from the amount of MMA added. Hence, no termination by the hydroxyl protons was apparent.

Next, the polymerizable UV stabilizers BDHM and 4-methacryloxy-2-hydroxybenzophenone (MHB) (which contains a hydroxyl group intramolecularly hydrogen bonded to a carbonyl) were introduced in a similar fashion to living GTP PMMA followed by additional MMA to theoretically double the molecular weight (Figure 3-41). MW changes were determined by setting the GPC detector wavelength at 232 nm for PMMA absorption and at 332 nm for MHB (Figure 3-42). The broader distribution observed at 232 nm as compared to that observed at 332 nm indicates that some termination occurred when MHB was added. However, this could also be because of trace impurities in the monomer.

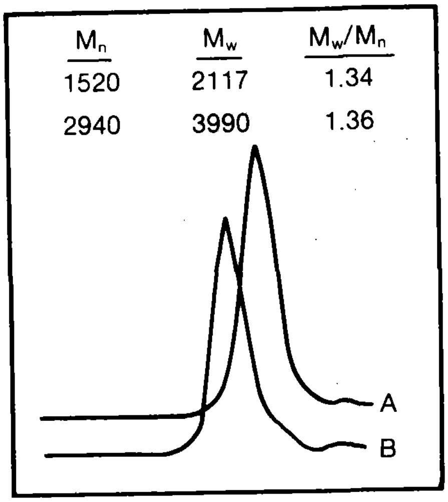

A - 10 g MMA + 10 mmol initiator (predicted MW = 1000)
B - After addition of (Tinuvin-P) followed by 10 g MMA

Figure 3-40. GPC Traces of a GTP Polymer (A) Before, and (B) After Addition of Tinuvin P Followed by a Second Batch of MMA

A similar result was obtained for the incorporation of BDHM. A UV spectrum of the PMMA-co-BDHM (Figure 3-43) after purification by precipitation in methanol, showed the expected λ_{max} at 335 nm. As a comparison, the spectra of pure BDHM and PMMA-co-BDHM obtained by free radical polymerization are included. All spectra were measured at 2×10^{-5} mol/L stabilizer concentration (assuming 100% of the feed is incorporated in the copolymer and extinction coefficients remain constant). Thus, the lower extinction coefficient for the copolymer via GTP indicates that approximately 70% of the BDHM in the feed was incorporated.

Another way of incorporating 2(2-hydroxyphenyl) 2H-benzotriazoles was by termination of the GTP PMMA with the bromide, 2[2-hydroxy-4-(3-bromopropoxyl) phenyl] 2H-benzotriazole (BDHPBr). BDHPBr was

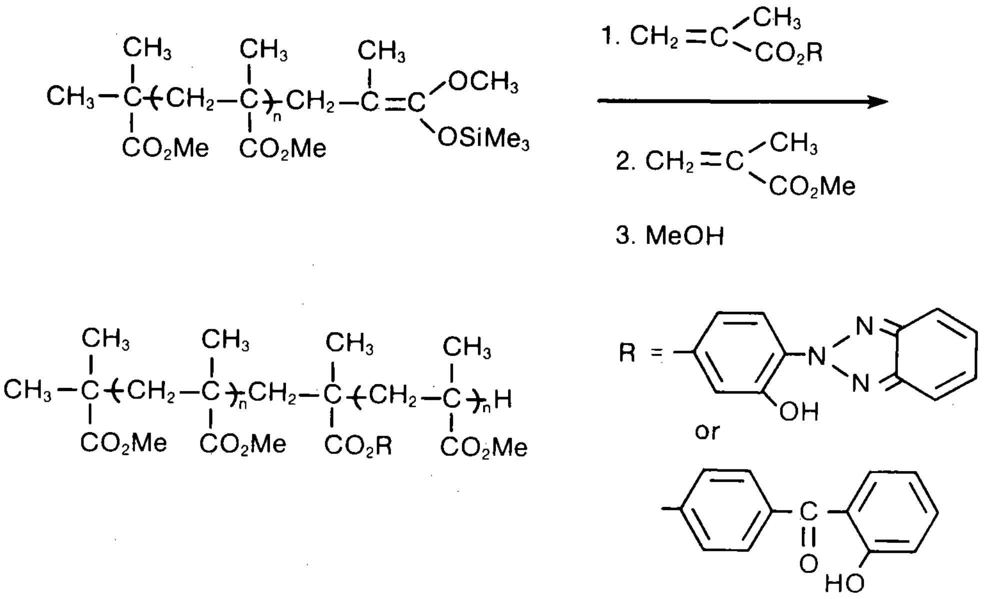

Figure 3-41. Reaction Scheme for the Incorporation of UV Stabilizers into PMMA Prepared by Group Transfer Polymerization

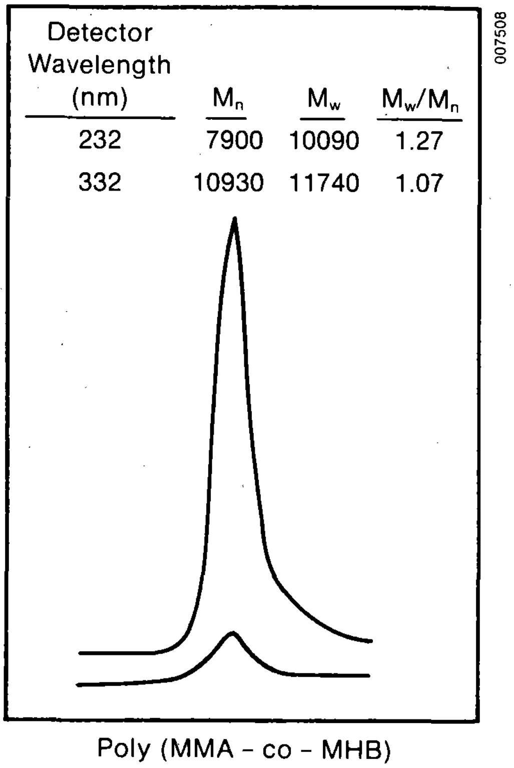

Detector Wavelength (nm)	M_n	M_w	M_w/M_n
232	7900	10090	1.27
332	10930	11740	1.07

Figure 3-42. GPC Results for a GTP Polymer with Incorporated MHB

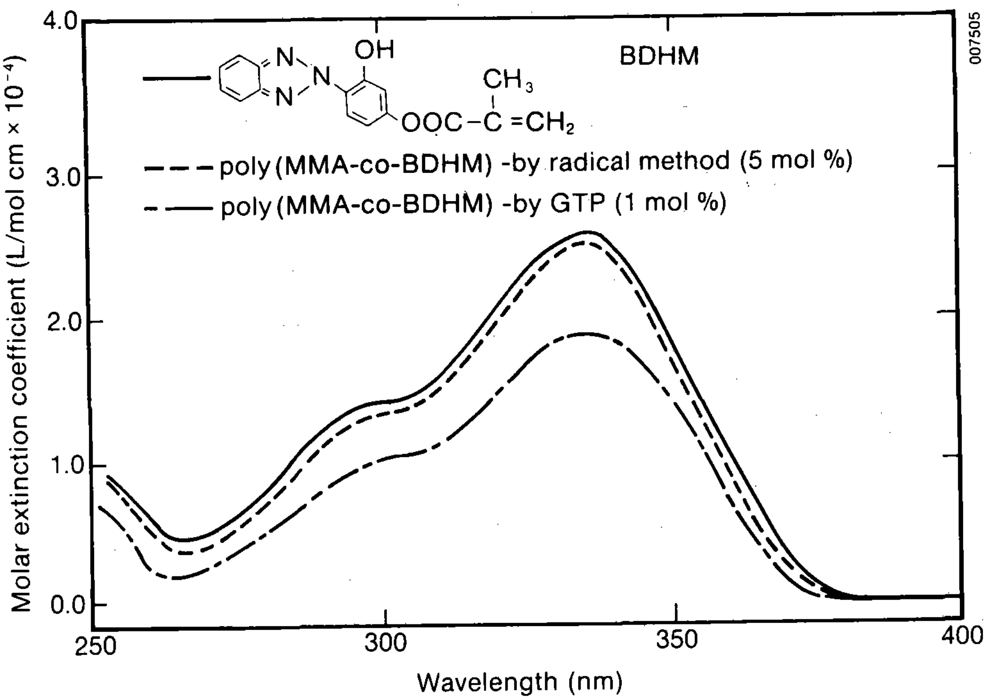

Figure 3-43. Ultraviolet Spectra of BDHM and p-MMA-co-BDHM

prepared in 65% yield by selective alkylation of the free -OH group in BDH with dibromopropane (Figure 3-44) in the presence of the base potassium-t-butoxide. Its UV spectrum (Figure 3-45) showed the characteristic absorption of the hydrogen bonded -OH in an α-position relative to a benzotriazole ring with λ_{max} at 344 nm. GPC results of the copolymer after incorporation (Figure 3-46) showed M_n of 5740 at detector wavelength 232 nm and M_n of 6300 at the benzotriazole absorption of 344 nm. The content of the 2(2-hydroxyphenol)2H-benzotriazole end groups as determined from the UV spectrum (Figure 3-45) indicated that only 55% of the PMMA contained the functional end groups. Incomplete coupling could be because of loss of living ends of PMMA before addition of BDHBr or side reactions with impurities introduced during addition of BDHBr.

In conclusion, polymerizable UV stabilizers based on 2(2-hydroxphenyl)2H-benzotriazoles and 2-hydroxybenzophenones containing unmasked, intra-molecularly hydrogen bonded hydroxyl groups can be readily copolymerized with acrylic type monomers by GTP. In other experiments, hindered hydroxyl protons of stabilizers based on 2,6-di-tert-butylphenols (in the form of Goodrite 3125) and hindered amine protons of 2,2,6,6-tetramethylpiperidine derivatives (in the form of Goodrite 3034) were found to be too labile when added to living PMMA mixture; in the case of hindered phenol, a yellow color formation in the GTP mixture was indicative of the formation of the phenoxide anion.

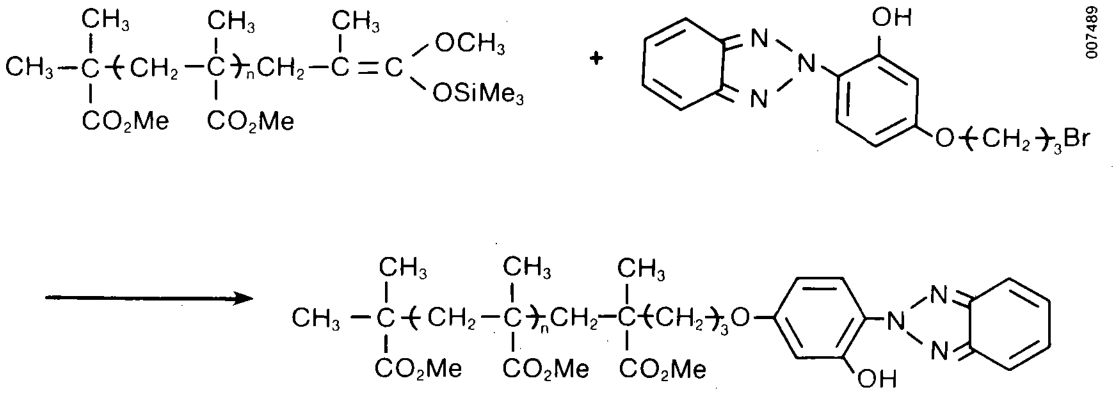

Figure 3-44. Reaction Scheme for the Coupling of BDHPBr to a PMMA prepared by Group Transfer Polymerization

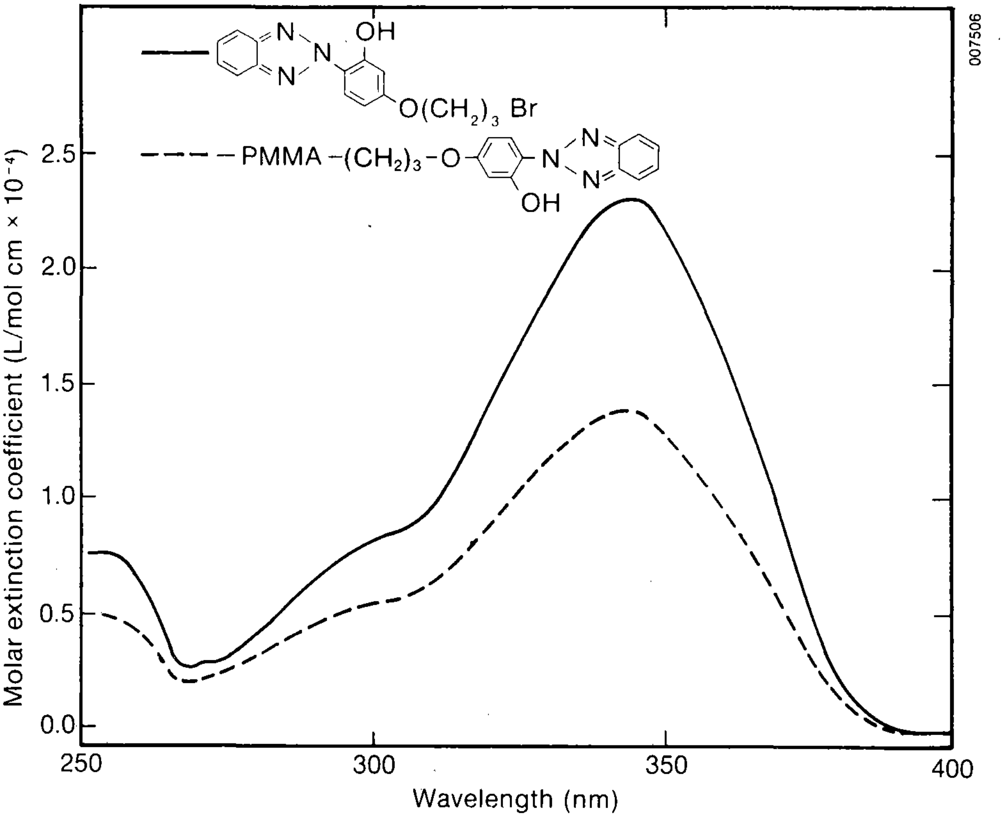

Figure 3-45. Ultraviolet Spectra of BDHPBr and PMMA Endcapped with BDHPBr

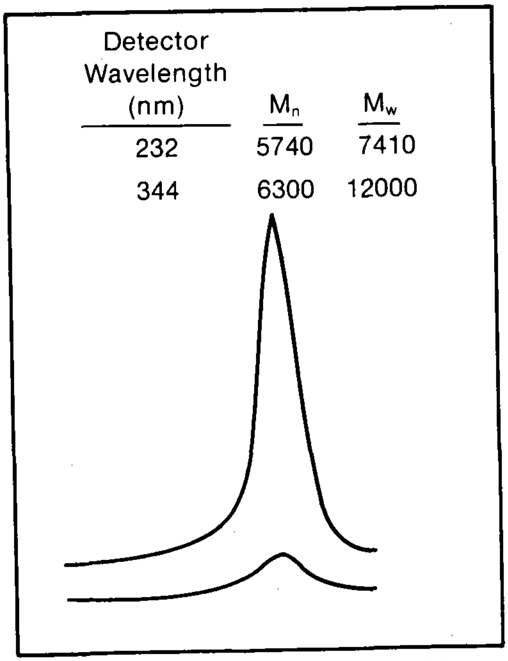

Detector Wavelength (nm)	M_n	M_w
232	5740	7410
344	6300	12000

PMMA Endcapped with BDHPBr

Figure 3-46. GPC Results for a GTP-PMMA Endcapped with BDHPBr

4.0 CONCLUSIONS AND RECOMMENDATIONS

The most significant results for this project are the following:

- We designed and constructed a state-of-the-art specular reflectometer.
- We have proved that both the initial specular reflectance and initial specularity of silvered polymers can greatly exceed the long-range goals.
- We demonstrated that optical goals can be exceeded when the silvered polymer is mounted with an adhesive onto a firm, flat, smooth substrate or when the silvered polymer is stretched in a membrane configuration.
- Outdoor weathering tests in Colorado show that silvered polymers resist corrosion for nearly 3 years, and tests are continuing.
- Further tests in Colorado show that the long-term performance goals (reflectance greater than 90% into a 4 mrad acceptance angle for 5 years) are maintained for nearly 1 year and tests are continuing.
- UV stabilizers added to the polymer impede the degradation of polymer glazings and of polymer/silver mirrors.
- Polymerizable stabilizer monomers of the hydroxy-benzophenone, hydroxy-benzotriazole, and hindered amine classes have been successfully synthesized and copolymerized with methyl methacrylate.
- We have demonstrated that the copolymeric SERI stabilizers minimize physical loss of UV screening agents from polymer films.
- Despite the high inherent UV stability of the UV absorbers tested, we observe a deactivation of the stabilizers in film surfaces, which is similar for polymeric and low-molecular-weight species. Deactivation is slow enough not to limit mirror lifetimes outdoors for at least several years; however, it may become a factor after more prolonged use.

Further results include the following:

- Mirrors mounted on painted aluminum are more durable than those mounted on unpainted aluminum both during outdoor exposure in Arizona and during some accelerated tests at SERI.
- Initial experiments show that hard-coated silvered polymer mirrors are more scratch resistant and durability tests are encouraging.
- The adhesion between PMMA and silver deteriorates in the presence of moisture but regains the initial adherence when dried. The lower adherence may be a problem for some applications.
- Mirror corrosion can be site specific; for example, Sandia reports substantial corrosion for silvered polymers outdoors at Solar One for about 2 years. Similar corrosion is not yet seen in Colorado, Arizona, Florida, or Minnesota.
- Outdoor exposures in Arizona and Florida are harsher than in Colorado or Minnesota; outdoor tests in Arizona show deterioration of reflectance below long-range goals; however, improved stabilizers enhance performance in Arizona.
- A new polymerization technique (group transfer polymerization) has been successfully used to introduce UV-stabilizers as end groups to PMMA.

- UV absorption bands and extinction coefficients of the monomeric stabilizers are preserved upon polymerization.

The results of this investigation suggest the following additional work to be done:

- Exploit the similarity in the degradation of optics in accelerated tests and outdoors in Arizona to understand the causes and cures of optical deterioration.
- Extend the chemistry to address surface coatings that are anti-soiling and/or more easily cleaned.
- Extend the favorable results with scratch-resistant coats to incorporate polymeric UV screens in fluorinated, hard-coated surface layers to attain optimum placement of a nonleachable UV screen in a soil-resistant, cleanable surface coat.
- Extend optical measurements to soiled surfaces.
- Elucidate the interfacial corrosion constituents as observed in test mirrors at Solar One to understand causes and cures.
- Elucidate factors controlling adherence between PMMA and silver.
- Exploit the observations on solvent effects to enable fabricators to roll coat protective coatings with performance comparable to extruded films.
- Elucidate the process factors that control polymer film smoothness and mechanical properties to enable fabrication of inexpensive, all-polymer membrane mirrors that are not limited in performance by a metal backing membrane.
- Continue optimization of polymeric stabilizer systems to attain the long-term goals for durability and maintenance of high specularity over the required life.

5.0 REFERENCES

1. U.S. DOE, *Solar Thermal Energy Systems, Annual Evaluation Report FY 1984*, July 1985 (available from NTIS).
2. Nine papers, *Solar Energy Materials*, Vol. 3, 1980, pp. 117-224.
3. Thomas, T. M., J. R. Pitts, and A. W. Czanderna, *Appl. Surface Sci.*, Vol. 15, 1983, p. 75.
4. Murphy, L. M., J. V. Anderson, W. D. Short, and T. J. Wendelin, *System Performance and Cost Sensitivity Comparison of Stretched Membrane Heliostat Reflectors with Current Generation Glass/Metal Concepts*, SERI/TR-253-2694, Golden, CO: Solar Energy Research Institute, Dec. 1985.
5. Brauman, S. K., D. B. MacBlane, and F. R. Mayo, *Reactivity of Polymers with Mirror Materials*, Golden, CO: Solar Energy Research Institute, SRI International, Menlo Park, CA.
6. Schissel, P., H. H. Neidlinger, and A. W. Czanderna, *Polymer Reflectors Research During FY 1985*, SERI/PR-255-2835, Golden, CO: Solar Energy Research Institute, May 1986.
7. Susemihl, I., and P. Schissel, "Specular Reflectance Properties of Silvered Polymer Materials," *SPIE 30th Annual International Technical Symposium on Optical and Optoelectronic Applied Sciences and Engineering*, Bellingham, WA: SPIE August 1986, Proceedings forthcoming.
8. Susemihl, I., and G. Lensch, *Untersuchungen zur Lichtstreuung in der Naehe des gerichteten Strahls mittles hochaufloesendem Spektral - und Gonioreflektometer an Scheiben und Spiegeln fuer Solarenergieanlagen und Literaturauswertung zum Thema*, internal report No. 7/85, FH Wedel, West Germany, 1985.
9. Hampton, H. L., J. S. Hartman, and M. A. Lind, "Specularity Measurements by Fourier Transform Examination," IES Solar Seminar on *Testing Solar Energy Materials and Systems*, Gaithersburg, MD, May 22-24, 1978.
10. Pettit, R. B., and E. P. Roth, *Solar Mirror Materials: Their Properties and Uses in Solar Concentrating Collectors*, SAND-79-2190, Albuquerque, NM: Sandia National Laboratories, June 1980.
11. Pettit, R. B., "Characterization of the Reflected Beam Profile of Solar Mirror Materials," *Solar Energy*, Vol. 19, 1977, pp. 733-741.
12. Muir, J. F., ed., *Proceedings of the Distributed Receiver Solar Thermal Technology Conference*, SAND84-2454, Albuquerque, NM: Sandia National Laboratories, April 1985.
13. Fu, S., A. Gupta, A. C. Albertsson, and O. Vogl, "New Polymerizable 2 (2-Hydroxyphenyl) 2H-Benzotriazole Ultraviolet Absorbers: 2[2,4-Dihydroxy-5-Vinyl (Isopropenyl) Phenyl] 1,3-2H-Dibenzotriazole," in *New Trends in the Photochemistry of Polymers*, edited by N. S. Allen and J. F. Rabek, London: Elsevier Applied Science Publishers, 1985, p. 247.
14. Li, S., A. C. Albertsson, A. Gupta, W. Bassett, Jr., and O. Vogl, "Functional Polymers XXVII: 2[2-Hydroxy-4-acryloxy(methacryloxy) phenyl] 2H-benzotriazole: Monomers, Polymers, and Copolymers," *Monatshefte fur Chemie*, Vol. 115, 1984, p. 853.

15. Raether, H., "Surface Plasmons and Roughness," Ch. 9 in *Surface Polaritons, Electromagnetic Waves at Surfaces and Interfaces*, edited by V. M. Agronovich and D. L. Mills, Amsterdam: North-Holland Publishing Co., 1982.

16. Barrich, D. E., "Rough Surfaces," Ch. 9 in *Radar Cross Section Handbook*, edited by G. T. Ruch, New York: Plenum Press, 1979, p. 719.

17. Beckman, P., A. Spizzichino, *Scattering of Electromagnetic Waves*, New York: Pergamon Press Limited, 1963.

18. Bennett, J. M., "Measurement of the rms Roughness, Autoconvariance Function and Other Statistical Properties of Optical Surfaces Using a FECO Scanning Interferometer," *Applied Optics*, Vol. 15, 1976, p. 2705.

19. Bennett, J. M., and D. L. Decker, "Surface Characterization of Diamond-Turned Metal Optics," *SPIE* Vol. 288, Los Alamos Conference on Optics, 1981.

20. Elson, J. M., and J. M. Bennett, *Optical Engineering*, Vol. 18, No. 2, 1979, p. 116.

21. Sung, C. C., and W. D. Eberhardt, "Scattering of an Electromagnetic Wave from a Very Rough Semi-Infinite Dielectric Plane (Exact Treatment of the Boundary Conditions)," *J. Appl. Phys.*, Vol. 49, No. 3, 1978, p. 994.

22. Holzer, J. A., and C. C. Sung, "Scattering of Electromagnetic Waves from a Rough Surface II," *J. Appl. Phys*, Vol. 49, No. 3, 1978, p. 1002.

23. Sung, C. C., and W. D. Eberhardt, "Explanation of the Experimental Results of Light Backscattered from a Very Rough Surface," *J. Opt. Soc. Am.*, Vol. 68, No. 3, 1978, p. 323.

24. Wood, R. L., *Single, Stretched Membrane, Structural Module Experiments*, SERI/TR-255-2736, Golden, CO: Solar Energy Research Institute, Feb. 1986.

25. Dellin, T. A., M. J. Fish, and C. L. Yang, *A User's Manual for DELSOL2: A Computer Code for Calculating the Optical Performance and Optical System Design for Solar Thermal Central Receiver Plants*, SAND81-8237, Sandia National Laboratories, Aug. 1981.

26. Neidlinger, H. H., *The Effect of the Size of Structural Bulk Inhomogeneities on the Specular Transmittance of Polymer Films*, SERI/TP-255-2995, Golden, CO: Solar Energy Research Institute, July 1986.

27. Schissel, P., H. H. Neidlinger, and A. W. Czanderna, *Identification of Chemical and Physical Phemonena Affecting the Durability of Silvered Polymer (PMMA) Mirrors*, SERI/PR-255-2493, Golden, CO: Solar Energy Research Institute, May 1985.

28. Neidlinger, H. H., and P. Schissel, *Polymer Synthesis and Modification Research During FY 1984*, SERI/TR-255-2590, Golden, CO: Solar Energy Research Institute, July 1985.

29. Ranby, B., and J. F. Rabek, *Photodegradation, Photooxidation, and Photostabilization of Polymers*, NY: John Wiley and Sons, 1975, p. 362.

30. Schissel, P., and A. W. Czanderna, "Reactions at the Silver/Polymer Interface: A Review," *Solar Energy Materials*, Vol. 3, 1980, p. 225.

31. Shultz, A. R., *J. Phys. Chem.*, Vol. 65, 1961, p. 967.

32. Allison, J. P., *J. Polym. Sci.*, Part A-1, Vol. 4, 1966, p. 1209.

33. Morimoto, K., et al., *J. Appl. Polym. Sci.*, Vol. 16, 1972, p. 294.

34. Webster, O. W., W. R. Hertler, D. Y. Sogah, W. B. Farnham, and T. V. RajanBabu, "Group Transfer Polymerization 1. A New Concept for Addition Polymerization with Organosilicon Initiators," *J. Am. Chem. Soc.*, Vol. 105, 1983, p. 5706.

35. Sogah, D. Y., and O. W. Webster, "Telechelic Polymers by Group Transfer Polymerization," *J. Polym. Sci., Polym. Lett. Ed.*, Vol. 21, 1983, p. 927.

36. Webster, O. W., W. R. Hertler, D. Y. Sogah, W. B. Farnham, and T. V. RajanBabu, "Group Transfer Polymerization — Addition Polymerization with Organosilicon Initiators," *Polymer Preprints*, Am. Chem. Soc., Div. Polym. Chem., Vol. 24, No. 2, 1983, p. 52.

37. Webster, O. W., "Group Transfer Polymerization — An Overview," *Polymer Preprints*, Am. Chem. Soc., Div. Polym. Chem., Vol. 27, No. 1, 1986, p. 161.

38. Asami, R., Y. Kondo, and M. Takaki, "Synthesis of Poly(methyl methacrylate) Macromer by Group Transfer Polymerization and Polymerization of the Macromer," *Polymer Preprints*, Am. Chem. Soc., Div. Polym. Chem., Vol. 27, No. 1, 1986, p. 186.

39. Li, S., A. Gupta, and O. Vogl, "Functional Polymers XXI. Synthesis of Compounds with More than One Benzotriazole Group in the Molecule," *Monatshefte fur Chemie*, Vol. 114, 1983, p. 937.

APPENDIX A

PHOTOSTABILIZATION AND ATMOSPHERIC SOILING RESISTANCE STUDIES OF SILVER-BACKED POLYACRYLONITRILE FILMS

C. A. Sergides, A. R. Chughtai, D. M. Smith
University of Denver

The combination of Irganox 1010* (antioxidant) with Irgastab 2002* (quencher), found to significantly retard the photodegradation of silver-backed polyacrylonitrile (PAN) films, was further examined. It was found that both stabilizers also behaved as quenchers in PAN/Ag films above 365 nm. Long-term durability tests, however, showed that the Irgastab 2002 was partially depleted in aqueous media, while no corresponding depletion products were detected from Irganox 1010 and PAN, respectively. The copolymer PAN-A7 yielded less photodegradation products than did the homopolymer PAN. Also, the PAN-A7/Ag film, after 6 months in an outdoor environmental test, showed higher specularity than the PAN-Ag film. Decreases in the photodegradation of PAN/SiO-Ag films were observed and compared with that of PAN/Ag film. The presence of about 10 nm SiO surface layer on PAN/Ag film was found to increase its specularity, retard to some extent its photodegradation, and increase its atmospheric soiling resistance and cleaning ease. Comparative photodegradation and specularity studies of PAN/Ag-Corning 7809 glass versus PAN/Ag float glass have suggested the use of the float glass (having a high specularity) for future studies of metal-backed polymer films.

A new photostabilizer, pentaerythritol, was also examined. In our earlier studies of the thermophysical properties of pentaerythritol [$C-(CH_2OH)_4$], it was found that this compound is thermally stable. A limited photostabilization of PAN was achieved with this additive.

---

*Ciba-Geigy Corporation

APPENDIX B

INDUSTRIAL SUPPORT ON SILVERED POLYMER R&D CONTRACT ZX-4-04052-1

The 3M Company is providing industrial support for the silvered polymer reflector task. The following is our brief summary of some of the work.

Outdoor Weathering Studies

Outdoor weathering data for ECP 300 Lot 7 (dry laminated to 0.025 in. thick, acid-etched aluminum) are compared for three locations (Arizona, Florida, Minnesota) in Table B-1. Performance in Minnesota is better than that for Florida and Arizona. At Minnesota, similar to SERI results in Golden, Colo. (see Table C-2), the data continue to show reflectance greater than 90%; however, after 15 months outdoors in both Florida and Arizona, reflectances less than 90% are obtained. The data as obtained with the D&S instrument are probably limited by that instrument and the thin aluminum substrates at the smallest (8.4 mrad) aperture.

Table B-1. Outdoor Weathering, ECP 300 Lot 7

	% Specular Reflectance			Total Solar Reflectance (%) 0.3-2.2 μ
	25 mrad	15 mrad	8.4 mrad	
Minnesota Aging				
None	97.7	97.3	94.9	95.0
12 Months	96.2	95.8	92.7	93.7
18 Months	94.7	94.1	87.4	90.5
Florida Aging, 5°				
None	98.1	97.5	92.2	94.3
3 Mos	97.1	96.5	90.1	94.1
6 Mos	96.1	95.6	90.5	94.5
9 Mos	94.0	93.8	88.9	92.7
12 Mos	91.0	90.6	84.3	89.8
15 Mos	86.7	86.0	77.2	89.3
Arizona Aging, 45°				
None	98.1	97.5	92.2	96.2
3 Mos	97.2	96.5	91.1	95.9
6 Mos	97.0	96.2	91.9	94.4
9 Mos	95.9	95.4	92.8	93.2
12 Mos	91.5	91.1	88.2	90.0
15 Mos	85.3	84.2	78.1	84.7

Four lots of ECP 300 have been produced; two lots, Lot 7 and Lot 8, with the original UV absorber in the PMMA and two lots, Lot 9 and Lot 10, with an alternate UV absorber in the PMMA layer and now designated ECP 300A. This alternate UV absorber is showing improved accelerated and outdoor weathering resistance. Tables B-2 and B-3 compare Lots 8 and 9 for outdoor weathering at Arizona and Florida, respectively. Tables B-2 and B-3 also compare bare aluminum to coil-coated aluminum substrates. The superior performance of the new stabilizer system is evident and also the coil-coated substrate appears effective.

Mar Resistant Coats

The cleaning of silvered polymer membrane mirrors is a technical problem that can be approached in several ways. One approach is to place mar resistant coats (MRC) on the polymer to provide a harder surface that resists abrasion during the cleaning process. Demonstration of the effectiveness and durability of MRC in solar applications is yet to be demonstrated. As a beginning, the 3M Company is testing two types of MRC on silvered polymer mirrors.

Table B-2. Arizona 45° Weathering of ECP 300 Lot 8 and ECP 300A Lot 9

ECP 300 Lot #	Substrate	Arizona Aging, 45°	% Specular Reflectance			% Total Solar Reflectance 0.3-2.2 µ
			25 mrad	15 mrad	8.4 mrad	
8	Aluminum	None	98.1	97.8	96.8	94.5
8	Aluminum	3 Mos	96.7	96.3	93.1	95.1
8	Aluminum	6 Mos	95.5	95.4	91.7	93.0
8	Aluminum	8 Mos	95.4	95.0	91.4	92.1
8	Aluminum	9 Mos	95.0	94.6	91.6	94.6
8	Aluminum	12 Mos	89.9	89.7	89.1	89.2
9	Aluminum	None	97.8	97.7	94.5	93.7
9	Aluminum	3 Mos	96.8	96.4	93.9	92.2
9	Aluminum	6 Mos	96.9	96.8	95.3	94.1
9	Aluminum	8 Mos	97.7	97.2	94.7	92.9
9	Aluminum	9 Mos	94.5	94.1	92.3	87.2
9	Aluminum	12 Mos	96.3	95.9	94.6	94.4
8	Coil alum	None	98.0	97.6	94.8	95.0
8	Coil alum	3 Mos	96.7	96.2	91.9	94.8
8	Coil alum	6 Mos	95.7	95.3	92.5	90.8
8	Coil alum	8 Mos	95.6	95.2	92.2	93.6
8	Coil alum	9 Mos	93.7	93.2	87.1	91.6
8	Coil alum	12 Mos	90.5	90.0	85.1	88.9
9	Coil alum	None	97.9	97.7	94.4	94.9
9	Coil alum	3 Mos	96.8	96.3	92.0	95.7
9	Coil alum	6 Mos	96.9	96.6	93.2	94.2
9	Coil alum	8 Mos	97.3	97.1	94.4	94.1
9	Coil alum	9 Mos	96.4	93.4	82.3	94.3
9	Coil alum	12 Mos	97.2	96.7	94.1	91.6

Table B-3. Florida 5° Weathering of ECP 300 Lot 8 and ECP 300A Lot 9

ECP 300 Lot #	Substrate	Florida Aging, 5°	% Specular Reflectance			% Total Solar Reflectance 0.3-2.2 μ
			25 mrad	15 mrad	8.4 mrad	
8	Aluminum	None	97.6	97.3	93.4	94.5
8	Aluminum	3 Mos	96.3	95.9	92.1	95.0
8	Aluminum	6 Mos	97.0	96.6	94.8	93.9
8	Aluminum	8 Mos	95.3	94.9	91.7	92.2
8	Aluminum	9 Mos	93.2	92.9	86.0	93.5
8	Aluminum	12 Mos	86.6	86.4	83.4	92.1
9	Aluminum	None	97.5	97.2	96.0	93.7
9	Aluminum	3 Mos	96.0	95.4	92.5	92.2
9	Aluminum	6 Mos	96.1	95.7	92.2	94.1
9	Aluminum	8 Mos	96.3	95.8	94.0	92.9
9	Aluminum	9 Mos	96.1	95.5	87.9	90.8
9	Aluminum	12 Mos	94.0	93.6	85.0	93.6
8	Coil alum	None	97.5	97.2	95.3	95.0
8	Coil alum	3 Mos	96.6	96.1	91.5	94.0
8	Coil alum	6 Mos	96.3	96.1	93.5	93.8
8	Coil alum	8 Mos	95.7	95.3	90.5	92.4
8	Coil alum	9 Mos	95.4	95.0	91.2	93.3
8	Coil alum	12 Mos	92.9	92.4	84.9	91.3
9	Coil alum	None	97.6	97.3	94.3	94.9
9	Coil alum	3 Mos	96.5	96.3	90.4	95.6
9	Coil alum	6 Mos	97.1	97.1	94.6	94.7
9	Coil alum	8 Mos	96.7	96.1	92.2	93.6
9	Coil alum	9 Mos	95.7	95.2	87.9	92.2
9	Coil alum	12 Mos	96.4	96.0	91.6	94.4

To test the effectiveness of MRC before weathering, ECP 300 Lot 7 film, 12-in. wide, was coated in Pilot Plant equipment with abrasion resistant coating types Lot 1B and Lot 2, and laminated to 0.062-in. aluminum panels for Taber Abraser Testing. The CS-O wheel with a 500-g weight was used for a 1100 cycle test with the results given in Table B-4.

Table B-4. Abrasion Tests

Test Film	% Reflectance (25 mrad)		Reflectance Loss, %
	Control	1100 Cycles	
ECP 300	98.2	73.4	25.3
ECP 300 with Lot 1B-ARC	97.4	85.3	12.4
ECP 300 with Lot 2-ARC	97.6	95.9	1.7

The results of Table B-5 were noted for each abrasion resistant coating after 12 months aging in Arizona and Florida:

Table B-5. Abrasion Tests

ECP 300 Lot 7 Coated with:	After 12 Months Arizona, 45°	After 12 Months Florida, 5°
Lot 1B		
Abrasion Resistance	Fair by #0000 Steel wool test	Poor by #0000 steel wool test
Coating Adhesion	Poor adhesion by tape test	Poor adhesion by tape test
Lot 2		
Abrasion Resistance	Good by #0000 steel wool test	Fair by #0000 steel wool test
Coating Adhesion	Good adhesion by tape test	Good adhesion by tape test

The data of Table B-5 suggest that the abrasion resistant properties of coating type Lot 2-ARC are better than Lot 1B-ARC. Weathering tests and optical measurements are also in progress (Table B-6). Table B-6 shows that ECP 300 Lot 7 fails our long-term goals when coated with either MRC and exposed in Arizona or Florida. Recall that ECP 300 Lot 7 alone also did not maintain the required reflectance (Table B-1) in Arizona or Florida while ECP 300A Lot 9 (Table B-2, B-3) is performing well. ECP 300A Lot 9 has not yet been top-coated with MRC. The SERI outdoor data (Table C-2) in Golden, Colo., remains good (at 8 mrad, results at smaller acceptance angles are limited by substrates) for each MRC type, these data again suggest that the Colorado environment is less harsh than Arizona or Florida. Clearly, more work is needed on MRC development and testing.

Silver/Polymer Adhesion

It has been noted that ECP 300, laminated to an aluminum substrate, loses a substantial amount of the adhesion between PMMA and the silver metallization after 1-2 h of water immersion. The adhesion is essentially all restored after 1-2 h drying time at room temperature and completely restored after 16 h of drying time. 3M is currently investigating methods of improving the silver to PMMA wet bond strength. Evidence to date shows that proper ECP 300 film application, with the use of the recommended 1/2-in. wide ECP 244 edge tape, prevents field failure from excess water exposure.

Membrane Mirrors

A promising candidate stretched membrane reflector was prepared by squeeze roll lamination of ECP 300A to 7-mil polyester (PET) film. The resultant film construction has the excellent weathering properties typical of acrylic films and the mechanical properties offered by polyester films.

Table B-6. Natural Weathering of ECP 300 Lot 7 with Abrasion Resistant Coatings

Substrate = 0.025 in. acid etched aluminum

Test Film	Aging	% Specular Reflectance			% Total Solar Reflectance, 0.3-2.2 μ
		25 mrad	15 mrad	8.4 mrad	
ECP 300 Lot 7 with Lot 1B ARC	None	97.4	97.1	91.6	96.5
	6 Mos AZ 45°	92.2	90.4	80.6	92.2
	9 Mos AZ 45°	92.9	92.4	79.6	91.5
	12 Mos AZ 45°	80.9	79.5	71.6	83.7
ECP 300 Lot 7 with Lot 1B ARC	6 Mos FL 5°	94.5	93.6	89.3	92.2
	9 Mos FL 5°	92.2	91.9	85.2	91.3
	12 Mos FL 5°	87.2	86.3	76.9	88.6
ECP 300 Lot 7 with Lot 2 ARC	None	97.2	97.0	91.7	95.9
	6 Mos AZ 45°	96.3	95.4	92.1	93.5
	9 Mos AZ 45°	92.6	92.5	91.2	92.0
	12 Mos AZ 45°	68.6	68.3	59.8	77.5
ECP 300 Lot 7 with Lot 2 ARC	6 Mos FL 5°	93.9	93.4	88.8	91.6
	9 Mos FL 5°	94.9	94.3	90.7	91.9
	12 Mos FL 5°	89.4	88.3	72.2	89.5

The following specular reflectance readings were measured on this construction using a D & S Model 15R Reflectometer: 25 mrad, 98.3; 15 mrad, 97.7; 8.4 mrad, 95.6. Values as measured at SERI are: 12 mrad, 96.0; 8 mrad, 95.6; 4 mrad, 93.7. The mechanical properties of the construction were tested in the machine direction (MD) and transverse direction (TD) with the following results:

	MD	TD
Break Strength	14,492 psi	19,784 psi
Std. Dev.	1,095 psi	3,067 psi
Break Elongation	113%	36%
Std. Dev.	22%	24%

Also the stress levels for 1%, 3%, and 5% strain were approximately 56, 138, and 162 lb/in. (TD) and 46, 121, and 154 lb/in. (MD).

APPENDIX C

EMPIRICAL RESULTS, DURABILITY OF SILVERED POLYMERS

This appendix lists the results (current to January 15, 1987) for optical reflectance measurements for silvered polymeric films as a continuation of earlier results [24,25]. The earlier data were obtained with a portable reflectometer of limited precision at small acceptance apertures. All data in Appendix C were obtained with Reflectometer II (see Sections 2.1.2 and 3.2) as a continuation of the same and new test samples. The commercially available silvered polymers are listed in Table C-1 along with one aluminized film. The outdoor weathering data, the QUV data, and the Weather-Ometer data are listed in Tables C-2, C-3, and C-4, respectively.

At the initiation of these tests our optical measurements were limited to hemispherical values only. Later specular measurements at 15-mrad acceptance angle were begun, and still later the acceptance angle was improved to 7 mrad and now Reflectometer II provides an optical capability consistent with our long-range goals. Mirrors are cleaned with deionized water and detergent before optical measurements.

Table C-1. Commercial Polymeric Mirrors

Designation	Metallization	Manufacturer	Comments
FEK 244	aluminized	3M Company	
YS 94	silvered	3M Company	
Polycarbonate	silvered	Sheldahl	
Teflon FEP	silvered	Sheldahl	
B2-111-1 to 4	silvered	Deposition Technology	
ECP300X	silvered	3M Company	
M084064	silvered	3M Company	
4321, J2	silvered	3M Company	
4322, J1	silvered	3M Company	
AX 9000 Lot 238	silvered	3M Company	
ECP 300 Lot 7	silvered	3M Company	
ECP 300 Lot 7	silvered	3M Company	Coated substrate
ECP 300 Lot 8	silvered	3M Company	
ECP 300 Lot 8	silvered	3M Company	Coated substrate
ECP 300 Lot 7	silvered	3M Company	Abrasion resistant coat Lot 2
ECP 300 Lot 7	silvered	3M Company	Abrasion resistant coat Lot 1B
ECP 300A Lot 9	silvered	3M Company	Modified stabilizers
ECP 300A Lot 10	silvered	3M Company	Modified stabilizers

Table C-2. Reflectance of Commercial Mirrors After Outdoor Weathering in Golden, Colo.

Sample	Exposure Time[b]	Aperture (mrad) Full-Cone Angle[a]							Film/Substrate
		4	6	8	10	12	H_s^c	H_{66}^d	
GROUP #1 EXPERIMENTAL SAMPLES									
B2-34-1	116W	76.9		88.3		90.0	90.9		3M, exp., Al
B2-34-1	129W	68.9		85.4		88.5	90.4		3M, exp., Al
B2-34-1	142W	57.7		87.2		90.2	90.6		3M, exp., Al
B2-34-2	116W	47.0		84.0		90.8			3M, exp., Al
B2-34-2	129W	41.7		82.1		90.7			3M, exp., Al
B2-34-2	142W	48.0		76.8		88.3	90.5		3M, exp., Al
B2-34-7	90W	59.3	88.9	92.2	92.8	92.9	90.9		3M, exp., Al
B2-34-7	116W	68.2		89.5		92.1			3M, exp., Al
B2-34-7	129W	74.6		90.6		92.5			3M, exp., Al
B2-34-7	142W	80.6		90.7		92.5	89.9		3M, exp., Al
B2-34-8	90W						90.5		3M, exp., Al
B2-34-8	116W	82.0		90.0		91.9			3M, exp., Al
B2-34-8	129W	90.5		90.7		91.9			3M, exp., Al
B2-34-8	142W	48.3		90.6		92.6	90.6		3M, exp., Al
B2-34-17	90W	72.1	84.7	86.9	97.6	88.1	89.8		3M, exp., Al
B2-34-17	116W	71.6		80.8		82.7			3M, exp., Al
B2-34-17	129W	78.5		85.5		87.6			3M, exp., Al
B2-34-17	142W	62.4		85.4		83.9	90.8		3M, exp., Al
B2-34-18	90W	61.0	78.0	81.9	82.6	83.0	--		3M, exp., Al
B2-34-18	116W	64.8		85.1		87.6			3M, exp., Al
B2-34-18	129W	72.6		78.2		80.4			3M, exp., Al
B2-34-18	142W	16.0		76.5		82.6	89.9		3M, exp., Al
B2-111-1	64W	73.2	79.2	81.8	83.1	84.3	92.3		Deposition Tech. Glass
B2-111-1	83W	65.4		71.2		75.2	92.9		Deposition Tech. Glass
B2-111-1	95W	45.4		55.8		59.8			Deposition Tech. Glass,D[e]
B4-25-2	16W	61.5	84.3	93.7	95.6	96.1	92.3		3M, exp., Al
B4-25-2	40W	21.8		95.6		96.4			3M, exp., Al
B4-25-2	54W	77.0		95.0		96.6			3M, exp., Al
B4-25-2	67W	65.2		89.3		94.8	91.1		3M, exp., Al
B4-25-4	16W	37.5	67.8	88.9	95.1	95.7	92.1		3M, exp., Al
B4-25-4	40W	46.5		92.1		96.1			3M, exp., Al
B4-25-4	54W	73.3		95.4		96.1			3M, exp., Al
B4-25-4	67W	46.2		90.4		94.9	91.6		3M, exp., Al
B4-25-13	16W	73.6	92.2	96.1	96.2	96.4	92.2		3M, exp., Al
B4-25-13	40W	72.3		95.1		95.9			3M, exp., Al
B4-25-13	54W	78.2		94.5		96.3			3M, exp., Al
B4-25-13	67W	72.4		93.0		94.3	91.6		3M, exp., Al
B4-25-14	16W	65.2	91.2	95.3	95.5	96.0	92.0		3M, exp., Al
B4-25-14	40W	73.6		95.0		96.4			3M, exp., Al
B4-25-14	54W	80.3		95.6		97.0			3M, exp., Al
B4-25-14	67W	71.2		92.9		95.8	91.7		3M, exp., Al
B4-25-23	16W	51.2	73.6	83.1	85.6	88.0	92.7		3M, exp., Al
B4-25-23	40W	52.1		81.0		87.4			3M, exp., Al
B4-25-23	54W	50.0		81.1		88.4			3M, exp., Al
B4-25-23	67W	47.1		79.7		87.3	92.3		3M, exp., Al

Table C-2. Reflectance of Commercial Mirrors After Outdoor Weathering in Golden, Colo. (Continued)

Sample	Exposure Time[b]	Aperture (mrad) Full-Cone Angle[a] 4	6	8	10	12	H_s^c	H_{66}^d	Film/Substrate
B4-25-24	16W	58.3	77.2	85.0	87.7	89.0	92.8		3M, exp., Al
B4-25-24	40W	60.8		86.5		91.2			3M, exp., Al
B4-25-24	54W	60.5		86.2		91.4			3M, exp., Al
B4-25-24	67W	60.8		84.5		89.3	92.2		3M, exp., Al
GROUP #2 ECP 300 Lot 7									
B4-150-3	1M						91.5		3M, ECP 300, Al
B4-150-3	7M	47.9	81.8	93.3	95.1	94.9	92.0	97.9	3M, ECP 300, Al
B4-150-3	10M	70.2		92.7		94.1			3M, ECP 300, Al
B4-150-3	13M	78.8		95.0		95.4			3M, ECP 300, Al
B4-150-3	16M	76.0		93.4		94.1			3M, ECP 300, Al
B4-151-6	1M						91.9		3M, ECP 300, Al
B4-151-6	7M	65.2	87.7	92.8	94.2	94.4			3M, ECP 300, Al
B4-151-6	10M	70.7		89.3		89.9	90.1		3M, ECP 300, Al
B4-151-6	10M	71.6		93.3		94.2			3M, ECP 300, Al, D[f]
B4-151-8	1M						92.0		3M, ECP 300, Al
B4-151-8	7M	56.8	86.6	94.0	94.4	94.6			3M, ECP 300, Al
B4-151-8	10M	69.6		92.2		92.8			3M, ECP 300, Al
B4-151-8	13M	79.3		94.8		95.6			3M, ECP 300, Al
B4-151-8	16M	76.0		93.4		94.1			3M, ECP 300, Al
B4-152-3	1M						92.1		3M, ECP 300, PAl[g]
B4-152-3	7M	67.8	89.2	94.3	95.3	95.6	92.1	97.9	3M, ECP 300, PAl
B4-152-3	10M	68.7		89.0		90.2			3M, ECP 300, PAl
B4-152-3	13M	79.5		93.8		94.3			3M, ECP 300, PAl
B4-152-3	16M	76.6		93.7		94.2			3M, ECP 300, PAl
B4-153-5	1M						92.4		3M, ECP 300, PAl
B4-153-5	7M	70.3	70.4	89.8	94.1	94.9			3M, ECP 300, PAl
B4-153-5	10M	78.4		92.8		93.2			3M, ECP 300, PAl
B4-153-5	13M	77.8		93.7		94.0			3M, ECP 300, PAl
B4-153-5	16M	71.1		92.8		93.6			3M, ECP 300, PAl
B4-153-6	1M						92.2		3M, ECP 300, PAl
B4-153-6	7M	59.6	89.4	94.8	95.8	96.1			3M, ECP 300, PAl
B4-163-6	10M	73.9		93.9		94.9			3M, ECP 300, PAl
B4-163-6	13M	79.2		94.4		94.9			3M, ECP 300, PAl
B4-163-6	16M	72.1		93.2		93.7			3M, ECP 300, PAl

This sample set has developed (at 10M) a mottled appearance that casual inspection would suggest is a light surface dirt layer; however, it does wash away but only under special cleaning conducted at 3M. At 13M, surface scratches and a mottled appearance are visible but the optics remain good at 8 mrad.

GROUP #3 ECP 300 Lot 8, Acrylic Seal

B4-157-1	1M						91.6		3M, ECP 300, PAl
B4-157-1	4M	70.5	90.6	95.3	95.5	96.0	91.7		3M, ECP 300, PAl
B4-157-1	7M	83.5		95.2		95.6	91.6		3M, ECP 300, PAl
B4-157-1	10M	87.3		94.9		95.6			3M, ECP 300, PAl
B4-157-1	13M	82.6		93.7		94.5			3M, ECP 300, PAl

Table C-2. Reflectance of Commercial Mirrors After Outdoor Weathering in Golden, Colo. (Continued)

Sample	Exposure Time[b]	Aperture (mrad) Full-Cone Angle[a]							Film/Substrate
		4	6	8	10	12	H_s^c	H_{66}^d	
B4-157-3	1M						92.0		3M, ECP 300, PAl
B4-157-3	4M						92.1		3M, ECP 300, PAl
B4-157-3	7M	84.8		94.6		95.0	91.6		3M, ECP 300, PAl
B4-157-3	10M	81.7		94.3		94.8			3M, ECP 300, PAl
B4-157-3	13M	77.4		93.1		94.1			3M, ECP 300, PAl
B4-159-10	1M						92.1		3M, ECP 300, PAl
B4-159-10	4M	29.9	66.4	91.0	94.1	95.4	92.3		3M, ECP 300, PAl
B4-159-10	7M	61.8		89.9		90.8	93.1		3M, ECP 300, PAl
B4-159-10	10M	66.8		89.6		90.6			3M, ECP 300, PAl
B4-159-10	13M	64.7		81.7		82.9			3M, ECP 300, PAl
B4-160-5	1M						91.9		3M, ECP 300, Al
B4-160-5	4M	66.1	92.3	95.9	96.5	95.9	92.0		3M, ECP 300, Al
B4-160-5	7M	82.6		96.1		96.7	91.9		3M, ECP 300, Al
B4-160-5	10M	84.8		94.7		95.6			3M, ECP 300, Al
B4-160-5	13M	80.5		94.6		95.0			3M, ECP 300, Al
B4-160-8	1M						91.9		3M, ECP 300, Al
B4-160-8	4M	71.3	94.0	95.7	95.9	96.0	92.0		3M, ECP 300, Al
B4-160-8	7M	83.6		93.0		93.5	93.1		3M, ECP 300, Al
B4-160-8	10M	81.3		92.4		92.9			3M, ECP 300, Al
B4-160-8	13M	81.3		89.4		90.2			3M, ECP 300, Al
B4-160-9	1M						92.2		3M, ECP 300, Al
B4-160-9	4M	64.0	88.4	92.2	93.1	91.1	92.5		3M, ECP 300, Al
B4-160-9	7M	72.7		91.4		92.0	92.6		3M, ECP 300, Al
B4-160-9	10M	81.5		90.1		90.8			3M, ECP 300, Al
B4-160-9	13M	73.5		86.4		87.2			3M, ECP 300, Al
GROUP #4 ECP 300 Lot 7									
Y1-14-3	13W	63.6	92.4	95.5	94.6	95.5	92.0		3M, ECP 300, Al
Y1-14-3	26W	77.9		94.5		95.0			3M, ECP 300, Al
Y1-14-3	10M	76.5		95.7		96.0			3M, ECP 300, Al
Y1-14-3	13M	83.5		94.5		94.8			3M, ECP 300, Al
Y1-14-5	13W	68.0	92.4	95.6	95.8	95.6		98.5	3M, ECP 300, Al
Y1-14-5	26W	81.5		93.9		94.6			3M, ECP 300, Al
Y1-14-5	10M	86.1		95.3		95.5			3M, ECP 300, Al
Y1-14-5	13M	81.7		95.3		95.6			3M, ECP 300, Al
Y1-14-10	13W	77.3	93.4	95.3	95.5	95.7		98.5	3M, ECP 300, Al
Y1-14-10	26W	75.5		93.3		94.2			3M, ECP 300, Al
Y1-14-10	10M	78.0		95.0		95.2			3M, ECP 300, Al
Y1-14-10	13M	84.1		92.9		93.2			3M, ECP 300, Al
ECP 300 Lot 7, Lot 2 ARC									
Y1-14-11	13W	43.8	80.8	93.8	95.6	95.9	92.5		3M, ECP 300, Al
Y1-14-11	26W	57.0		91.1		93.7			3M, ECP 300, Al
Y1-14-11	10M	57.5		90.8		94.4			3M, ECP 300, Al
Y1-14-11	13M	60.8		92.9		94.5			3M, ECP 300, Al

Table C-2. Reflectance of Commercial Mirrors After Outdoor Weathering in Golden, Colo. (Continued)

Sample	Exposure Time^{b}	Aperture (mrad) Full-Cone Angle^{a}							Film/Substrate
		4	6	8	10	12	H_s^c	H_{66}^d	
Y1-14-12	13W	40.9	71.4	89.7	94.7	95.4		98.7	3M, ECP 300, Al
Y1-14-12	26W	50.8		85.4		94.4			3M, ECP 300, Al
Y1-14-12	10M	57.1		93.0		94.7			3M, ECP 300, Al
Y1-14-12	13M	61.8		91.7		95.3			3M, ECP 300, Al
Y1-14-13	13W	42.1	74.6	91.6	94.7	95.5		99.1	3M, ECP 300, Al
Y1-14-13	26W	49.2		91.4		95.8			3M, ECP 300, Al
Y1-14-13	10M	56.5		91.7		93.5			3M, ECP 300, Al
Y1-14-13	13M	55.1		90.1		94.7			3M, ECP 300, Al
ECP 300 Lot 7, Lot 1B ARC									
Y1-14-22	13W	42.0	76.7	92.5	94.6	95.1	92.3		3M, ECP 300, Al
Y1-14-22	26W	54.8		92.0		95.3			3M, ECP 300, Al
Y1-14-22	10M	66.1		90.7		93.4			3M, ECP 300, Al
Y1-14-22	13M	48.7		89.9		93.7			3M, ECP 300, Al
Y1-14-23	13W	45.3	79.6	92.1	94.4	95.2		98.2	3M, ECP 300, Al
Y1-14-23	26W	58.4		90.7		95.3			3M, ECP 300, Al
Y1-14-23	10M	65.8		91.6		94.2			3M, ECP 300, Al
Y1-14-23	13M	72.2		93.4		95.0			3M, ECP 300, Al
Y1-14-30	13W	46.0	78.8	92.0	94.0	94.6		98.5	3M, ECP 300, Al
Y1-14-30	26W	53.9		91.9		94.5			3M, ECP 300, Al
Y1-14-30	10M	60.9		92.8		94.6			3M, ECP 300, Al
Y1-14-30	13M	57.9		90.4		93.4			3M, ECP 300, Al
GROUP #5 ECP 300A Lot 9									
Y1-30-5	4M	53.4	88.0	96.2	96.9	97.1	92.9		3M, ECP 300A, Al
Y1-30-5	7M	66.4		92.6		94.4			3M, ECP 300A, Al
Y1-30-5	10M	71.5		93.4		94.5			3M, ECP 300A, Al
Y1-30-5	13M	76.7		94.6		95.9			3M, ECP 300A, Al
Y1-30-6	4M	57.5	89.8	96.0	97.1	97.1	93.0		3M, ECP 300A, Al
Y1-30-6	7M	69.5		93.3		94.3			3M, ECP 300A, Al
Y1-30-6	10M	72.7		94.7		95.7			3M, ECP 300A, Al
Y1-30-6	13M	78.9		93.9		94.9			3M, ECP 300A, Al
Y1-30-8	4M	59.7	89.3	96.0	96.8	96.9	92.5		3M, ECP 300A, Al
Y1-30-8	7M	73.5		93.0		94.2			3M, ECP 300A, Al
Y1-30-8	10M	74.4		93.4		95.5			3M, ECP 300A, Al
Y1-30-8	13M	79.0		94.7		95.4			3M, ECP 300A, Al
Y1-30-14	4M	66.2	92.3	96.4	97.4	97.6	93.0		3M, ECP 300A, PAl
Y1-30-14	7M	76.3		93.1		93.6			3M, ECP 300A, PAl
Y1-30-14	10M	81.9		95.2		95.9			3M, ECP 300A, PAl
Y1-30-14	13M	68.3		92.1		93.6			3M, ECP 300A, PAl
Y1-30-16	4M	71.4	93.0	95.6	96.1	95.8	92.8		3M, ECP 300A, PAl
Y1-30-16	7M	82.0		93.8		94.1			3M, ECP 300A, PAl
Y1-30-16	10M	85.0		95.1		94.5			3M, ECP 300A, PAl
Y1-30-16	13M	83.1		94.8		95.8			3M, ECP 300A, PAl

Table C-2. **Reflectance of Commercial Mirrors After Outdoor Weathering in Golden, Colo.** (Concluded)

Sample	Exposure Time[b]	Aperture (mrad) Full-Cone Angle[a]							Film/Substrate
		4	6	8	10	12	H_s[c]	H_{66}[d]	
Y1-30-18	4M	62.6	89.8	95.0	96.2	96.2	92.7		3M, ECP 300A, PAl
Y1-30-18	7M	72.4		93.2		94.1			3M, ECP 300A, PAl
Y1-30-18	10M	78.5		94.5		95.4			3M, ECP 300A, PAl
Y1-30-18	13M	75.5		94.6		95.6			3M, ECP 300A, PAl
Y1-105-4	0	94.5		96.6		96.6	92.8		3M, ECP 300A, AlP[h]
Y1-105-4	1M	95.4		96.8		96.5	93.4		3M, ECP 300A, AlP
Y1-105-4	2M	95.4		96.7		97.0	92.5		3M, ECP 300A, AlP
Y1-105-5	0	92.0		96.2		96.5	92.9		3M, ECP 300A, AlP
Y1-105-5	1M	93.2		96.6		96.0	93.1		3M, ECP 300A, AlP
Y1-105-5	2M	92.6		96.9		97.4	92.6		3M, ECP 300A, AlP
Y1-107-1	0	93.6		95.8		95.8	92.9		3M, ECP 300A, SS[i]
Y1-107-1	1M	95.8		97.1		97.1	93.1		3M, ECP 300A, SS
Y1-107-1	2M	96.3		96.9		97.3	92.5		3M, ECP 300A, SS
Y1-107-2	0	92.6		95.5		95.5	92.7		3M, ECP 300A, SS
Y1-107-2	1M	94.3		96.1		96.0	93.1		3M, ECP 300A, SS
Y1-107-2	2M	93.8		96.2		96.6	92.2		3M, ECP 300A, SS
GROUP #6 ECP 300 Lot 7									
Y1-62-1	10W	96.8				96.4	92.3		3M, ECP 300, Glass
Y1-62-1	20W	96.0		96.4		92.4	92.4		3M, ECP 300, Glass
Y1-62-1	35W	93.3		94.3		94.6			3M, ECP 300, Glass
Y1-62-1	48W	95.7		96.6		96.4			3M, ECP 300, Glass
Y1-62-2	10W	95.1				96.4	92.3		3M, ECP 300, Glass
Y1-62-2	20W	95.4		95.6		95.9	92.4		3M, ECP 300, Glass
Y1-62-2	35W	94.0		94.9		94.4			3M, ECP 300, Glass
Y1-62-2	48W	95.7		96.4		96.9			3M, ECP 300, Glass
Y1-62-3	10W	95.0				96.3	92.3		3M, ECP 300, Glass
Y1-62-3	20W	91.6		94.9		95.2	92.4		3M, ECP 300, Glass
Y1-62-3	35W	90.8		93.7		93.7			3M, ECP 300, Glass
Y1-62-3	48W	94.2		93.6		96.7			3M, ECP 300, Glass
Y1-62-32	0	93.1		96.0		96.3	92.7		3M, ECP 300, AlP
Y1-62-32	1M	94.8		96.9		96.7	92.9		3M, ECP 300, AlP
Y1-62-32	2M	94.8		96.7		97.5	92.3		3M, ECP 300, AlP
Y1-70-2	1Y	47.8	83.0	94.5	95.6	96.1	--		3M, ECP 300, Al, MN[j],D[e]

---

[a] Wavelength = 660 nm; angle of incidence = 20°; beam diameter = 10 mm.
[b] W = weeks, M = months, Y = years.
[c] Solar-weighted hemispherical reflectance (AM 1.5).
[d] Hemispherical reflectance at 660 nm.
[e] D = discontinued.
[f] Sent to 3M, cleaned specially at 3M.
[g] PA1 is painted aluminum.
[h] AlP = polished aluminum
[i] SS = stainless steel.
[j] Minnesota.

Table C-3. Reflectance of Commercial Mirrors After QUV Exposure

Sample	Exposure Time^b	Aperture (mrad) Full-Cone Angle^a					H_s^c	H_{66}^d	Film/Substrate
		4	6	8	10	12			
Experimental Samples									
B2-34-4	38W	24.5	41.9	49.9	52.3	53.0			3M, EXP, Al, D^e
B2-34-12	38W	43.8	50.1	51.8	52.5	52.9			3M, EXP, Al, D
B2-34-13	38W	50.8	66.4	70.0	71.3	71.3			3M, EXP, Al, D
B4-25-5	20W	18.9	36.6	52.5	60.8	65.5	82.0		3M, EXP, Al
B4-25-5	28W	22.8	45.4	62.2	70.0	72.4	80.2	83.8	3M, ECP, Al, D
B4-25-6	20W	28.8	52.1	64.3	68.1	68.9	78.2		3M, EXP, Al
B4-25-6	28W	19.0	40.6	60.5	65.5	66.4	81.7	76.0	3M, EXP, Al, D
B4-25-7	20W	24.7	42.2	59.3	68.8	72.2	82.0		3M, EXP, Al
B4-25-7	28W	22.6	44.4	58.7	65.8	68.8	80.1	83.6	3M, EXP, Al, D
B4-25-15	20W	33.1	59.8	73.0	75.3	75.7	80.4		3M, EXP, Al
B4-25-15	28W	30.2	56.8	70.0	72.5	72.9	79.2	84.1	3M, EXP, Al, D
B4-25-16	20W	42.4	67.8	74.8	75.8	76.2	81.0		3M, EXP, Al
B4-25-16	28W	37.5	62.0	70.3	72.2	72.3	79.4	83.1	3M, EXP, Al, D
B4-25-17	20W	35.5	59.0	71.1	73.2	74.0	80.3		3M, EXP, Al
B4-25-17	28W	31.5	56.6	66.6	70.0	70.1	79.0	83.8	3M, EXP, Al, D
B4-25-25	20W	29.1	49.8	64.4	69.6	71.8	88.0		3M, EXP, Al
B4-25-25	28W	18.4	41.1	54.4	60.1	62.0	81.8	86.3	3M, EXP, Al, D
B4-25-26	20W	23.1	44.9	57.5	61.4	64.1	82.8		3M, EXP, Al
B4-25-26	28W	16.4	33.0	43.8	49.2	51.3	80.8	84.4	3M, EXP, Al, D
B4-25-27	20W	28.5	54.4	72.7	80.8	83.9	89.7		3M, EXP, Al
B4-25-27	28W	21.9	48.5	70.3	79.2	82.5	88.6	94.4	3M, EXP, Al, D
ECP 300 Lot 7									
B4-150-2	1M						87.4		3M, ECP 300, Al
B4-150-2	5.5M	34.9	60.7	73.0	76.8	77.7	80.6		3M, ECP 300, Al
B4-150-2	6.5M	5.5		17.2		29.4			3M, ECP 300, Al, D
B4-151-7	1M						86.3		3M, ECP 300, Al
B4-151-7	5.5M	37.3	64.4	77.3	79.8	80.2	80.2		3M, ECP 300, Al
B4-151-7	6.5M	5.3		16.1		27.7			3M, ECP 300, Al, D
B4-152-9	1M						86.5		3M, ECP 300, Al
B4-152-9	5.5M	14.7	33.1	48.9	57.4	61.9	80.0		3M, ECP 300, Al
B4-152-9	6.5M	3.6		11.9		22.1			3M, ECP 300, Al, D
B4-153-4	1M						86.4		3M, ECP 300, PAl^f
B4-153-4	5.5M	15.4	29.0	41.6	48.0	51.2	76.7		3M, ECP 300, PAl
B4-153-4	6.5M	1.2		4.5		8.8			3M, ECP 300, PAl, D
B4-153-7	1M						85.4		3M, ECP 300, PAl
B4-153-7	5.5M	24.5	43.2	55.2	61.4	64.4	78.7		3M, ECP 300, PAl
B4-153-7	6.5M	3.5		10.2		18.0			3M, ECP 300, PAl, D
B4-154-10	1M						84.7		3M, ECP 300, PAl
B4-154-10	5.5M	7.3	17.3	29.0	37.3	41.8	76.6		3M, ECP 300, PAl
B4-154-10	6.5M	1.4		4.9		9.6			3M, ECP 300, PAl, D

Samples B4-150-2 through B4-154-10 all badly crazed at 6.5 months (was not noticed at 5.5 months). No difference bare or painted aluminum substrates. White edge tape intact, clear edge tape attacked, no blisters.

Table C-3. Reflectance of Commercial Mirrors After QUV Exposure (Continued)

Sample	Exposure Time[b]	Aperture (mrad) Full-Cone Angle[a]					H_s^c	H_{66}^d	Film/Substrate
		4	6	8	10	12			
ECP 300, Lot 8, Acrylic Seal									
B4-157-2	1M						89.2		3M, ECP 300, PAl
B4-157-2	5M	40.9	71.2	78.6	79.9	80.1	82.2		3M, ECP 300, PAl
B4-157-2	6M	48.6		73.7		76.4			3M, ECP 300, PAl, D
B4-158-6	1M						89.4		3M, ECP 300, PAl
B4-158-6	5M	35.0	62.7	77.5	80.5	80.8	82.0		3M, ECP 300, PAl
B4-158-6	6M	5.1		16.6		29.6			3M, ECP 300, PAl, D
B4-158-7	1M						89.3		3M, ECP 300, PAl
B4-158-7	5M	33.3	64.6	78.4	80.5	81.1	83.1		3M, ECP 300, PAl
B4-158-7	6M	19.9		48.6		62.3			3M, ECP 300, PAl, D
B4-159-2	1M						90.4		3M, ECP 300, Al
B4-159-2	5M	35.3	64.7	77.8	79.8	80.5	81.6		3M, ECP 300, Al
B4-159-2	6M	41.3		71.6		76.0			3M, ECP 300, Al, D
B4-160-7	1M						90.5		3M, ECP 300, Al
B4-160-7	5M	46.1	70.1	76.2	78.2	78.5	81.8		3M, ECP 300, Al
B4-160-7	6M	41.9		62.9		68.1			3M, ECP 300, Al, D
B4-161-10	1M						88.5		3M, ECP 300, Al
B4-161-10	5M	34.6	59.2	70.1	73.7	74.3	80.5		3M, ECP 300, Al
B4-161-10	6M	7.8		22.3		36.1			3M, ECP 300, Al, D

Samples B4-157-2 through B4-161-10 all badly crazed, little difference between painted and unpainted aluminum substrate, no blisters.

Sample	Exposure Time[b]	4	6	8	10	12	H_s^c	H_{66}^d	Film/Substrate
EXP 300 Lot 7									
Y1-14-1	13W	33.4	65.4	78.5	81.2	81.6	84.1		3M, ECP 300, Al
Y1-14-1	17W	30.0	61.8	77.7	79.7	79.7			3M, ECP 300, Al
Y1-14-1	21W	37.7		75.1		77.8	81.3		3M, ECP 300, Al
Y1-14-1	26W	14.5		36.2		51.4			3M, ECP 300, Al, D
Y1-14-2	13W	39.0	68.4	80.8	83.5	84.1		95.9	3M, ECP 300, Al
Y1-14-2	17W	42.3	73.7	84.2	86.2	86.3			3M, ECP 300, Al
Y1-14-2	21W	45.0		78.0		80.9	81.9		3M, ECP 300, Al
Y1-14-2	26W	40.0		71.5		75.3			3M, ECP 300, Al, D
Y1-14-6	13W	37.4	72.1	83.8	85.2	85.6		96.6	3M, ECP 300, Al
Y1-14-6	17W	35.6	72.2	82.6	83.5	83.7			3M, ECP 300, Al
Y1-14-6	21W	44.0		79.8		82.2	82.6		3M, ECP 300, Al
Y1-14-6	26W	51.0		79.0		79.4			3M, ECP 300, Al, D

Samples Y1-14-1, 2, and 6 discontinued, all badly crazed.

Sample	Exposure Time[b]	4	6	8	10	12	H_s^c	H_{66}^d	Film/Substrate
ECP 300 Lot 7, Lot 2 ARC									
Y1-14-15	13W	33.1	67.0	82.7	86.6	87.1	86.5		3M, ECP 300, Al
Y1-14-15	17W	34.0	66.0	81.7	84.9	85.7			3M, ECP 300, Al
Y1-14-15	21W	46.9		80.6		84.5	83.7		3M, ECP 300, Al
Y1-14-15	26W	46.5		77.6		81.4			3M, ECP 300, Al
Y1-14-15	30W	36.5		74.1		79.6			3M, ECP 300, Al, D

Table C-3. Reflectance of Commercial Mirrors After QUV Exposure (Continued)

Sample	Exposure Time[b]	Aperture (mrad) Full-Cone Angle[a] 4	6	8	10	12	H_s^c	H_{66}^d	Film/Substrate
Y1-14-19	13W	40.6	68.3	81.9	87.0	85.6		97.7	3M, ECP 300, Al
Y1-14-19	17W	31.2	65.7	83.1	85.4	85.6			3M, ECP 300, Al
Y1-14-19	21W	39.6		79.8		85.2	84.0		3M, ECP 300, Al
Y1-14-19	26W	41.7		75.8		82.5			3M, ECP 300, Al
Y1-14-19	30W	35.7		75.0		80.4			3M, ECP 300, Al, D
Y1-14-20	13W	34.6	64.0	80.5	83.6	84.3		96.1	3M, ECP 300, Al
Y1-14-20	17W	23.3	50.8	69.2	79.5	82.7			3M, ECP 300, Al
Y1-14-20	21W	29.3		63.1		78.1	82.6		3M, ECP 300, Al
Y1-14-20	26W	42.8		74.1		79.1			3M, ECP 300, Al
Y1-14-20	30W	27.4		58.6		66.7			3M, ECP 300, Al, D

Samples Y1-14-15, Y1-14-19, and Y1-14-20 discontinued, all slightly crazed.

ECP 300 Lot 7, Lot 1B ARC

Sample	Exposure Time	4	6	8	10	12	H_s^c	H_{66}^d	Film/Substrate
Y1-14-26	13W	32.7	61.5	79.4	83.5	83.5	85.7		3M, ECP 300, Al
Y1-14-26	17W	34.4	55.6	78.2	81.4	81.7			3M, ECP 300, Al
Y1-14-26	21W	34.0		72.3		79.3	83.0		3M, ECP 300, Al
Y1-14-26	26W	19.2		44.5		59.6			3M, ECP 300, Al, D
Y1-14-27	13W	30.3	60.9	76.9	80.0	80.6		95.6	3M, ECP 300, Al
Y1-14-27	17W	30.4	58.5	75.5	80.3	81.1			3M, ECP 300, Al
Y1-14-27	21W	24.8		52.3		66.5	81.5		3M, ECP 300, Al
Y1-14-27	26W	7.0		19.6		32.9			3M, ECP 300, Al, D
Y1-14-29	13W	25.5	52.0	69.9	75.4	77.7		94.5	3M, ECP 300, Al
Y1-14-29	17W	23.4	51.2	70.9	76.6	78.4			3M, ECP 300, Al
Y1-14-29	21W	18.3		41.9		56.7	81.0		3M, ECP 300, Al
Y1-14-29	26W	8.3		20.7		29.9			3M, ECP 300, Al, D

Samples Y1-26, 27, and 29 discontinued, all badly crazed.

ECP 300A Lot 9

Sample	Exposure Time	4	6	8	10	12	H_s^c	H_{66}^d	Film/Substrate
Y1-30-2	4M	29.6	59.1	77.3	81.6	82.1	85.5		3M, ECP 300A, Al
Y1-30-2	7M	15.3		37.5		52.8			3M, ECP 300A, Al, D
Y1-30-3	4M	34.6	63.8	80.3	85.6	86.5	87.0		3M, ECP 300A, Al
Y1-30-3	7M	12.9		33.2		49.2			3M, ECP 300A, Al, D
Y1-30-9	4M	36.9	72.7	87.9	91.6	92.2	89.3		3M, ECP 300A, Al
Y1-30-9	7M	11.0		30.3		47.4			3M, ECP 300A, Al, D
Y1-30-11	4M	37.6	68.9	86.6	88.8	89.3	87.6		3M, ECP 300A, PAl
Y1-30-11	7M	16.0		38.4		55.0			3M, ECP 300A, PAl, D
Y1-30-12	4M	39.3	74.8	88.3	91.3	91.9	88.7		3M, ECP 300A, PAl
Y1-30-12	7M	19.2		46.6		62.7			3M, ECP 300A, PAl, D
Y1-30-15	4M	34.3	69.4	90.2	93.4	93.5	90.1		3M, ECP 300A, PAl
Y1-30-15	7M	50.4		78.9		82.9			3M, ECP 300A, PAl, D
Y1-105-1	0	88.6		96.5		96.9	93.1		3M, ECP 300A, AlP[g]
Y1-105-1	1M	87.9		95.6		95.9	92.1		3M, ECP 300A, AlP
Y1-105-1	2M	83.9		94.8		95.7	91.2		3M, ECP 300A, AlP
Y1-105-3	0	89.9		96.4		96.9	92.8		3M, ECP 300A, AlP
Y1-105-3	1M	85.9		95.0		95.4	92.0		3M, ECP 300A, AlP
Y1-105-3	2M	86.8		95.9		96.6	91.0		3M, ECP 300A, AlP

Samples Y1-30-2, 3, 9, 11, 12, and 15 discontinued, all except Y1-30-15, badly crazed.

Table C-3. Reflectance of Commercial Mirrors After QUV Exposure (Concluded)

Sample	Exposure Time[b]	Aperture (mrad) Full-Cone Angle[a]					H_s[c]	H_{66}[d]	Film/Substrate
		4	6	8	10	12			
Y1-107-3	0	90.8		93.9		93.9	92.6		3M, ECP 300A, SS[h]
Y1-107-3	1M	90.2		95.2		95.3	92.2		3M, ECP 300A, SS
Y1-107-3	2M	85.1		91.4		93.3	90.7		3M, ECP 300A, SS
Y1-62-31	0	90.8		95.0		95.3	92.7		3M, ECP 300A, AIP
Y1-62-31	1M	85.0		94.8		94.9	91.9		3M, ECP 300A, AIP
Y1-62-31	2M	87.7		95.0		95.8	90.6		3M, ECP 300A, AIP
ECP 300 Lot 7									
Y1-62-4	5W	94.8	95.2	95.1	94.0	93.9	89.3	95.7	3M, ECP 300, Glass
Y1-62-4	9W	84.8	87.4	87.6	87.9	88.1	86.8		3M, ECP 300, Glass
Y1-62-4	14W	83.1		82.6		83.6		84.7	3M, ECP 300, Glass
Y1-62-4	33W	75.3		75.3		75.6			3M, ECP 300, Glass, D
Y1-62-5	5W	92.2	92.2	93.7	93.9	94.0	89.0	95.6	3M, ECP 300, Glass
Y1-62-5	9W	85.5	87.4	88.4	88.7	88.8	86.9		3M, ECP 300, Glass
Y1-62-5	14W	83.2		84.3		85.3		85.3	3M, ECP 300, Glass
Y1-62-5	33W	23.3		43.0		52.2			3M, ECP 300, Glass, D
Y1-62-8	5W	94.0	94.3	94.4	94.5	93.7	89.2	95.8	3M, ECP 300, Glass
Y1-62-8	9W	86.5	87.7	88.3	88.3	88.5	86.7		3M, ECP 300, Glass
Y1-62-8	14W	82.3		82.8		83.5		85.0	3M, ECP 300, Glass
Y1-62-8	33W	69.0		69.8		70.0			3M, ECP 300, Glass, D
All crazed samples.									

---

[a] Wavelength = 660 nm; angle of incidence = 20°; beam diameter = 10 mm.
[b] W = weeks, M = months.
[c] Solar-weighted hemispherical reflectance (AM 1.5).
[d] Hemispherical reflectance at 660 nm.
[e] D = discontinued.
[f] PAl = painted aluminum.
[g] AlP = polished aluminum.
[h] SS = stainless steel.

Table C-4. Reflectance of Commercial Mirrors After Weather-Ometer Exposure

Sample	Exposure Time[b]	Aperture (mrad) Full-Cone Angle[a]							Film/Substrate
		4	6	8	10	12	H_s[c]	H_{66}[d]	
ECP 300 Lot 7									
B4-150-1	1M/NoUV						92.0		3M, ECP 300, Al
B4-150-1	1M						91.4		3M, ECP 300, Al
B4-150-1	4M/NoUV	55.1	85.0	94.1	95.7	96.1	91.8		3M, ECP 300, Al
B4-150-1	4M	41.3	72.7	84.4	85.4	85.8	82.4		3M, ECP 300, Al
B4-150-1	5M/NoUV	53.0	85.4	93.3	94.0	94.6			3M, ECP 300, Al
B4-150-1	5M	34.4	62.4	73.0	75.0	75.1			3M, ECP 300, Al
B4-150-1	6M/NoUV	61.5		89.6		92.6	91.3		3M, ECP 300, Al
B4-150-1	6M	35.6		61.4		63.4	71.4		3M, ECP 300, Al, D[e]
B4-151-4	1M/NoUV						92.1		3M, ECP 300, Al
B4-151-4	1M						91.2		3M, ECP 300, Al
B4-151-4	4M/NoUV	48.8	80.4	93.8	95.2	96.0	91.9		3M, ECP 300, Al
B4-151-4	4M	51.2	76.3	83.8	84.7	84.9	81.3		3M, ECP 300, Al
B4-151-4	5M/NoUV	41.6	77.4	92.8	95.0	95.1			3M, ECP 300, Al
B4-151-4	5M	41.6	66.6	72.5	73.7	73.9			3M, ECP 300, Al
B4-151-4	6M/NoUV	61.0		90.9		92.3	91.2		3M, ECP 300, Al
B4-151-4	6M	39.7		59.2		61.4	70.9		3M, ECP 300, Al, D
B4-151-5	1M/NoUV						92.0		3M, ECP 300, Al
B4-151-5	1M						91.4		3M, ECP 300, Al
B4-151-5	4M/NoUV	55.4	83.1	93.1	95.0	96.0	92.3		3M, ECP 300, Al
B4-151-5	4M	51.0	79.2	89.7	90.6	91.1	84.6		3M, ECP 300, Al
B4-151-5	5M/NoUV	53.5	80.9	92.6	94.6	94.8			3M, ECP 300, Al
B4-151-5	5M	48.1	74.6	85.2	87.3	87.3			3M, ECP 300, Al
B4-151-5	6M/NoUV	74.6		94.9		97.2	92.0		3M, ECP 300, Al
B4-151-5	6M	58.0		72.1		72.3	72.3		3M, ECP 300, Al, D
B4-152-1	1M/NoUV						92.5		3M, ECP 300, PAl[f]
B4-152-1	1M						92.2		3M, ECP 300, PAl
B4-152-1	4M/NoUV	45.5	76.6	89.3	92.1	93.0	91.6		3M, ECP 300, PAl
B4-152-1	4M	51.8	77.4	87.5	89.2	90.3	89.0		3M, ECP 300, PAl
B4-152-1	5M/NoUV	40.8	73.4	87.5	90.8	91.9			3M, ECP 300, PAl
B4-152-1	5M	46.7	72.9	84.2	86.3	87.0			3M, ECP 300, PAl
B4-152-1	6M/NoUV	53.9		89.9		91.4	92.0		3M, ECP 300, PAl
B4-152-1	6M	47.0		76.9		82.8	87.2		3M, ECP 300, PAl, D
B4-153-8	1M/NoUV						91.2		3M, ECP 300, PAl
B4-153-8	1M						91.0		3M, ECP 300, PAl
B4-153-8	4M/NoUV	54.3	80.4	92.8	94.2	94.6	90.7		3M, ECP 300, PAl
B4-153-8	4M	63.6	85.4	90.9	91.3	91.5	88.8		3M, ECP 300, PAl
B4-153-8	5M/NoUV	47.0	79.0	89.9	92.4	93.0			3M, ECP 300, PAl
B4-153-8	5M	57.6	80.6	87.2	88.2	88.3			3M, ECP 300, PAl
B4-153-8	6M/NoUV	64.1		93.3		94.6	90.6		3M, ECP 300, PAl
B4-153-8	6M	59.9		86.2		87.1	87.7		3M, ECP 300, PAl
B4-153-8	9M/NoUV	66.8		91.6		92.9			3M, ECP 300, PAl
B4-153-8	9M	61.8		83.0		84.2			3M, ECP 300, PAl
B4-153-8	12M/NoUV	66.8		91.6		92.6			3M, ECP 300, PAl
B4-153-8	12M	62.4		79.4		80.8			3M, ECP 300, PAl

Table C-4. Reflectance of Commercial Mirrors After Weather-Ometer Exposure (Continued)

Sample	Exposure Time[b]	Aperture (mrad) Full-Cone Angle[a]					H_s[c]	H_{66}[d]	Film/Substrate
		4	6	8	10	12			
B4-154-11	1M/NoUV						91.5		3M, ECP 300, PAl
B4-154-11	1M						91.8		3M, ECP 300, PAl
B4-154-11	4M/NoUV	52.5	79.3	90.3	91.9	92.7	89.9		3M, ECP 300, PAl
B4-154-11	4M	52.6	80.6	91.9	93.0	93.5	89.8		3M, ECP 300, PAl
B4-154-11	5M/NoUV	47.6	77.9	88.8	91.3	91.6			3M, ECP 300, PAl
B4-154-11	5M	47.2	74.6	86.5	90.0	90.5			3M, ECP 300, PAl
B4-154-11	6M/NoUV	63.5		90.6		91.4	89.0		3M, ECP 300, PAl
B4-154-11	6M	58.3		86.8		90.9	88.2		3M, ECP 300, PAl
B4-154-11	9M/NoUV	61.8		88.1		91.2			3M, ECP 300, PAl
B4-154-11	9M	62.7		85.1		86.3			3M, ECP 300, PAl
B4-154-11	12M/NoUV	69.4		89.4		91.0			3M, ECP 300, PAl
B4-154-11	12M	65.6		83.2		84.0			3M, ECP 300, PAl

Samples B4-150-1, B4-151-4, and B4-151-5 after 6 months have intact, clear edge tape, minor surface scratches, no blisters, sharp demarcation and graying at the UV/No UV edge. Same for B4-152-1, B4-153-8, and B4-154-11, except the effect of UV is much less severe with painted aluminum substrate, also latter three have intact white Teflon edge tape. The first three samples have been discontinued, the latter three will be continued until they degrade about the same amount as the first three.

ECP 300 Lot 8, Acrylic Seal

Sample	Exposure Time[b]	4	6	8	10	12	H_s[c]	H_{66}[d]	Film/Substrate
B4-157-4	1M						92.2		3M, ECP 300, PAl
B4-157-4	4M/NoUV	41.9	78.5	94.3	96.1	96.6	91.8		3M, ECP 300, PAl
B4-157-4	4M	36.4	75.7	90.7	92.0	92.3	88.7		3M, ECP 300, PAl
B4-157-4	5M/NoUV	35.4		86.2		93.1	91.1		3M, ECP 300, PAl
B4-157-4	5M	41.1		82.4		86.8	87.9		3M, ECP 300, PAl
B4-157-4	8M/NoUV	61.1		91.7		94.3			3M, ECP 300, PAl
B4-157-4	8M	54.8		86.0		87.8			3M, ECP 300, PAl
B4-157-4	12M/NoUV	52.6		93.6		96.0			3M, ECP 300, PAl
B4-157-4	12M	47.7		82.8		85.1			3M, ECP 300, PAl
B4-158-5	1M						91.8		3M, ECP 300, PAl
B4-158-5	4M/NoUV	57.4	87.6	95.0	95.9	96.1	91.6		3M, ECP 300, PAl
B4-158-5	4M	54.0	82.3	90.6	91.5	91.7	88.2		3M, ECP 300, PAl
B4-158-5	5M/NoUV	58.2		90.3		93.2	93.2		3M, ECP 300, PAl
B4-158-5	5M	55.3		86.3		88.2	86.2		3M, ECP 300, PAl
B4-158-5	8M/NoUV	76.6		94.3		94.1			3M, ECP 300, PAl
B4-158-5	8M	65.5		86.2		86.8			3M, ECP 300, PAl
B4-158-5	12M/NoUV	78.0		96.2		96.7			3M, ECP 300, PAl
B4-158-5	12M	76.6		86.5		86.9			3M, ECP 300, PAl
B4-158-8	1M						92.1		3M, ECP 300, PAl
B4-158-8	4M/NoUV	39.7	77.7	94.6	96.5	96.9	91.6		3M, ECP 300, PAl
B4-158-8	4M	44.0	78.8	91.0	92.6	92.8	88.8		3M, ECP 300, PAl
B4-158-8	5M/NoUV	52.5		89.4		91.5	91.4		3M, ECP 300, PAl
B4-158-8	5M	53.8		85.2		87.5	88.0		3M, ECP 300, PAl

Table C-4. Reflectance of Commercial Mirrors After Weather-Ometer Exposure (Continued)

Sample	Exposure Time[b]	Aperture (mrad) Full-Cone Angle[a]					H_s[c]	H_{66}[d]	Film/Substrate
		4	6	8	10	12			
B4-158-8	8M/NoUV	66.8		91.6		92.9			3M, ECP 300, PAl
B4-158-8	8M	61.8		83.0		84.2			3M, ECP 300, PAl
B4-158-8	12M/NoUV	74.6		95.8		96.7			3M, ECP 300, PAl
B4-158-8	12M	63.8		86.2		86.9			3M, ECP 300, PAl
B4-159-3	1M						91.9		3M, ECP 300, Al
B4-159-3	4M/NoUV	51.2	85.5	94.9	96.3	96.6	92.1		3M, ECp 300, Al
B4-159-3	4M	41.7	75.1	87.2	89.0	89.3	84.3		3M, ECP 300, Al
B4-159-3	5M/NoUV	58.3		90.6		93.6	91.5		3M, ECP 300, Al
B4-159-3	5M	46.1		74.1		76.5	78.8		3M, ECP 300, Al, D
B4-159-4	1M						91.6		3M, ECP 300, Al
B4-159-4	4M/NoUV	53.7	85.3	94.9	96.3	96.5	93.0		3M, ECP 300, Al
B4-159-4	4M	57.5	85.0	90.7	91.1	91.1	87.6		3M, ECP 300, Al
B4-159-4	5M/NoUV	58.3		90.6		93.6	91.0		3M, ECP 300, Al
B4-159-4	5M	60.9		84.5		86.3	86.6		3M, ECP 300, Al, D
B4-160-6	1M						92.1		3M, ECP 300, Al
B4-160-6	4M/NoUV	63.1	89.8	95.0	95.5	95.9	91.7		3M, ECP 300, Al
B4-160-6	4M	39.8	65.5	72.9	73.7	74.0	76.7		3M, ECP 300, Al
B4-160-6	5M/NoUV	68.0		91.2		92.9	91.6		3M, ECP 300, Al
B4-160-6	5M	35.6		50.1		51.9	64.8		3M, ECP 300, Al, D

Samples B4-157-4, B4-158-5, and B4-158-8 have intact acrylic edge bead, minor surface scratches, no blisters, sharp demarcation and graying at the UV/No UV edge and these samples with painted aluminum substrates are less degraded by UV than those with unpainted substrates (B4-159-3, B4-159-4, and B4-160-6).

ECP 300 Lot 7

Y1-14-4	13W/NoUV	45.2	83.6	95.3	96.1	96.0	92.8		3M, ECP 300, Al
Y1-14-4	13W	33.0	70.4	89.9	91.9	92.0	89.2		3M, ECP 300, Al
Y1-14-4	26W/NoUV	61.2		91.4		93.1			3M, ECP 300, Al
Y1-14-4	26W	45.3		85.5		87.5			3M, ECP 300, Al
Y1-14-4	39W/NoUV	60.0		92.8		95.1			3M, ECP 300, Al
Y1-14-4	39W	51.5		87.8		89.1			3M, ECP 300, Al
Y1-14-4	52W/NoUV	64.2		94.0		95.8			3M, ECP 300, Al
Y1-14-4	52W	52.3		82.3		83.8			3M, ECP 300, Al
Y1-14-8	13W/NoUV	49.8	83.5	94.2	95.5	95.9		99.7	3M, ECP 300, Al
Y1-14-8	13W	31.0	67.9	89.3	91.8	92.1		96.7	3M, ECP 300, Al
Y1-14-8	26W/NoUV	59.4		91.1		92.9			3M, ECP 300, Al
Y1-14-8	26W	43.6		83.0		87.8			3M, ECP 300, Al
Y1-14-8	39W/NoUV	73.5		94.9		95.8			3M, ECP 300, Al
Y1-14-8	39W	50.9		87.5		89.1			3M, ECP 300, Al
Y1-14-8	52W/NoUV	54.3		94.4		96.9			3M, ECP 300, Al
Y1-14-8	52W	46.9		84.2		86.1			3M, ECP 300, Al

Table C-4. Reflectance of Commercial Mirrors After Weather-Ometer Exposure (Continued)

Sample	Exposure Time[b]	Aperture (mrad) Full-Cone Angle[a] 4	6	8	10	12	H_s^c	H_{66}^d	Film/Substrate
Y1-14-9	13W/NoUV	48.3	82.9	94.0	95.4	95.7		98.7	3M, ECP 300, Al
Y1-14-9	13W	36.5	72.1	90.4	92.4	92.6		97.6	3M, ECP 300, Al
Y1-14-9	26W/NoUV	60.3		91.3		93.4			3M, ECP 300, Al
Y1-14-9	26W	43.5		83.1		87.2			3M, ECP 300, Al
Y1-14-9	39W/NoUV	71.8		94.1		95.3			3M, ECP 300, Al
Y1-14-9	39W	59.1		84.8		87.5			3M, ECP 300, Al
Y1-14-9	52W/NoUV	60.0		94.6		94.9			3M, ECP 300, Al
Y1-14-9	52W	45.2		79.9		82.2			3M, ECP 300, Al

ECP 300 Lot 7, Lot 2 ARC

Sample	Exposure Time[b]	Aperture (mrad) Full-Cone Angle[a] 4	6	8	10	12	H_s^c	H_{66}^d	Film/Substrate
Y1-14-14	13W/NoUV	32.8	68.4	89.2	94.6	96.0	93.3		3M, ECP 300, Al
Y1-14-14	13W	35.7	69.8	88.3	93.6	94.0	91.0		3M, ECP 300, Al
Y1-14-14	26W/NoUV	42.6		87.9		93.5			3M, ECP 300, Al
Y1-14-14	26W	43.5		83.9		89.8			3M, ECP 300, Al
Y1-14-14	39W/NoUV	48.9		89.7		95.1			3M, ECP 300, Al
Y1-14-14	39W	52.9		85.9		90.7			3M, ECP 300, Al
Y1-14-14	52W/NoUV	46.7		84.4		94.3			3M, ECP 300, Al
Y1-14-14	52W	42.9		83.2		87.9			3M, ECP 300, Al
Y1-14-16	13W/NoUV	28.8	63.8	87.2	94.8	95.8		99.2	3M, ECP 300, Al
Y1-14-16	13W	41.8	73.0	89.6	92.6	93.1		96.9	3M, ECP 300, Al
Y1-14-16	26W/NoUV	42.9		88.7		93.4			3M, ECP 300, Al
Y1-14-16	26W	44.5		84.3		88.9			3M, ECP 300, Al
Y1-14-16	39W/NoUV	53.9		93.2		94.1			3M, ECP 300, Al
Y1-14-16	39W	52.7		86.5		89.3			3M, ECP 300, Al
Y1-14-16	52W/NoUV	39.8		85.5		96.6			3M, ECP 300, Al
Y1-14-16	52W	33.3		80.9		87.0			3M, ECP 300, Al
Y1-14-18	13W/NoUV	31.4	65.0	89.5	94.8	95.8		99.0	3M, ECP 300, Al
Y1-14-18	13W	36.0	67.6	87.5	94.0	94.7		98.0	3M, ECP 300, Al
Y1-14-18	26W/NoUV	46.0		94.7		102.2			3M, ECP 300, Al
Y1-14-18	26W	45.1		92.1		99.1			3M, ECP 300, Al
Y1-14-18	39W/NoUV	53.0		91.1		94.8			3M, ECP 300, Al
Y1-14-18	39W	55.0		87.8		90.2			3M, ECP 300, Al
Y1-14-18	52W/NoUV	45.7		90.4		96.4			3M, ECP 300, Al
Y1-14-18	52W	45.5		83.8		88.9			3M, ECP 300, Al

ECP 300 Lot 7, Lot 1B ARC

Sample	Exposure Time[b]	Aperture (mrad) Full-Cone Angle[a] 4	6	8	10	12	H_s^c	H_{66}^d	Film/Substrate
Y1-14-21	13W/NoUV	30.0	64.4	90.8	95.0	96.2	92.9		3M, ECP 300, Al
Y1-14-21	13W	35.6	68.5	89.4	93.1	92.2	90.1		3M, ECP 300, Al
Y1-14-21	26W/NoUV	44.5		85.5		95.7			3M, ECP 300, Al
Y1-14-21	26W	41.4		86.1		91.8			3M, ECP 300, Al
Y1-14-21	39W/NoUV	51.3		89.0		95.7			3M, ECP 300, Al
Y1-14-21	39W	45.8		85.8		89.8			3M, ECP 300, Al
Y1-14-21	52W/NoUV	46.5		91.3		96.8			3M, ECP 300, Al
Y1-14-21	52W	48.6		75.3		79.4			3M, ECP 300, Al

Table C-4. Reflectance of Commercial Mirrors After Weather-Ometer Exposure (Continued)

Sample	Exposure Time[b]	Aperture (mrad) Full-Cone Angle[a]					H_s[c]	H_{66}[d]	Film/Substrate
		4	6	8	10	12			
Y1-14-25	13W/NoUV	31.4	68.6	87.7	92.4	93.6		98.7	3M, ECP 300, Al
Y1-14-25	13W	35.3	72.3	90.5	93.5	94.0		97.3	3M, ECP 300, Al
Y1-14-25	26W/NoUV	45.8		89.4		94.2			3M, ECP 300, Al
Y1-14-25	26W	51.7		88.9		92.7			3M, ECP 300, Al
Y1-14-25	39W/NoUV	47.4		87.3		92.3			3M, ECP 300, Al
Y1-14-25	39W	30.3		86.1		89.8			3M, ECP 300, Al
Y1-14-25	52W/NoUV	42.0		88.9		96.5			3M, ECP 300, Al
Y1-14-25	52W	40.7		77.9		87.8			3M, ECP 300, Al
Y1-14-28	13W/NoUV	37.7	73.9	91.3	94.4	95.0		98.7	3M, ECP 300, Al
Y1-14-28	13W	32.8	62.2	84.5	90.2	91.6		96.4	3M, ECP 300, Al
Y1-14-28	26W/NoUV	53.8		91.3		95.9			3M, ECP 300, Al
Y1-14-28	26W	36.3		83.5		91.0			3M, ECP 300, Al
Y1-14-28	39W/NoUV	52.4		90.3		93.7			3M, ECP 300, Al
Y1-14-28	39W	57.4		87.3		89.6			3M, ECP 300, Al
Y1-14-28	52W/NoUV	55.6		81.3		96.0			3M, ECP 300, Al
Y1-14-28	52W	51.3		82.9		85.8			3M, ECP 300, Al
ECP 300A Lot 9									
Y1-30-1	4M/NoUV	39.9	73.9	92.4	95.8	96.1	92.4		3M, ECP 300A, Al
Y1-30-1	4M	44.5	76.1	88.4	90.7	91.2	87.3		3M, ECP 300A, Al
Y1-30-1	7M/NoUV	57.0		89.5		95.8	91.7		3M, ECP 300A, Al
Y1-30-1	7M	46.2		68.6		70.5	75.4		3M, ECP 300A, Al
Y1-30-1	10M/NoUV	60.2		92.2		95.3			3M, ECP 300A, Al
Y1-30-1	10M	21.4		35.7		36.7			3M, ECP 300A, Al
Y1-30-1	13M/NoUV	49.2		91.9		96.2			3M, ECP 300A, Al
Y1-30-1	13M	22.0		36.6		38.5			3M, ECP 300A, Al, D
Y1-30-4	4M/NoUV	45.1	81.1	95.5	96.7	96.8	91.8		3M, ECP 300A, Al
Y1-30-4	4M	31.6	63.3	85.4	89.0	89.6	84.9		3M, ECP 300A, Al
Y1-30-4	7M/NoUV	63.8		92.7		95.9			3M, ECP 300A, Al
Y1-30-4	7M	34.0		57.7		65.1			3M, ECP 300A, Al
Y1-30-4	10M/NoUV	63.8		94.5		99.8			3M, ECP 300A, Al
Y1-30-4	10M	18.5		31.9		17.5			3M, ECP 300A, Al
Y1-30-4	13M/NoUV	59.9		91.5		95.6			3M, ECP 300A, Al
Y1-30-4	13M	8.8		16.8		17.6			3M, ECP 300A, Al, D
Y1-30-10	4M/NoUV	44.4	77.7	93.7	96.1	96.3	91.7		3M, ECP 300A, Al
Y1-30-10	4M	25.7	57.9	82.4	88.0	88.4	84.7		3M, ECP 300A, Al
Y1-30-10	7M/NoUV	51.6		91.0		94.5			3M, ECP 300A, Al
Y1-30-10	7M	28.4		57.3		60.4			3M, ECP 300A, Al
Y1-30-10	10M/NoUV	64.1		93.8		96.7	93.9		3M, ECP 300A, Al
Y1-30-10	10M	16.6		31.2		32.7	54.0		3M, ECP 300A, Al
Y1-30-10	13M/NoUV	58.8		91.2		98.4			3M, ECP 300A, Al
Y1-30-10	13M	7.5		14.4		15.0			3M, ECP 300A, Al, D

Table C-4. Reflectance of Commercial Mirrors After Weather-Ometer Exposure (Concluded)

Sample	Exposure Time[b]	Aperture (mrad) Full-Cone Angle[a]							Film/Substrate
		4	6	8	10	12	H_s^c	H_{66}^d	
Y1-30-13	4M/NoUV	45.2	81.0	96.3	97.5	97.7	92.7		3M, ECP 300A, PAl
Y1-30-13	4M	44.4	79.9	93.9	96.4	96.4	91.6		3M, ECP 300A, PAl
Y1-30-13	7M/NoUV	56.8		94.2		96.3	93.2		3M, ECP 300A, PAl
Y1-30-13	7M	59.4		92.9		94.6	90.8		3M, ECP 300A, PAl
Y1-30-13	10M/NoUV	71.5		96.6		97.7	93.6		3M, ECP 300A, PAl
Y1-30-13	10M	64.5		93.5		95.1	89.7		3M, ECP 300A, PAl
Y1-30-13	13M/NoUV	50.4		92.4		94.9			3M, ECP 300A, PAl
Y1-30-13	13M	56.5		86.4		88.4			3M, ECP 300A, PAl
Y1-30-19	4M/NoUV	34.4	68.1	92.7	96.4	96.8	92.9		3M, ECP 300A, PAl
Y1-30-19	4M	27.8	65.8	88.4	94.9	95.5	91.4		3M, ECP 300A, PAl
Y1-30-19	7M/NoUV	49.6		92.1		95.7			3M, ECP 300A, PAl
Y1-30-19	7M	40.4		86.5		92.4			3M, ECP 300A, PAl
Y1-30-19	10M/NoUV	65.6		94.5		97.7			3M, ECP 300A, PAl
Y1-30-19	10W	44.1		88.7		93.1			3M, ECP 300A, PAl
Y1-30-19	13M/NoUV	42.8		88.2		94.9			3M, ECP 300A, PAl
Y1-30-19	13M	45.6		84.2		88.0			3M, ECP 300A, PAl
Y1-30-20	4M/NoUV	38.5	77.5	94.6	96.3	96.6	92.4		3M, ECP 300A, PAl
Y1-30-20	4M	41.5	73.8	92.3	95.4	95.5	91.5		3M, ECP 300A, PAl
Y1-30-20	7M/NoUV	58.1		92.8		95.5			3M, ECP 300A, PAl
Y1-30-20	7M	61.2		92.1		94.3			3M, ECP 300A, PAl
Y1-30-20	10M/NoUV	55.4		94.4		97.5			3M, ECP 300A, PAl
Y1-30-20	10M	65.0		92.6		93.5			3M, ECP 300A, PAl
Y1-30-20	13M/NoUV	62.7		93.9		94.1			3M, ECP 300A, PAl
Y1-30-20	13M	50.2		86.0		88.1			3M, ECP 300A, PAl
Y1-105-2	0	86.3		96.1		97.1	92.8		3M, ECP 300A, AlP[g]
Y1-105-2	1M	83.3		95.9		96.1	92.8		3M, ECP 300A, AlP
Y1-105-2	2M						92.2		3M, ECP 300A, AlP

[a] Wavelength = 660 nm; angle of incidence = 20°; beam diameter = 10 mm.
[b] W = weeks, M = months.
[c] Solar-weighted hemispherical reflectance (AM 1.5).
[d] Hemispherical reflectance at 660 nm.
[e] d = discontinued.
[f] PAl is painted aluminum.
[g] AlP = polished aluminum.

APPENDIX D

REFLECTANCE OF SOLUTION CAST PMMA/SILVER MIRRORS AS A FUNCTION OF ENVIRONMENTAL DEGRADATION

This appendix lists the results for optical reflectance measurements of silver mirrors with cast polymeric films. The additives used, together with their concentrations in the polymeric films, are given in Tables D-1 and D-2. The outdoor weathering data, the QUV data, and the Weather-Ometer data are listed in Tables D-3 to D-15.

Optical measurements were limited to hemispherical values in the wavelength range from 300 to 1000 nm and selected specular measurements at 15-mrad acceptance angle (660 nm). Mirrors were cleaned with deionized water and detergent after degradation and before the optical measurements.

Table D-1. Stabilizer Additives Incorporated into Multiple PMMA Coatings on Wet-Processed Silver (Effective stabilizer concentration = 1.5%; total average film thickness range: 0.5-3.0 μm)

SERI Sample #	Additives to PMMA	
	Bottom Layer	Top Layer
R12-178-1 to -4	None	None
-5 to -8	V	V
-9 to -12	None	V
-13 to -16	V	None
-17 to -20	VI	VI
-21 to -24	None	VI
-25 to -28	VI	None
-29 to -32	VIII	VIII
-33 to -36	None	VIII
-37 to -40	VIII	None
-41 to -44	IX	IX
-45 to -48	None	IX
-49 to -52	IX	None
-53 to -56	X	X
-57 to -60	None	X
-61 to -64	X	None
-65 to -68	XI	XI
-69 to -72	None	XI
-73 to -76	XI	None
-77 to -80	XII (MS1-11-5)	XII (MS1-11-5)
-81 to -84	None	XII (MS1-11-5)
-85 to -88	XII (MS1-11-5)	None
-89 to -92	XII (MS1-13-2)	XII (MS1-13-2)
-93 to -96	XII (MS1-13-2)	None
-97 to -100	None	XII (MS1-13-2)
-101 to -104	XIII	XIII
-105 to -108	None	XIII
-109 to -112	XIII	None

Table D-2. Stabilizer Additives Incorporated into Solution Cast PMMA Coatings

SERI Sample #	Additives to PMMA	Film Thickness (μm)
R13-100-1	No Additive	14
-2	1.5% TIN-P	13
-3	3.0% NS	18
-4	1.5% UV	17
-5	3.0% NS + 1.0% G-31	18
-6	1.5% TIN-2	16
-7	1.5% IRG	14
-8	1.5% G-31	16
-9	1.5% IST	16
-10	1.5% CH	14
-11	1.5% SP	11
-12	10% SERI-JPL-2H5V-15 (p-MMA-co-2H5V)	25
-13	20% SERI/MS1-11-5 (p-MMA-co-MHB)	12
-14	20% SERI-MS1-13-2 (p-MMA-co-MHB)	12
-15	1.5% MHB	14

Table D-3. Hemispherical Reflectance (H) and Specular Reflectance (S) at 15 mrad of Multiple PMMA Coatings onto Wet-Processed Silver After Outdoor Weathering

SERI Sample #	Hemispherical (%) Weeks Weeks			Specular — 15 mrad (%)		
	0	8	18	0	8	18
R-12-178-1	87.9	86.3	74.9 d	94	95	87 d
R-12-178-6	87.7	85.9	86.1	96	95	92
R-12-178-10	86.5	85.6	85.1	95	95	94
R-12-178-13	87.6	83.7	85.0	94	95	89
R-12-178-18	88.0	86.4	85.6	95	96	92
R-12-178-23	87.5	--	85.4	95	--	85
R-12-178-26	87.2	84.0	84.9	94	93	83
R-12-178-31	87.4	80.1	63.9 d	96	94	88 d
R-12-178-34	87.5	85.3	86.4	96	95	93
R-12-178-39	87.5	84.9	71.6 d	94	94	89 d
R-12-178-43	86.5	85.0	85.3	92	95	91
R-12-178-47	87.1	84.9	d	94	92	d
R-12-178-51	86.6	81.1	84.7	95	94	92
R-12-178-55	86.9	84.8	d	94	94	d
R-12-178-59	86.4	84.5	85.4	92	95	91
R-12-178-63	86.5	84.9	d	94	93	90 d
R-12-178-67	86.3	84.0	84.8	94	93	91
R-12-178-70	86.2	83.4	64.6 d	94	93	d
R-12-178-75	87.0	83.8	83.0	94	95	91
R-12-178-78	85.2	82.5	84.4	96	94	92
R-12-178-83	87.4	84.9	85.1	96	95	92
R-12-178-87	86.0	83.8	64.5 d	96	92	d
R-12-178-90	86.5	83.2	85.5	93	93	73
R-12-178-94	86.9	85.1	84.2	96	95	86
R-12-178-99	87.2	83.8	d	96	90	d
R-12-178-101	87.8	--	85.7	96	--	88
R-12-178-105	85.5	82.8	83.4	94	94	93
R-12-178-109	86.0	d	d	95	d	30 d

d = delaminated.

Table D-4. Hemispherical Reflectance (H) and Specular Reflectance (S) at 15 mrad of Multiple PMMA Coatings onto Wet-Processed Silver After QUV Exposures

SERI Sample #	Hemispherical (%) Weeks Weeks			Specular — 15 mrad (%)		
	0	8	18	0	8	18
R-12-178-2	87.5	86.8	86.0	96	94	87
R-12-178-8	87.9	86.8	86.0	94	94	90
R-12-178-12	86.9	86.9	86.3	95	92	85
R-12-178-16	86.5	86.7	86.1	95	95	91
R-12-178-20	88.3	86.0	85.7	95	95	94
R-12-178-22	87.0	86.3	87.1	94	94	90
R-12-178-25	86.0	86.8	77.8 d	92	91	91 d
R-12-178-30	87.8	87.2	84.7	94	94	84
R-12-178-36	86.7	86.8	d	96	94	91 d
R-12-178-38	86.0	86.6	87.0	95	95	94
R-12-178-42	87.2	87.9	d	94	89	86 d
R-12-178-46	88.2	88.0	d	95	94	d
R-12-178-50	87.2	86.8	84.5	95	92	77
R-12-178-54	86.9	85.9	85.5	93	94	95
R-12-178-58	84.7	86.5	86.5	95	95	95
R-12-178-62	86.5	85.3	85.4	93	94	94
R-12-178-66	86.3	85.9	d	96	94	d
R-12-178-72	86.7	86.1	d	94	95	d
R-12-178-74	85.9	85.9	86.6	96	93	91
R-12-178-80	85.8	83.1	d	95	90	d
R-12-178-82	85.8	85.3	83.7	96	92	72
R-12-178-86	87.4	86.7	d	97	92	d
R-12-178-92	86.4	84.0	81.2	96	95	66
R-12-178-96	86.3	86.2	85.9	95	94	91
R-12-178-98	86.0	86.0	83.1	96	91	85
R-12-178-103	85.2	84.1	82.8	95	92	88
R-12-178-107	86.1	86.9	d	95	94	d
R-12-178-111	87.4	88.1	86.8	94	95	94

d = delaminated.

Table D-5. Hemispherical Reflectance (H) and Specular Reflectance (S) at 15 mrad of Selected Multiple PMMA Coatings onto Wet-Processed Silver After Weather-Ometer Exposures

SERI Sample #	Hemispherical (%) Weeks					Specular — 15 mrad (%) Weeks				
	0	^{8}UV	^{8}NoUV	^{18}UV	^{18}NoUV	0	^{8}UV	^{8}NoUV	^{18}UV	^{18}NoUV
R-12-178-4	88	d	86	d	d	95	d	91	d	d
R-12-178-7	88	85	87	d	d	95	21	85	d	d
R-12-178-11	88	86	84	d	d	96	24	86	d	d
R-12-178-15	87	82	87	d	d	96	52	83	d	d
R-12-178-32	88	84	87	d	d	96	85	93	51 d	92 d
R-12-178-56	87	84	86	d	d	94	65	93	87 d	92 d
R-12-178-64	87	82	83	83	83	94	58	91	74	92
R-12-178-68	86	84	85	d	d	92	29	87	84 d	92 d
R-12-178-71	86	78	86	d	d	93	26	85	73 d	92 d
R-12-178-76	86	84	86	83	85	95	78	93	88	93
R-12-178-79	87	82	85	78	75	94	32	30	76	89
R-12-178-84	86	85	86	d	d	96	73	91	46 d	90 d
R-12-178-88	87	85	86	d	86	94	--	86	53 d	81
R-12-178-91	87	86	86	84	86	94	28	88	45	89
R-12-178-95	87	86	86	81	86	96	63	92	84	93
R-12-178-100	86	85	86	85	86	96	76	93	44	95
R-12-178-102	87	83	88	87	87	96	44	93	56	95
R-12-178-106	86	86	86	86	86	95	65	89	82	93
R-12-178-110	87	85	87	87	87	95	92	94	49	94

d = delaminated.

Table D-6. Hemispherical Reflectance (H) and Specular Reflectance (S) at 15 mrad of Solution Cast PMMA Coatings onto Wet-Processed Silver After Outdoor Weathering

SERI Sample #	Hemispherical (%) Weeks					Specular — 15 mrad (%) Weeks				
	0	1	3	6	15	0	1	3	6	15
R13-100-1	88	88	89	76 d	d	95	94	95	d	d
-2	85	85	85	85	85	95	94	95	94	59
-3	86	86	86	d	d	95	95	74	d	d
-4	85	84	85	84	84	94	92	47	93	42
-5	85	85	90	d	d	94	95	77	d	d
-6	88	88	88	89	22	97	94	92	95	63
-7	87	88	88	87	d	96	94	83	94	d
-8	88	88	88	88	13	97	95	94	94	12
-9	86	86	86	86	85	96	94	85	86	74
-10	89	d	d	d	d	94	88 d	d	d	d
-11	85	d	d	d	d	94	84 d	d	d	d
-12	86	d	d	d	d	96	92 d	d	d	d
-13	87	87	87	87	86	94	91	91	94	69
-14	88	88	--	87	49	94	93	93	93	3
-15	87	87	87	86	73	94	94	94	94	54

d = delaminated.

Table D-7. Hemispherical Reflectance (H) and Specular Reflectance (S) at 15 mrad of Solution Cast PMMA Coatings onto Wet-Processed Silver After QUV Exposures

SERI Sample #	Hemispherical (%) Weeks					Specular — 15 mrad (%) Weeks				
	0	1	3	6	15	0	1	3	6	15
R13-100-1	86	84	80	88	69	95	93	92	91	76
-2	85	84	--	82	76	96	94	94	93	35
-3	86	86	--	d	d	95	95	95	71 d	d
-4	85	85	84	d	d	95	94	93	74 d	d
-5	85	85	85	82	83	93	92	93	93	87
-6	88	87	87	87	80	97	94	95	96	60
-7	87	85	--	82	37	96	93	94	90	30
-8	88	87	84	88	69	97	95	95	91	66
-9	87	85	84	82	72	96	94	95	95	82
-10	87	86	84	84	d	94	92	91	85	d
-11	84	80	82	d	d	94	84	69	d	d
-12	86	86	--	80	67	96	94	93	95	77
-13	87	86	84	87	44	94	91	94	91	37
-14	85	83	80	82	64	92	92	92	64	54
-15	87	86	84	85	47	94	94	94	72	44

d = delaminated.

Table D-8. Hemispherical Reflectance (H) and Specular Reflectance (S) at 15 mrad of Solution Cast PMMA Coatings onto Wet-Processed Silver After Weather-Ometer Exposures

SERI Sample #	Hemispherical (%) Weeks									Specular 15 mrad (%) Weeks								
	0	^{1}UV	^{1}NoUV	^{3}UV	^{3}NoUV	^{6}UV	^{6}NoUV	^{15}UV	^{15}NoUV	0	^{1}UV	^{1}NoUV	^{3}UV	^{3}NoUV	^{6}UV	^{6}NoUV	^{15}UV	^{15}NoUV
R13-100-1	88	87	86	84	86	83	87	84	86	95	93	94	96	96	92	95	87	93
-2	85	84	84	80	84	64	84	44	84	96	93	93	96	96	82	93	37	91
-3	86	86	86	86	86	86	86	86	86	95	93	94	97	97	96	91	42	86
-4	85	85	85	85	85	85	85	85	85	95	93	94	97	90	95	69	73	94
-5	88	88	88	88	88	88	88	88	88	95	94	95	98	98	96	97	94	95
-6	89	89	89	89	89	89	90	88	91	97	95	95	99	100	98	98	95	96
-7	88	88	87	87	86	87	87	87	87	97	93	94	98	98	96	93	94	95
-8	88	88	88	88	88	88	88	88	88	97	94	94	98	97	94	84	93	86
-9	87	87	89	87	86	87	87	88	86	96	94	94	98	96	96	94	94	93
-10	88	89	89	88	89	89	90	89	91	95	94	94	96	97	89	95	d	d
-11	84	d	d	d	d	d	d	d	d	93	d	d	d	d	d	d	d	d
-12	87	87	87	87	90	d	d	d	d	96	94	95	99	98	d	d	d	d
-13	87	84	87	71	87	73	87	75	87	94	91	93	83	98	89	96	86	94
-14	88	86	86	84	85	86	86	86	85	94	91	91	97	96	93	92	93	89
-15	87	86	86	86	87	86	87	86	87	94	93	93	95	93	89	79	89	79

d = delaminated.

Table D-9. **Hemispherical Reflectance (H) and Specular Reflectance (S) at 15 mrad of Filtered Solution Cast PMMA Coatings onto Wet-Processed Silver After Weather-Ometer Exposures** (Filter: R13-100-1, transmittance characteristics given in Figure 3-16)

SERI Sample #	Hemispherical (%) Weeks					Specular — 15 mrad (%) Weeks				
	0	1	3	6	15	0	1	3	6	15
R13-100-1	86	84	84	82	83	95	93	79	92	91
-2	86	83	77	62	50	96	94	78	86	38
-3	86	85	86	87	86	94	94	69	94	91
-4	87	86	87	87	87	96	95	83	96	94
-5	85	86	86	87	86	94	94	75	95	93
-6	89	88	87	89	78 d	97	95	95	96	d
-7	87	87	86	88	88	97	95	75	95	94
-8	88	87	87	88	88	97	95	95	96	92
-9	87	87	87	88	88	96	95	85	95	94
-10	88	--	87	d	d	91	--	49	d	d
-11	84	d	d	d	d	93	d	d	d	d
-12	86	86	83	81	78	97	94	91	91	83
-13	88	85	83	85	86	93	92	72	93	93
-14	86	84	82	83	84	93	92	89	94	92
-15	87	87	86	85	86	94	94	94	96	94

d = delaminated.

Table D-10. **Hemispherical Reflectance (H) and Specular Reflectance (S) at 15 mrad of Filtered Solution Cast PMMA Coatings onto Wet-Processed Silver After Weather-Ometer Exposures** (Filter: R13-100-2, transmittance characteristics given in Figure 3-16)

SERI Sample #	Hemispherical (%) Weeks					Specular — 15 mrad (%) Weeks				
	0	1	3	6	15	0	1	3	6	15
R13-100-1	86	85	84	82	78	95	93	90	90	90
-2	86	84	80	72	58	96	94	95	65	65
-3	86	85	86	87	87	94	94	96	94	94
-4	87	85	86	87	87	96	95	96	94	95
-5	85	86	86	87	87	94	94	94	94	95
-6	89	89	88	88	88	97	94	96	96	95
-7	87	88	87	87	88	97	95	96	96	95
-8	88	87	87	88	88	97	95	96	96	95
-9	87	87	87	88	88	96	95	95	95	94
-10	88	--	87	d	d	91	--	93	d	d
-11	84	d	d	d	d	93	d	d	d	d
-12	86	86	86	85	83 d	97	94	92	92	d
-13	88	85	87	87	87	93	94	94	92	94
-14	86	84	84	82	81	93	92	92	94	93
-15	87	87	86	86	86	94	94	94	95	94

d = delaminated.

Table D-11. **Hemispherical Reflectance (H) and Specular Reflectance (S) at 15 mrad of Filtered Solution Cast PMMA Coatings onto Wet-Processed Silver After Weather-Ometer Exposures** (Filter: R13-100-4, transmittance characteristics given in Figure 3-16).

SERI Sample #	Hemispherical (%) Weeks					Specular — 15 mrad (%) Weeks				
	0	1	3	6	15	0	1	3	6	15
R13-100-1	87	86	86	84	79	96	94	91	91	91
-2	86	82	73	57	45	97	94	95	75	36
-3	86	84	86	87	86	95	95	97	96	94
-4	86	84	85	86	85	96	94	76	94	94
-5	86	87	86	87	92 d	94	94	76	95	d
-6	89	89	88	88	88	97	95	95	96	95
-7	88	87	87	87	87	97	95	96	96	94
-8	87	87	87	88	88	97	95	93	97	95
-9	87	87	88	88	88	96	95	74	96	94
-10	89	--	91	d	d	94	--	90	d	d
-11	85	d	d	d	d	94	d	d	d	d
-12	86	87	86	86	86	97	95	93	96	89
-13	86	85	83	81	80	93	92	73	93	91
-14	86	85	81	82	83	93	92	73	93	92
-15	86	85	84	82	79	93	93	73	94	91

d = delaminated.

Table D-12. **Hemispherical Reflectance (H) and Specular Reflectance (S) at 15 mrad of Filtered Solution Cast PMMA Coatings onto Wet-Processed Silver After Weather-Ometer Exposures** (Filter: R13-100-13, transmittance characteristics given in Figure 3-16)

SERI Sample #	Hemispherical (%) Weeks					Specular — 15 mrad (%) Weeks				
	0	1	3	6	15	0	1	3	6	15
R13-100-1	87	86	86	85	81	96	93	72	93	92
-2	86	--	76	65	48	97	95	82	93	53
-3	86	85	87	87	86	95	95	94	96	95
-4	86	84	85	85	84	96	94	94	94	93
-5	86	86	86	87	87	94	95	96	89	94
-6	89	89	88	88	88	97	95	94	96	95
-7	88	87	86	87	87	97	95	97	94	94
-8	87	87	87	89	89	97	95	97	96	91
-9	87	87	87	88	87	96	95	87	96	93
-10	89	--	90	d	d	94	--	94	d	d
-11	85	d	d	d	d	94	d	d	d	d
-12	86	86	85	83	82	97	94	95	95	88
-13	86	85	82	81	80	93	92	92	93	92
-14	86	84	82	82	84	93	92	90	90	92
-15	86	86	85	83	83	93	93	93	94	92

d = delaminated.

Table D-13. **Hemispherical Reflectance (H) of Solution Cast Unstabilized PMMA Coatings onto Irradiation Treated Wet-Processed Silver (R14-26-1,2) After Weather-Ometer Exposures** (A wet-processed silver sample was exposed to WOM radiation for 2 h before coating)

SERI Sample #	Time of WOM Exposure (h)	Hemispherical (%) Weeks								
		0	^{1}UV	^{1}NoUV	^{3}UV	^{3}NoUV	^{9}UV	^{9}NoUV	^{20}UV	^{20}NoUV
R14-26-1	0	87	87	87	87	87	87	86	87	87
R14-26-2	2	87	87	86	87	87	87	86	87	86

Table D-14. **Hemispherical Reflectance (H) of Solution Cast Unstabilized PMMA Coatings onto HCl-Treated Wet-Processed Silver (R14-26-4,5,6) After Weather-Ometer Exposures** (The wet-processed silver sample was exposed to HCl vapor for various times before coating)

SERI Sample #	Time of HCl Exposure (min)	Hemispherical (%) Weeks											
		0 (Ag only)	0	^{1}UV	^{1}NoUV	^{3}UV	^{3}NoUV	^{6}UV	^{6}NoUV	^{12}UV	^{12}NoUV	^{20}UV	^{20}NoUV
R14-26-4	15	92	84	83	82	84	84	83	83	80	80	83	84
R14-26-5	5	94	87	86	86	87	87	86	86	83	82	86	86
R14-26-6	1	94	86	86	85	87	86	86	86	83	86	86	85

Table D-15. Hemispherical Reflectance (H) of Solution Cast PMMA Coatings on Various Silver Surfaces After Weather-Ometer Exposures

SERI Sample #	Coating Type^{a}	Hemispherical (%) Weeks									
		0 (metal only)	0	^{1}UV	^{1}NoUV	^{6}UV	^{6}NoUV	^{15}UV	^{15}NoUV	^{26}UV	^{26}NoUV
Wet Processed Ag											
R14-74-A1	1	95	89	90	90	90	90	89	89	88	89
-A2	2	95	89	90	90	89	89	89	88	88	88
-A3	3	95	87	87	87	84	87	84	86	84	86
Sputtered Ag											
R14-74-B1	1	96	95	95	95	95	95	95	94	93	94
-B2	2	96	95	95	95	94	94	94	94	92	94
-B3	3	96	92	93	92	92	92	91	91	90	91
Sputtered Al on Wet-Processed Ag											
R14-74-C1	1	67	64	62	62	64	65	66	60	67	60
-C2	2	81	69	71	61	72	62	73	61	71	60
-C3	3	81	60	60	69	61	70	61	72	57	74

[a] Coating type:
1: PMMA, purified
2: PMMA, as received
3: 2 + 1.5% TIN-P

APPENDIX E

TRANSMITTANCE OF SOLUTION CAST PMMA FILMS AS A FUNCTION OF ENVIRONMENTAL DEGRADATION

This appendix lists the results for optical transmittance measurements of cast polymer films. The additives used, together with their concentrations in the polymeric films, are given in Tables D-2 and E-1. The accelerated exposure data are listed in Tables E-2 to E-4.

The optical measurements were limited to solar weighted specular transmittance values in the wavelength range from 200 to 600 nm as measured with the Perkin-Elmer spectrometer PE 340. The films were cleaned with deionized water after exposure and before the optical measurements.

Table E-1. Stabilizer Additives Incorporated into Solution Cast PMMA Films

SERI Sample #	Additives to PMMA
R13-100-1 to R13-100-15	see Table D-2
R13-100-16	14% SERI-MS1-49-2
R14-145-1	15% SERI-PG1-27-2
R14-145-2	7.5% SERI-PG1-27-3

Table E-2. Specular Transmittance (200-600 nm) of Solution Cast Thin Films After Weather-Ometer Exposures

SERI Sample #	Film Thickness (μm)	T(%) Weeks		
		0	6	15
R13-100-1	22	92	90	90
-2	19	82	81	84
-4	20	87	86	82
-13	22	86	86	86

Table E-3. Specular Transmittance (200-600 nm) of Solution Cast Thick Films (ca. 3.5 mil = 89 μm) After Weather-Ometer (WOM) and QUV Exposures

SERI Sample #	T(%) Weeks WOM					T(%) Weeks QUV				
	0	1	3	6	15	0	1	3	6	15
R13-100-1	91	91	91	90	90	91	86	80	75	b
-2	82	81	81	81	81	82	81	80	80	55[c]
-3	85	86	85	85	84	85	83	84	83	85
-14	82	82	81	82	82	82	77	65	46	0[c]
R14-145-1	79	79	79	79	79	79	78	77	76	63[c]
ECP 300[a]	81	81	81	81	78	81	81	78	78	78

[a] Melt extruded film.
[b] Brittle failure.
[c] Surface crazing.

Table E-4 Specular Transmittance (200-600 nm) of Solution Cast Thin Films (ca. 0.5-1.0 mil = 13-25 μm) After QUV Exposures

SERI Sample #	T(%) Weeks									
	0	^{1}UV	^{1}Filt[a]	^{1}NoUV	^{3}UV	^{3}Filt[a]	^{3}NoUV	^{6}UV	^{6}Filt[a]	^{6}NoUV
R13-100 -1	92	90	90	91	c	90	91	--	90	92
-2	83	82	81	83	82	82	83	82	82	83
-3	89	88	89	88	89	88	88	90	88	89
-4	85	86	86	86	86	86	87	86	86	87
-16	88	87	88	87	c	88	86	--	b	86
R14-145-2	83	83	83	83	82	83	83	81	81	83
ECP 300[b]	81	79	80	80	79	81	80	79	78	80

[a] ECP 300 filter.
[b] Melt-extruded film.
[c] Brittle failure.

DISTRIBUTION LIST

Bartkus, Ed
Rohm and Haas Company
New Products Development
Independence Mall West
Philadelphia, PA 19105

Belfiore, Larry
Dept. of Chemical Engineering
Colorado State University
Fort Collins, CO 80523

Bell, William
Gila River Products
6615 West Boston Street
Chandler, AZ 85224
(602) 961-1244

Benson, Burton A. (Bud)
The 3M Company
St. Paul, MN 55144
(612) 733-1031

Braun, Gerald
Pacific Gas & Electric
3400 Crow Canyon Road
San Ramon, CA 94583
(415) 820-2000 x559

Bronstein, Allen
Sunsteam Ltd.
715 Florales Drive
Palo Alto, CA 94306

Butler, Barry L.
Science Applications, Inc.
San Diego, CA 92121
(619) 458-3844

Chughtai, Abdul R.
University of Denver
Department of Chemistry
Boettcher West
2050 E. Iliff Ave.
Denver, CO 80208
(303) 871-4404

De Laquil, Pascal (Pat)
Bechtel
P.O. Box 3965
San Francisco, CA 94119
(415) 768-1947

Department of Energy/HQ
Forrestal Building
1000 Independence Ave., SW
Washington, DC 20585
Dr. H. Coleman
Mr. S. Gronich
Mr. M. Scheve
Mr. Frank Wilkins

Firca, D. J.
BF Goodrich Company
Specialty Polymers and
Chemicals Division
6100 Oak Tree Blvd.
Cleveland, OH 44131

Gee, Randy and Ken May
Industrial Solar Technology
5775 W. 52nd Avenue
Denver, CO 80212
(303) 431-8348

Hallman, Dennis
Dunmore Corp.
Newtown Industrial Commons
207 Penns Trail
Newtown, PA 18940
(215) 968-4774

Harder, John
Black & Veatch
Consulting Engineers
1500 Meadow Lake Parkway
Kansas City, MO 64114

Heldt, Walter Z.
Helix Associates, Inc.
P.O. Box 4694
Newark, DE 19715
(302) 738-6581

Hess, Walter
Entech, Inc.
1015 Royal Lane
P.O. Box 612246
DFW Airport, Texas 75261

Hull, Jacques L.
Acurex Solar Corporation
485 Clyde Avenue
Mountain View, CA 94042
(415) 964-3200

Hutchison, J. A.
Solar Kinetics, Inc.
10635 King William Drive
Dallas, TX 75220
(214) 556-2376

Idle, James
Vice President for
Research and Development
Ashland Chemical Co.
P.O. Box 2219
Columbus, OH 43216

Jones, William
Texas Tech University
Lubbock, TX 79409

Kainer, Helmuth
Director for Technical Liaison
BASF Wyandotte Corp.
100 Cherry Hill Rd.
P.O. Box 181
Parsippany, NJ 07054

Kearney, David
Luz Engineering Corp.
924 Westwood
Suite 1000
Los Angeles, CA 90024
(213) 208-7444

Lampert, Carl
Lawrence Berkeley Laboratory
One Cyclotron Rd.
Berkeley, CA 94720
(415) 486-6093

Learn, Martin
Alternate Energy Institute
P.O. Box 1432
La Jolla, CA 92038
(619) 692-2015

Lensch, Guenther
Nordische Universitat Tech. GmbH
Ilsahl 5
2350 Neumuenster
West Germany

Lutley, John H.
The Silver Institute
Suite 101
1026 16th Street, NW
Washington, DC 20036

McCusker, Mark
Additives Department
Ciba-Geigy Corp.
Three Skyline Drive
Hawthorne, NY 10532

McGlaun, Monte
LaJet Energy Co.
3130 Antilley Road
Abilene, TX 79606
(915) 698-8800

Pettit, R. B.
Sandia National Laboratories
Albuquerque, NM 87115

Porter, Prof. Roger S.
Co-Director Materials Research
Laboratory
Department of Polymer Science and
Engineering
University of Massachusetts
Amherst, MA 01003

Seki, Art
Hawaii Natural Energy Institute
University of Hawaii at Manoa
2540 Dole Street
Honolulu, HI 96822

Shannon, W. E.
WES Consulting Inc.
20380 Town Center Lane
Suite 170
Cupertino, CA 95014
(408) 446-0860

Smith, Dwight M.
University of Denver
Office of the Chancellor
2301 South Gaylord
Denver, CO 80208

Susemihl, Ingo
DFVLR
Abt. RF-ET
Linger Höhe 90
Postfach 906058
5000 Köln 90
West Germany

Touryan, Kenell
Moriah Research Company
6200 Plateau Drive
Englewood, CO 80111
(303) 771-1101

Vogl, Prof. O.
Polytechnic Institute of New York
333 Jay Street
Brooklyn, NY 11201

Walty, Robert J.
Deposition Technology, Inc.
8963 Carroll Way
San Diego, CA 92121
(629) 578-9400

Washom, Byron
Advanco Corporation
1714 Ferrari Drive
Beverly Hills, CA 90210
(213) 273-9690

White, James and Miko Cakmak
Center for Polymer Engineering (APEC)
Dept. of Polymer Engineering
The University of Akron
Akron, OH 44325